EFFECT OF RAPID HEATING AND COOLING INJECTION MOLDING CONDITIONS ON SURFACE ROUGHNESS OF THERMOPLASTIC PRODUCTION

WASAN PALAPINYO

A THESIS SUBMITTED IN PARTIAL FULFILLMENT
OF THE REQUIREMENT FOR THE DEGREE OF
MASTER OF ENGINEERING IN AUTOMOTIVE ENGINEERING
(INTERNATIONAL PROGRAM)
INTERNATIONAL COLLEGE
KING MONGKUT'S INSTITUTE OF TECHNOLOGY LADKRABANG
2012

KMITL-2012-IC-M-004-022

Thesis Title	Effect of Rapid Heating and Cooling Injection molding Conditions on Surface Roughness of Thermoplastic Production
Student	Mr. Wasan Palapinyo
Student ID.	52600902
Degree	Master of Engineering
Program	Automotive Engineering (International Program)
Year	2012
Thesis Advisor	Dr.Nattawoot Depaiwa Dr.Wuttipong Rungseesantivanon Assoc. Prof. Takushi Saito Prof. Isao Satoh

ABSTRACT

Plastics and automotive industry are related with plastic molding technology that were used injection molding, blow molding, extrusion, and forming sheets in the production of automotive parts. In this work studies the technology of injection molding that use rapid heating and cooling injection molding to control appearance of products. Technique heating and cooling cycle help with the injection process is increased immediately temperatures. The injection molding process uses high temperature when the injection machine is injecting to the mold that called filling. Then, the machine decreases immediately temperature. The process uses low temperature in cooling process. In this study, the on-off controller controls between injection molding machine and heating and cooling machine. The parameter in control system is temperature. The temperature from mold can detect by three thermocouples. When the signal from them is going to set point temperature, the injection machine will switch on to first stage is closing mold. Then after packing stage, the heating and cooling machine is switch on to cooling stage. The final of injection is part ejection, the heating and cooling stage is heating.

From this experiment, the parameters in injection molding are five parameters, that are mold temperature, barrel temperature, packing pressure, packing time, and injection speed. The mold temperature is the major factor of surface roughness. The relationship between mold temperature and surface roughness is direct variant because the melt plastic is low viscosity at

high temperature. From the result in mold temperature condition at100°C, it is the comparison study between conventional injection molding and rapid heating and cooling injection molding. The optimum point is at 100°C condition in heating and cooling injection molding because the surface roughness is better than conventional condition and part is more complete than conventional technique. Moreover, the energy consumption was calculated and investigated. The relationship between surface roughness and energy consumption was obtained. It was found that the lower surface roughness value is the higher energy consumption molding condition.

ACKNOWLEDGEMENT

This thesis could not be completed without the assistance of many persons to whom I would like to express my sincere appreciation.

First, I would like to sincerely thank my advisor, Dr.Nattawoot Depaiwa, who has given me many helpful suggestions.

I would like to sincerely thank Dr.Wuttipong Rungseesantivanon for kind advising and helping, Assoc. Prof. Takushi Saito and Prof. Isao Satoh for the suggestion of Injection process.

Moreover, I would like to show gratitude to National Metal and Materials Technology Center (MTEC), especially the Plastics Technology Laboratory for providing the high performance equipment as well as financial supporting.

I am grateful to National Science and Technology Development Agency (NSTDA), which provided the full scholarship for studying in the master program.

Finally, I am very grateful to my family for all love, caring, understanding and motivation throughout my life.

Wasan Palapinyo

CONTENTS

Page

CONTENTS (CONT.)

Page

CONTENTS (CONT.)

CONTENTS (CONT.)

CONTENTS (CONT.)

CONTENTS (CONT.)

Page

CONTENTS (CONT.)

Page

CONTENTS (CONT.)

Page

CONTENTS (CONT.)

Page

LIST OF TABLES

Table Page

LIST OF TABLES (CONT.)

Table Page

LIST OF FIGURES

LIST OF FIGURES (CONT.)

LIST OF FIGURES (CONT.)

Figure Page

LIST OF FIGURES (CONT.)

Figure Page

LIST OF FIGURES (CONT.)

Figure Page

LIST OF FIGURES (CONT.)

Figure Page

LIST OF FIGURES (CONT.)

Figure Page

LIST OF FIGURES (CONT.)

Figure Page

LIST OF FIGURES (CONT.)

CHAPTER 1

INTRODUCTION

1.1 Significance and Background

There are three techniques to make up thermoplastic such as injection molding, extrusion, and blow molding. Conventional methods are usually had heating for melting polymer that is easy to production. Especially, injection molding is the most popular technique for making parts. It can make complex artefact, easy to adding extra component. For example, polymeric interior bodies at a lot of complex artefact, beam strength and connected joint part for making product. However, the other benefit is colourful production because this method is included the colour process.

The appropriate polymer in making up process is considered in melt viscosity. The suitable polymer for injection molding process is low melt viscosity, while in extrusion and blow molding process use until medium to high melt viscosity.

In injection molding process has many extra techniques. For instance, water injection, gas injection and rapid heat cycle injection. The rapid heat cycle molding is a molding process that the mold cavity is rapidly heated to a high temperature before polymer melt injection, and then cooled quickly once the cavity is completely filled. Heating and cooling efficiency and temperature uniformity of the rapid heat cycle molding system are two key technical parameters to ensure a high productivity and high – quality products. [1] In this study is divided into four sections.

1.1.1 To study in the data correcting that is temperature and pressure data in injection molding process. There are use a data logger that is correcting temperature and pressure data from thermocouple and load cell. The software is a new programming in Microsoft visual basic 6.0. The data were analyzed in terms of energy consumption.

1.1.2 To study in parameters in conventional injection molding process. In this cases have five parameters instance, mold temperature, barrel temperature, pack pressure, pack pressure time and injection speed, are affected in quality of surface's gloss and surface's roughness.

1.1.3 To study the rapid heat cycle molding. In this cases, the specimens have high quality in surface's gloss and surface's roughness. It has limiting controlled quality of mold's surface.

1.1.4 To study statistical process control. In three section above, the summary is a guide - line in quality production in energy consumption term. It is included all of parameters in injection molding and rapid heat cycle molding.

1.2 Objectives

1.2.1 To study injection molding.

1.2.2 To study the effects of temperature and pressure on appearance properties.

1.2.3 To study the energy consumption for process between conventional injection molding and injection molding via heating and cooling machine.

1.3 Scopes

1.3.1 The first part was to study the appropriate parameters for conventional injection molding such as mold temperature, barrel temperature, packing pressure, packing pressure time, and injection speed.

1.3.2 The second part was to study the parameters for rapid heat and cool in injection molding such as mold temperature and packing pressure time.

1.3.3 The third part was to examine surface's gloss, surface's roughness, and microstructure.

1.3.4 The final part was to calculation in energy consumption in injection molding.

1.4 Expected Benefits

1.4.1 Understanding the processing method of conventional injection molding.

1.4.2 Understanding the processing method of rapid heat and cool in injection molding.

1.4.3 Understanding the effects of parameters of injection molding process on appearance properties.

1.4.4 Understanding the controlling of injection molding machine and heating and cooling machine.

CHAPTER 2

THEORY AND LITERATURE REVIEWS

In this study is investigated in surface finish in polymer surface. The polymers in this case is thermoplastic. The thermoplastic is weaken and it is melt, when polymer was heat by processing. The kinds of the thermoplastic are amorphous polymer (see in **2.1**) and crystalline polymer (see in **2.2**).

The mostly thermoplastic processes are compression molding, blow molding, and injection molding. In this case, is concentrated in injection molding (see in **2.3**) because the advantages of injection molding are low cost production, automatic production, and complex part production. Injection molding has many technique for assist injection molding that are gas injection molding, injection compression molding, and rapid heating cooling injection molding (see in **2.3.3**). [1] The rapid heating cooling injection molding is a molding is a molding process, that the mold's surface is rapidly heat to a high temperature before plastic melt injection, and then cooled quickly once in the cooling state.

For the control system in rapid heating cooling injection molding was studied in statistic process control (see in **2.4**). [2] The statistic process control simply means the use of statistic methods to monitor, analyze, and control a process, in particular process variation. For monitor in this case concern with the measurement of temperature (see in **2.5**) and the measurement of pressure (see in **2.6**). Also there have a programming that monitor and correcting data from thermocouples and pressure sensor.

For the study, the analyze of surface finish is investigated in scanning electron microscope (see in **2.7**), viscosity (see in **2.8**), and melt flow index (see in **2.9**). They are the main factors of surface finish. The surface finish can be explain in surface modification (see in **2.10**). In the **2.11** is shown the thermal insulation. This part is calculated the energy consumption of injection molding (see the result in **4.4**). And the last part is literature review (see in **2.12**).

2.1 Amorphous polymers

A specific amorphous polymer, such as poly(methyl methacrylate) or polystyrene, can exist in a number of states according to the temperature and the average molecular weight of the polymer. This is shown diagrammatically in **Figure 2.1**. At low molecular weight the polymer will be solid below some given temperature whilst above that temperature it will be liquid. The melting point for such polymers will be quite sharp and is the temperature above which the molecules have sufficient energy to move independently of each other, i.e. they are capable of viscous flow. In high polymers this is rarely, if ever, the case.

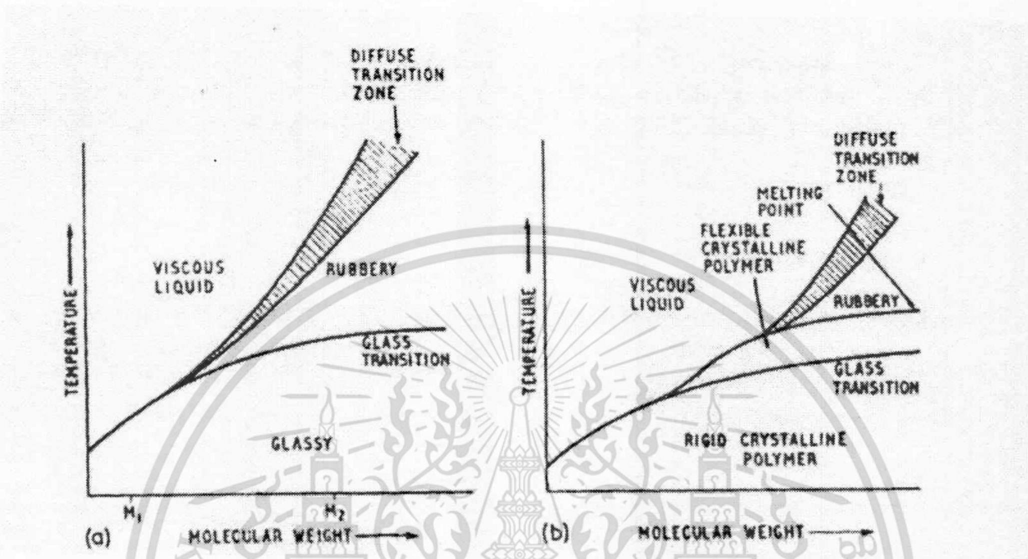

Figure2.1 Temperature – molecular weight diagrams for (a) amorphous and (b) moderately crystalline polymer (with highly crystalline polymers the glass transition is less apparent)

It is instructive to consider briefly the three states and then to consider the processes which define the transition temperatures. In the solid state, the polymer is hard and rigid. Amorphous polymers, under discussion in this section, are also transparent and thus the materials are glass-like and the state is sometimes referred to as the glassy state. Above the glass transition temperature the molecular has more energy and movement of molecular segments becomes possible. It has been established that, above a given molecular weight, movement of the complete molecule as a unit does not take place. Flow will occur only when there is a co-operative movement of the molecular segments. In the rubbery range such co-operative motion leading to flow is very limited because of such features as entanglements and secondary cross-linking

Whether or not a polymer is rubbery or glass-like depends on the relative values of t and τ_m. If t is much less than τ_m, the orientation time, then in the time available little deformation occurs and the rubber behaves like a solid. This is the case in tests normally carried out with a material such as polystyrene at room temperature where the orientation time has a large value, much greater than the usual time scale of an experiment. On the other hand if t is much greater than τ_m there will be time for deformation and the material will be rubbery, as is normally the case with tests carried out on natural rubber at room temperature. Thus a material which shows rubbery behavior in normal tensile tests could appear to be quite stiff if it were subjected to very high frequency vibrational stresses.

The rate constant τ_m is a measure of the ease at which the molecule can uncoil through rotation about the C-C or other backbone bonds. This is found to vary with temperature by the exponential rate constant law so that

$$\tau_m = Ae^{E/RT} \tag{2.1}$$

Equation2.2 is obtained.

$$D_{HE}(t) = D_{HE}(\infty)\left[1 - \exp\left(\frac{-t}{Ae^{E/RT}}\right)\right] \tag{2.2}$$

In effect this equation indicates that the deformation can be critically dependent on temperature, and that the material will change form a rubbery to a glass-like state over a small drop in temperature. Frith and Tuckett have illustrated (**Figure 2.2**) how a polymer of τ_m = 100 sec at 27 °C and an activation energy E of 60 kcal will change from being rubbery to glass-like as the temperature is reduced from about 30°C to about 15°C. The time of stressing in this example was 100 s.

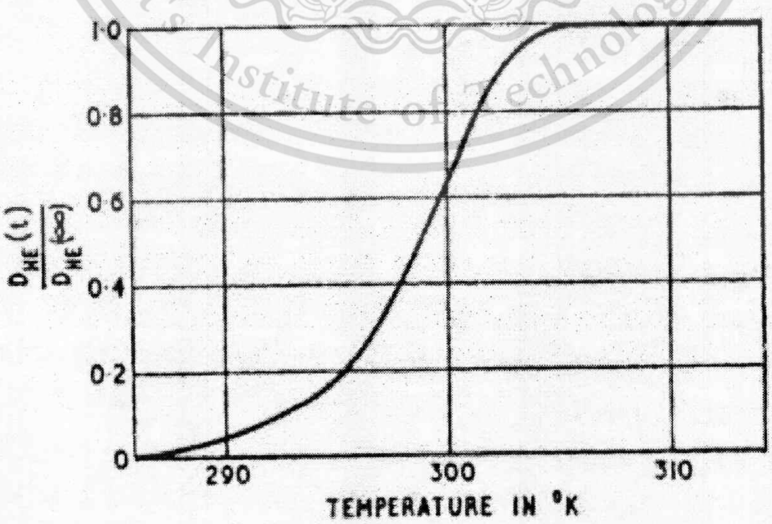

Figure 2.2 The ratio $D_{HE}(t)/D_{HE}(\infty)$ and its variation with temperature. (After Frith and Tuckett, reproduce by permission of Longmans, Green and Co. Ltd.)

2.1.1 Orientation in amorphous polymers

If a sample an amorphous polymer is heated to a temperature above its glass transition point and then subjected to a tensile stress the molecules will tend to align themselves in the general direction of the stress. If the mass is the cooled below its transition temperature while the molecule is still under stress the molecules will become frozen whilst in an oriented state.

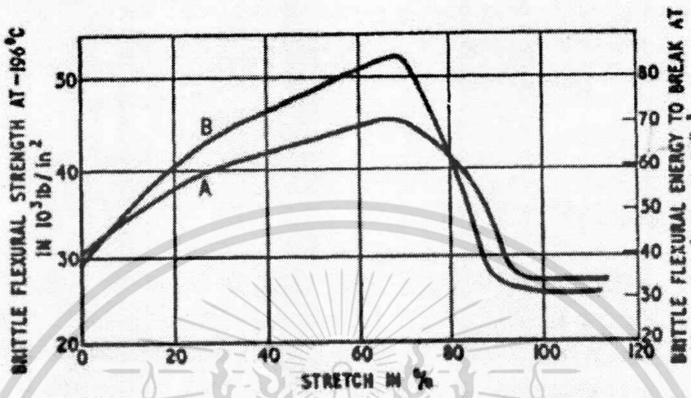

Figure 2.3 Biaxial orientation of polymethyl methacrylate. Variation of (a) brittle flexural strength and (b) brittle flexural energy with percentage stretch. (After Ladbury)

In addition to monoaxial orientation, biaxial stretching of amorphous polymers is possible. For example if poly(methyl methacrylate) sheet is heated above its glass temperature and stretched in two directions simultaneously there will be a planar disposition of the molecules. It has been found that with poly(methyl methacrylate) sheet such properties as tensile strength and brittle flexural strength increased with increased with increased orientation up to a percentage stretch of about 70% (**Figure 2.3**). Above this value there is a decrease in the numerical value of these properties, presumably due to the increase in flaws between the layers of molecules. Properties such as impact strength (**Figure 2.4**) and solvent crazing resistance, which are less dependent on these flaws than other properties, continue to improve with increased orientation.

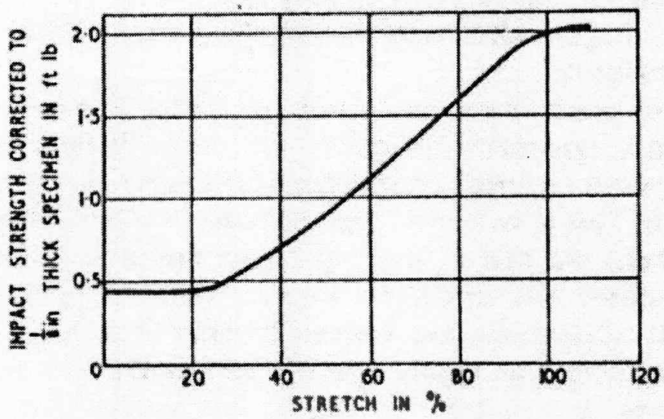

Figure 2.4 Biaxial orientation of polymethyl methacrylate. Variation of impact strength with percentage stretch. (After Ladbury)

In addition to the deliberate monoaxial or biaxial orientation carried out to produce oriented filament or sheet, orientation will often occur during polymer processing whether desired or not. Thus in injection molding, extrusion the shearing of the melt during flow will cause molecular orientation. If the plastic will contain frozen-in orientation with built-in, often undesirable, stresses. It is in order to reduce these frozen-in injection moulding. In the manipulation of poly(methyl methacrylate) sheet to form baths, light fittings and other objects biaxial stretching will frequently occur. Such acrylic products produced by double curvature forming will revert completely to the original flat sheet from which they were prepared if they are heated above their glass transition temperature

2.1.2 Acrylonitrile-butadiene-styrene polymers

ABS (acrylonitrile-butadiene-styrene) polymers are elastomeric and thermoplastic composites (qv) that exhibit excellent toughness and good dimensional stability (qv). The elastomeric component, usually polybutadiene or a butadiene copolymer, of styrene and crylonitrile (SAN). Grafying a styreane-acrylonitrile copolymer onto the elastomer permits the presence of a distinct rubber phase in a sufficiently compatible state. The flexibility in composition offered by the use of a three-monomer system combined with the option to alter molecular weight, degree of grafting, and rubber particle size and morphology allows the tailoring of properties to meet specific product needs. Consequently, ABS polymers provide one of the broadest selections of properties.

2.1.2.1 Polymer Properties

2.1.2.1.1 Melt flow

Factors influencing melt flow behavior include: (3) the presence of the grafted rubber domains, their weight fraction, graft to rubber ratio, particle size and distribution; the composition, molecular weight and molecular-weight distribution of the matrix; (4) additive, ie, lubricants, stabilizers, fillers, pigments, etc; (5) residual components from the polymerization process; and (6) water. The presence of the grafted rubber increases viscosity; the viscosity effect increases with decreasing shear rates and increasing rubber content. The rheological behavior of ABS has been discussed in the literature (7-10). Residual volatile components and lubricants can function as diluents to reduce viscosity. It has been suggested that their influence on viscosity may depend on whether such materials preferentially reside in the rubber or matrix phase (11).

2.1.2.1.2 Gloss

ABS plastics offer broad aesthetic choice. Surface gloss ranges from low mat finishes at <10% (60° Garner) to very high gloss in excess of 95%. Gloss values are determined experimentally as the fraction of incident light secularly reflected from a polished surface; measurements are conducted at a specified angle, since reflectance is a function of the angle of incidence. Gloss is determined by the number of disruptions and irregularities on the sample surface and is dependent on the specific grade and the mold or polishing roll finish.

2.1.2.1.3 Electron microscopy

Electron microscopy(qv) can be used to determine the size and distribution of the rubber domains. Image contrast between the rubber domain and surrounding matrix may be enhanced by treatment of the sample with osmium tetroxide, which adds to unsaturated polymeric regions. Example of various types of morphology observable by transmission electron microscopy are illustrated in **Figures 2.5** and **2.6**. **Figure 2.5** illustrates rubber domains obtained with a grafted emulsion substrate. Rubber domains characteristic of a suspension process are illustrated in **Figure 2.6**. Scanning electron microscopy can also be used in determining the morphology of ABS polymers by directly examining the surface of bulk samples. The rubber component is first etched out by treatment of the sample with an oxidizing agent to reveal a characteristic topography, as shown in **Figure 2.7**.

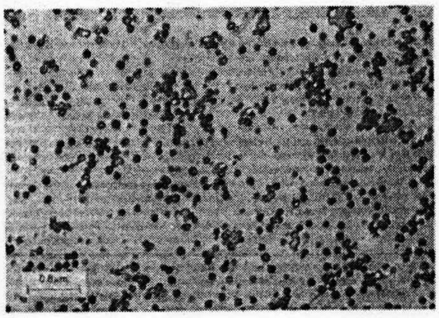

Figure2.5 Transmission electron micrograph of an emulsion-prepared ABS. Typically emulsion rubber domain little occluded copolymer of styrene and acrylonitrile

Figure2.6 Transmission electron micrograph of a suspension-prepared ABS. Typically rubber domain in suspension-derived polymer contain susstantial amounts of occluded copolymer of styrene and acylonitrile

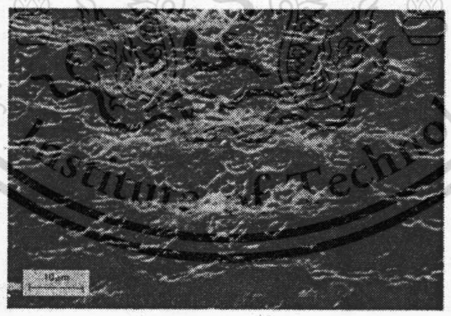

Figure2.7 Scanning electron micrograph of a suspension-prepared ABS. Surface relief is provided by etching out the rubber component

2.2 Crystalline polymers

If a polymer molecule has a sufficiently regular structure it may be capable of some degree of crystallization. In this study, the example of crystalline polymers is acetal resin (see in **2.2.1**).

From a brief consideration of the properties of the above three polymers it will be realized that there are substantial differences between the crystallization of simple molecules such as water and copper sulphate and of polymers such as polyethylene. The lack of rigidity, for example, of polyethylene indicates a much lower degree of crystalline than in the simple molecules. In spite of this the presence of crystalline regions in a polymer has large effects on such properties as density, stiffness and clarity.

The essential difference between the traditional concept of a crystal structure and crystalline polymers is that the former is a single crystal whilst the polymer is polycrystalline. By a single crystal is mean a crystalline particle grown without interruption from a single nucleus and relatively free from defects. The term polycrystalline refers to a state in which clusters of single crystal are involved, developed from the more or less simultaneous growth of many nuclei. The resulting conglomerate may possess no readily discernible symmetry. Polycrystalline occurs not only in polymers but also metals and, unless care is taken, in the large-scale commercial crystallization of materials such as sucrose and sodium chloride.

There have been, over the years, profound changes in the theories of crystallisation in polymers. For many years it was believed that the crystallinity present was based on small crystallites of the order of a few hundred Angstrom units in length. This is very much less than the length of a high polymer molecule and it was believed that a single polymer molecule actually passes through several crystallites. The crystallites thus consisted of a bundle of segments from separate molecules which had packed together in a highly regular order. The method of packing was highly specific and could be ascertained from X-ray diffraction data. It was believed that in between the crystallites the polymer passed through amorphous regions in which molecular disposition was random. Thus there is the general picture of crystallites embedded in an amorphous matrix (**Figure 2.8**). This theory known as the fringed micelle theory or fringed crystallite theory helped to explain many properties of crystalline polymers but it was difficult to explain the formation of certain larger structures such as spherulites which could posses a diameter as large as 0.1 mm.

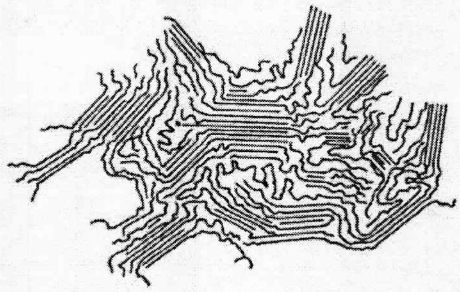

Figure 2.8 Two-dimensional representation of molecules in a crystalline polymer according to the fringed micelle theory showing ordered regions (crystallites) embedded in an amorphous matrix. (Afer Bryant)

As a result of work based initially on studies of polymer single crystals, it became realized that the fringed micelle theory was not entirely correct. It was found that in many circumstances the polymer molecules folded upon themselves at intervals of about 100 Å to form lamellae which appear to be the fundamental units in a mass of crystalline polymer. Crystallisation spreads by the growth of individual lamellae as polymer molecules align themselves align themselves into position and start to fold. For a variety of reasons, such as a point of branching or some other irregularity in the structure of the molecule, growth would then tend to proceed in many directions. In effect this would mean an outward growth from the nucleus and the development of spherulites. In this concept it is seen that a spherulite is simply caused by growth of the initial crystal structure, whereas in the fringed micelle theory it is generally postulated that formation of a spherulite required considerable reorganization of the disposition of the crystallites. Both theories are consistent with many observed effects in crystalline polymers. The closer packing of the molecules causes an increased density. The decreased intermolecular distances will increase the secondary forces holding the chain together and increase the value of properties such as tensile strength, stiffness and softening point. If it were not for crystallization, polyethylene would be rubbery at room temperature and many grades would be quite fluid at 100ºC.

The properties of a given polymer will very much depend on the way in which crystallization has taken place. A polymer mass with relatively few large spherulitic structures will be very different in its properties to a polymer with far more, but smaller, spherulites. It is thus useful to consider the affecting the formation of the initial nuclei of the nuclei for crystallization (nucleation) and on those which affect growth.

Homogeneous nucleation occurs when, as a result of statistically random segmental motion, a few segments have adopted the same conformation as they would have in a crystallite. At one time it was considered that the likelihood of the formation of such nuclei was greatest just above the transition temperature whilst the rate of growth was greatest just below the melting point. This provided an explanation of the common observation that the overall crystallization rate is greatest at a temperature about half-way between the glass transition temperature and the melting point. It is, however, now believed that both nucleation rates and growth rates are dependent on temperature in the same way so that the overall crystallization rate- temperature curve is of the same from as the nucleation-temperature and growth-temperature curve (**Figure 2.9**). By definition no crystallization occurs above the melting point.

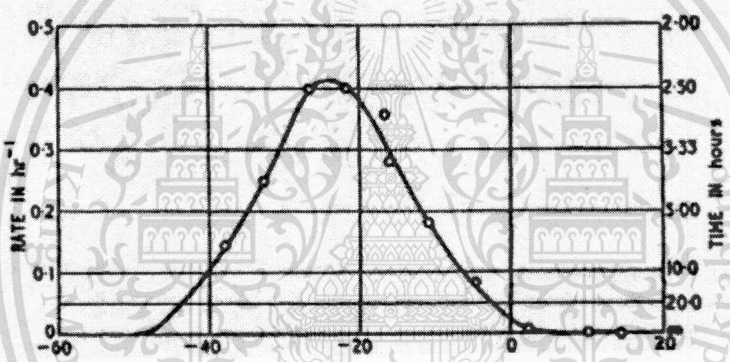

Figure 2.9 Rate of crystallisation of natural rubber as a function of temperature. (After Wood)

There are certain differences between the properties of a polymer crystallized under conditions of high nucleation/growth ratios as compared with those made under the opposite conditions. In the latter case the polymer develops large crystal structures which may be sufficiently large to interfere with light waves and cause opacity. It may also be somewhat brittle. In the former case the polymer mass, with smaller structures, is generally more transparent. The properties of the polymer will also depend on the time available for cooling. In the case of a polymer such as the bis-phenol A polycarbonate the glass temperature is about 140 ºC. There is in this case little time for crystallization to develop in cooling from the melt after injection moulding and extrusion and transparent polymers are usually obtained.

Mention may be made of the effect of the glass transition on the properties of a crystalline polymer. In a high crystalline polymer there is little scope for segmental motion since most of the segment are involved in a lattice formation in which they have low mobility. Such polymers are comparatively rigid in the mass and there is little difference in properties immediately above and below the glass transition. In fact with highly crystalline polymers it is difficult to find the glass temperature. With less crystalline materials some distinction may be possible because of the greater number of segments in a less organized state. Thus above the glass transition point the polymer may be flexible and below it quit stiff.

2.2.1 Orientation and Crystallisation

If a rubbery polymer of regular structure (e.g nature rubber) is stretched, the chain segment will be aligned and crystallization is induced by orientation. This crystallization causes a pronounced stiffening in natural rubber on extension. The crystalline structures are meta stable and on retraction of the sample they disappear.

Much of the success of the poly(ethylene terephthalate) bottle has arisen from the control of the biaxial orientation that occurs during manufacture to give a product both strong and of low gas permeability. In this study, the material of Crystalline polymers is Acetal resin(see in **2.2.2**).

2.2.2 Acetal Resins

Acetal resins are the family of polymers derived primarily from formaldehyde and therefore have a repeat unit, $(CH_2\text{-}O)_n$. The homopolymers are completely characterized by this repeat unit and the name polyoxymethylene is more structurally descriptive. Acetal copolymers have the oxymethylene structure occasionally interrupted by the comonomer unit. The designation aldehyde polymers (qv) generally refers to polymers of aldehydes larger than formaldehyde.

The successful development of these engineering resins is better appreciated it if one considers the modes of degradation that had to be overcome. These have been summarized and include unzippering from the chain ends to yield monomer formaldehyde, oxidation and chain scission followed by depolymerization, acidic attack on the acetic chain, and thermal scission, which occurs above 270 °C (12). Stabilization (qv) to prevent or limit these modes of degradation was essential to the commercial development of acetal resins. Throughout this discussion, the homo-polymers and copolymers referred to are generally DuPont's Delrin and Celanese's Celon, respectively.

2.2.3 Physical properties

Acetal resins are produced from either formaldehyde or its cyclic trimer, trioxane. Formaldehyde is a well-known, widely used commodity chemical. At room temperature, it is a colorless, pungent gas that is highly irritating to the mucous membranes of the eyes, nose, and throat. Formaldehyde is not commercially available in the anhydrous monomeric from, and is usually sold in aqueous solution, with methanol added as an inhibitor. Trioxane is the anhydrous trimer of formaldehyde. Trioxane is the anhydrous trimer of formaldehyde. It is a white, crystalline solid with a pleasant etherlike aroma unlike that of formaldehyde. Trioxane is soluble in alcohols and ethers and will also dissolve in water without depolymerization to formaldehyde. Both formaldehyde and trioxane are flammable. **Table 2.1** lists the physical properties of each.

Table 2. 1 Properties of Formaldehyde and Trioxane

Property	Formaldehyde	Trioxane	Refs.
Molecular weight	30.03	90.08	
formular	CH_2O	$C_3H_6O_3$	
Density, g/cm^3			
-20 °C	0.815		13
10 °C		1.17	14
Normal boiling point, °C	-19	114.4	15,16
Melting point, °C	-118	62	14,15
Vapor pressure, Antoine constants,			
Pa[a]	9.28176	10.040	
A	959.43	1849.920	16,17
B	243.392	253.270	
C			
Heat of vaporization at normal			
Boiling point, kJ/mol[b]	23.3	42.0	14,15
Heat of combustion, kJ/mol[b]	561	1488	14,18
Critacal constants[c]			
Temperature, °C	137.2	331.4	
Pressure, MPa[d]	6.784	5.797	
Flammability in air			
Lower/upper limit,vol%	7.0/7.3	3.6/29.0	19
Ignition temperature, °C	430	413.9	19

Table 2. 1 Properties of Formaldehyde and Trioxane (con.)

Property	Formaldehyde	Trioxane	Refs.
a Log10 P = A-B/(C+T); where T = ?C; To convert Pa (kPa) to mmHg, multiply by 0.0075 (7.5). b To convert J to cal, divide by 4.184. c Estimated by methods in refs. 20 and 21. d To convert MPa to psi, multiply by 145.			

2.2.4 Chemical properties

Formaldehyde is extremely reactive with itself and with other chemicals. It is readily soluble in water, with which it immediately reacts to form methylene glycol, $CH_2(OH)_2$, and poly (oxymethane) glycol, $HO\text{-}(CH_2O\text{-})_nH$. It can oxidize to formic acid, and in aqueous alkali, the Cannizzaro auto oxidation = reduction reaction may produce both formic acid and methanol (22).

At ambient temperatures, pure formaldehyde gas polymerizes slowly, yielding a white solid; traces of water markedly increase the polymerization rate. Polymerization of the dry gas can be avoided by maintaining the temperature above 100 °C.

Trioxane is chemically stable; pure material shows little decomposition at 224°C (23). Trioxane readily depolymerizes to monomeric formaldehyde in an acid environment at elevated temperatures.

2.2.5 Manufacture

Formaldehyde is manufactured from methanol. In a typical process, methanol and air are passed across a catalyst bed, consisting of a silver or a metaloxide catalyst (24). The reactor product, consisting of formaldehyde, unconverted methanol, and the by-product, carbon monoxide and dioxide, methyl formate, and formic acid, is cooled and then scrubbed with water in an absorption tower. The aqueous product is then purified by distillation.

Anhydrous formaldehyde used in the manufacture of acetal homopolymer must be extremely pure. Even very low concentrations of residual formic acid or hydroxyl compounds, such as water and methanol, in the monomer can result in unacceptably low molecular weight in the finished product; great care is taken to eliminate these species in monomer production. In order to obtain the necessary purity, the formaldehyde process is modified to scrub the product gases with cyclohexanol in a series of columns. The formaldehyde is absorbed and forms cyclohexyl hemiformal with the cyclohexanol (25). Residual formaldehyde and cyclohexanol carried over from the absorption columns are scrubbed out by water before the remaining gases are discharged. The cyclohexanol from the absorption columns containing the hemiformal, along with some water and methanol, is sent to a distillation column in which the water-cyclohexanol azeotrope and methanol are removed overhead at 95 °C. Bottoms from this column are then sent to a pyrolysis column, where they are heated to 160 °C in order to decompose the hemiformal; formaldehyde gas goes overhead. Removal of trace cyclohexanol and any remaining water is accomplished by condensation after chilling the formaldehyde gas to 1 °C. The purified monomer must then be introduced to the polymerization reaction immerdiately.

Acetal copolymer is commonly produced from trioxane, which is made from aqueous formaldehyde in the presence of a strong acid catalyst. Dilute formaldehyde solution is concentrated to 60% and introduced into the reactor, which contains 6 wt% sulfuric acid. The product is then distilled; a trioxane-formaldehyde-water azeotrope is taken overhead and the residue returned to the reactor. Extraction of the distillate with solvents, such as benzene or methylene chloride, separates the trioxane from the water and most of the formaldehyde. The dilute formaldehyde solution is send to recovery; separation of the trioxane from the solvent is accomplished by distillation. If necessary, the trioxane can be further purified by another distillation and treatment with molten sodium (26).

2.3 Injection molding

Injection molding produces parts in large volume at high production rates. Labor costs per unit are low and the process can be automated. The parts require little or no finishing and many different surface finishes and colors are available. The same article can be molded into different materials on the same equipment. Close tolerances can be maintained. Parts can be molded in a combination of plastic and fillers, eg, glass, asbestos, talc, and carbon; metallic and nonmetallic pieces can be inserted.

The process permits the manufacture of very small parts which are almost impossible to fabricate in quantity by other methods. Scrap losses are minimal, as runners, gates, and rejects can be reground and reused. Aside from die casting, it is the only commercial process where the scarp can be reused immediately by regrinding and remolding at the machine. Since energy costs are low, this process is the most economical way to fabricate many shapes.

2.3.1 Injection molding machines

A reciprocating-screw injection-molding machine with a clamping capacity of 300t and a 6.35-cm ($2\frac{1}{2}$-in.) reciprocating screw delivers a maximum of ~570 g (20 oz) of polystyrene per shot (see **Figure. 2.10**). The machine clamps the mold halves together, raises the temperature of the plastic to a point where it flows under pressure, injects the hot plastic into the mold, cools the plastic in the mold, opens the mold and ejects the hardened plastic piece.

The injection-molding machine performs these functions automatically under controllable temperature, time, speed, and pressure. Molecular structure, molecular weight, and molecular-weight distribution (all of which control melt viscosity), ortentation of the polymer molecules, and crystallizability play important roles in the process and must be considered for their effect on product properties.

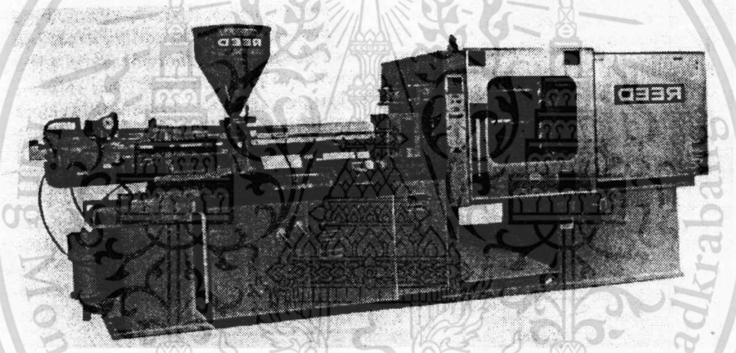

Figure2.10 A 300-t injection-molding machine with a 6.35-cm reciprocating screw. Courtesy of Reed-Prentice Division, Package Machinery Company

The injection end of the first commercial injection-molding machine was a plunger. It consists of a very heavy steel tube with a nozzle threaded into one end. The outside of the nozzle has a radius which fits into the reverse radius of the sprue bushing of the mold. The melts plastic material is forced into a small hole (3-9.5 mm) by the plunger.

The inside of the tube is taken up by a steel spreader or torpedo which distributes the material around the inside wall. The tube, called a heating cylinder, is heated by electrical resistance heaters (heating bands) and controlled by thermocouples attached to pyrometers. The plunger is a round steel bar that pushes the cold material from the open end of the cylinder toward the hot nozzle end. It is volumetrically fed through a hole in the top rear of the cylinder.

In plunger machines, both melting and injection take place in the same location, although each has different and opposing mechanical requirements. The first revolution in machine design separated the two functions by using two cylinders. The first cylinder, used for melting, is mounted at 45 or 90° to the second or shooting cylinder or pot. The pot is a small-bore plunger cylinder without the torpedo. The two cylinders are connected by a valve. When the valve is open, the melting or plasticizing cylinder pushes the material into the nozzle end of the pot, forcing the plunger back. When the plunger moves back an experimentally predetermined distance, filling stops and the valve closes because the return motion of the plunger contacts a limit switch. At the appropriate time in the cycle, the material is injected into the mold from the second cylinder, the so-called pot. This operation improves the mixing of the plastics, equalizes the temperature, and gives better control of speed, pressure, and material.

This type of machine is called a preplasticizing machine. Of the equipment in use today, 95% is preplasticizing, either with a reciprocating screw (**Figure.2.10**) or a screw-pot (**Figure.2.11**). In a reciprocating screw, the melted material is collected in front of the screw which continues to move backward as more material is melted. The area where the melted material is collected corresponds to the pot in a two-stage machine. A check valve (non return valve) is closed when the screw is pushed forward by the injection cylinders. At this time, the screw and non return valve act like a plunger.

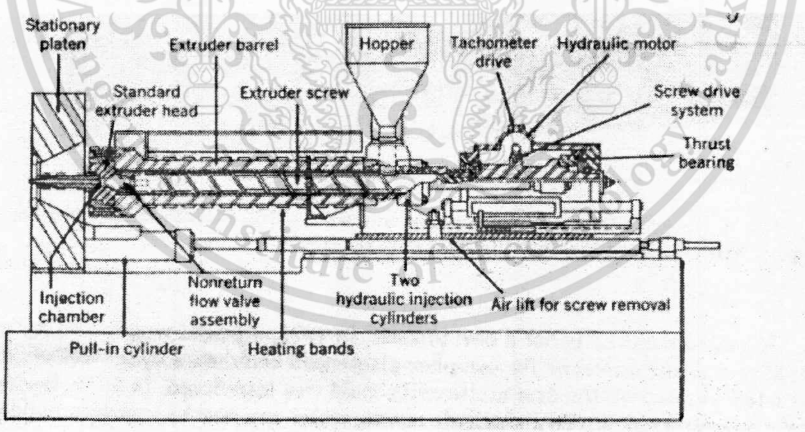

Figure.2.11 Reciprocating-screw machine, injection end. Courtesy of HPM Division of Koehring Company.

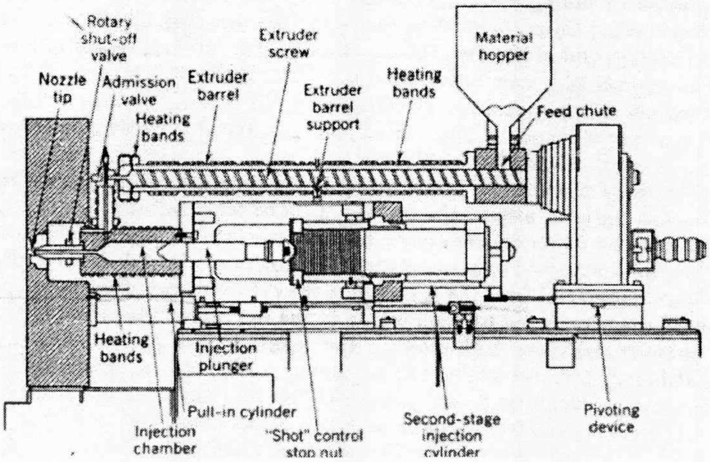

Figure.2.12 Two-stage screw-plunger machine. Courtesy of HPM Division of Koehring Company.

The plunger machine heats the material by conduction. Since plastic is an insulator, the material next to the outside wall is much hotter than that near the centre. The laminar flow in the plunger-type cylinder does not reduce the temperature differential. This produces residual stresses in the molded parts which can be very troublesome. The plunger machine is used now only for producing special effects, eg, for mottling: the two-stage plunger is also obsolete.

The second revolution in machine design was the reciprocating screw where the material is melted by the heat generated internally by the friction of molecules rubbing over each other throughout the plastic. The screw is an excellent mixer and quickly replaced the plunger machine.

The last significant change in machine design is the computer-controlled machine with feedback which further improves operation, productivity, and product quality.

Hydraulic molding-machine circuits have not changed in the last 50 years. For a description of hydraulic components, circuits, and nonsolid-state electrical circuits, see **Ref.1**.

2.3.2 Reciprocating-Screw Injection-Molding Machines

A hydraulic clamping system is shown in **Figure 2.12.** In order to minimize cost and power consumption, small-diameter cylinders (not shown) move the large clamp rapidly, using a prefill valve and gravity to force oil behind the large clamp ram. The injection end of an in-line reciprocating-screw plasticizing unit is shown in **Figure.2.10.** The ejection side of the mold is clamped to the moving platen. The cavity side is clamped to the stationary platen. The empty space of the mold is filled with melted plastic under high pressure.

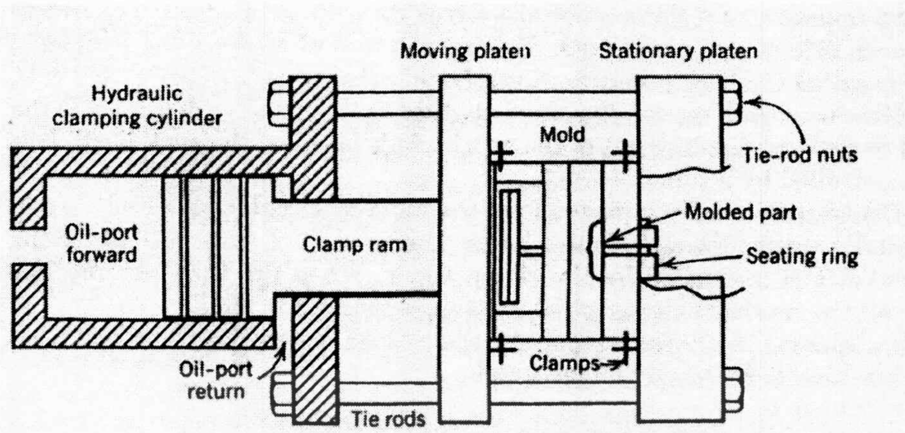

Figure 2.13 Hydraulic clamping system. time, temperature, and pressure controls are not shown.

The moving platen rides on four steel bars called tie rods or tie bars. The clamping force is generated by the hydraulic mechanism pushing against the moving platen and stretching the tie rods.

The molding process for reciprocating screw machine with hydraulic clamps includes the following steps:

1. Granulated plastic material is put into the hopper.

2. Oil is sent behind the clamp ram which moves the moving platen, closing the mold. The pressure behind the clamp ram builds up, developing enough force to keep the mold closed during the injection cycle. If the force of the plastic material is greater than the clamp force, the mold opens, an unacceptable condition causing plastic to flow past the parting line on the surface of the mold producing flash, which must be removed or the piece rejected and reground.

3. The two hydraulic injection cylinders, one on each side of the screw, bring the screw forward, injecting previously melted material into the mold cavity. The injection pressure is maintained for a predetermined length of time. A valve at the tip of the screw prevents material from leaking into the screw flights during injection. It opens when the screw is turning and melting material, permitting the plastic to flow in front of it to force the screw back.

4. The oil velocity and pressure in the two injection cylinders are high enough to fill the mold as quickly as needed and maintain sufficient pressure to mold a part free from marks, welds, and other defects.

5. As the material cools, it becomes more viscous and solidifies to the point where injection pressure is no long.

6. The material is melted primarily by the turning of the screw which converts mechanical energy into heat. It also absorbs heat from the heating bands on the plasticizing cylinder (extruder barrel). As the material melts, it moves forward along the screw flights to the front end of the screw. The pressure generated by the screw on the material force the screw, screw drive system, and the hydraulic motor back, leaving a reservoir of plasticized material in front of the screw. The screw continues to turn until the rearward motion of the injection assembly touches a limit switch stopping the rotation. This limit switch is adjustable, and its location determines the amount of material that remains in front of the screw (the size of the shot)

The pumping action of the screw slight also forces the hydraulic injection cylinders (one on each side of the screw) back. This return flow of oil from the hydraulic cylinder is called the back pressure; it can be adjusted 2.75 MPa (400 psi).

7. Most machines retract the screw slightly at this point to decompress the material to prevent drooling out of the nozzle. This is called the suck back; it is usually controlled by a timer

8. Heat is continually removed from the mold by circulating a cooling medium (usually water) through drilled holes. The amount of time needed for the part to solidify is controlled by the clamp timer. When the time expire, the movable platen returns to its original position, opening the mold.

9. An ejection mechanism separates the molded plastic part from the mold and the machine is ready for the next cycle.

The back safety gate is removed showing the operator lifting molded parts from a molding machine; the four tie bars upon which the movable platen rides are visible. The rubber hoses circulate fluid for temperature control. The temperature for each cavity and core can be controlled separately. The mold is held on the platen by clamps.

2.3.3 Closing system

2.3.3.1 Toggle clamping

A type clamping unit include various designs. An actuator moves the crosshead forward, extending the toggle links to push the moving platen toward a closed position. At the beginning of the movement, mechanical advantage is low and speed is high; but near the end of the stroke, the reverse is true. Thus, toggle clamps provide both high speed and high force at different points in the cycle when they are desirable. They are actuated either by hydraulic cylinders or ball screws driven by electric motors. Toggle-clamp units seem most suited to relatively low-tonnage machines.

2.3.3.2 Hydraulic clamping

Hydraulic clamping is used on higher-tonnage injection molding machines, typically in the range 1300 to 8900 kN (150 to 1000 tons). These units are also more flexible than toggle clamps in terms of setting the tonnage at given positions during the stroke.

Hydraulic Clamping System is using the direct hydraulic clamp of which the tolerance is still and below 1 %, of course, better than the toggle system. In addition, the Low Pressure Protection Device is higher than the toggle system for 10 times so that the protection for the precision and expensive mold is very good. The clamping force is focus on the central for evenly distribution that can make the adjustment of the mold flatness in automatically.

2.3.4 Heating and Cooling system

Heating and cooling system is controlling stream pressure about 4-10 bar. It increased rapidly high temperature between 140 $^{\circ}$C – 180 $^{\circ}$C (see in **Table 2.2**). In rapid heat temperature (higher than heat distortion temperature), melting plastic flow well. The produce is high gloss. Then the system reduce rapid high stream out of mould and fill up cool water into mould. The products can be eject.

Table 2.2 water boiling point and pressure

Absolute Pressure (bar)	Boiling point (C)	Density (steam) (kg/m^3)	Specific enthalpy of steam (total heat)	Latent heat of vaporization	Specific heat (kJ/kg)
1	99.63	639.02	2257.92	539.3	2.0267
1.5	111.37	643.3	2226.23	531.73	2.0768
2	120.23	646.39	2201.59	525.84	2.1208
2.4	126.09	648.36	2184.91	521.86	2.1531
3	133.54	650.77	2163.22	516.68	2.1981
3.5	138.87	652.44	2147.35	512.89	2.2331
4	143.63	653.87	2132.95	509.45	2.2664

Table 2.2 water boiling point and pressure (con.)

Absolute Pressure (bar)	Boiling point (C)	Density (steam) (kg/m^3)	Specific enthalpy of steam (total heat)	Latent heat of vaporization	Specific heat (kJ/kg)
4.5	147.92	655.13	2119.71	506.29	2.2983
5	151.85	656.24	2107.42	503.35	2.3289
5.5	155.47	657.23	2095.9	500.6	2.3585
6	158.84	658.13	2085.03	498	2.3873
6.5	161.99	658.94	2074.73	495.54	2.4152
7	164.96	659.69	2064.92	493.2	2.4424
7.5	167.76	660.37	2055.53	490.96	2.469
8	170.42	661	2046.53	488.8	2.4951
8.5	172.94	661.58	2037.86	486.73	2.5206
9	175.36	662.11	2029.49	484.74	2.5456
9.5	177.67	662.61	2021.4	482.8	2.5702
10	179.88	663.07	2013.56	480.93	2.5944

http://www.engineeringtoolbox.com/saturated-steam-properties-d_457.html

1. The instructor of rapid heating and cooling system

1.1 System use computer for controlling Programmable Logic Control (PLC). PLC is control system that controls temperature, flow rate and pressure (see in **Figure2.13(a)**)

1.2 Controllable of valve is feeding hot water into mould. The actual temperature is read by thermocouples that were installed in the mould. For this system can control hot and cool water flow in injection process (see in **Figure2.13(b)**).

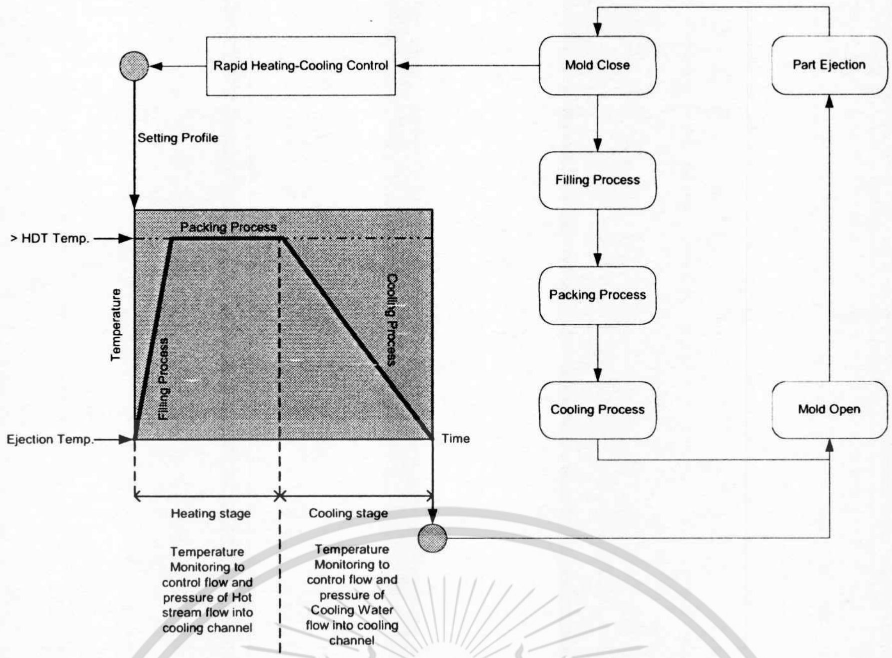

(a)

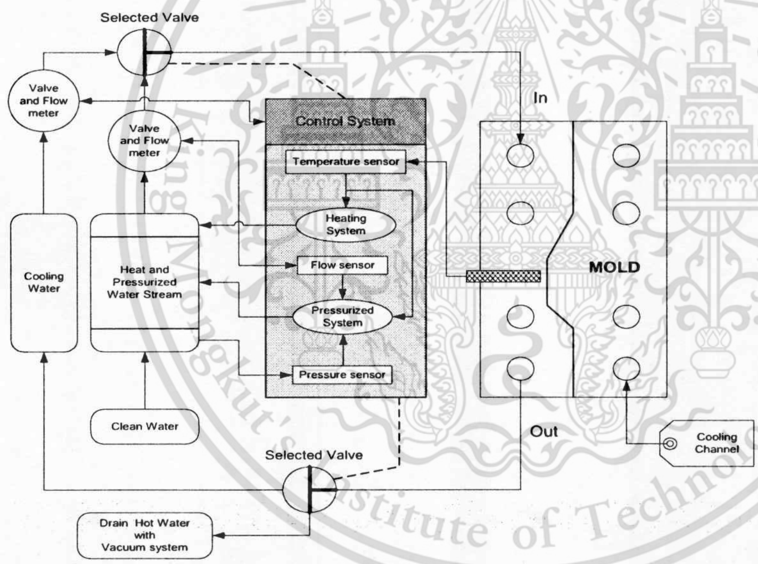

(b)

Figure2.14 (a) heating and cooling in injection moulding process (b) heating and cooling control system.

2.4 Statistical Process Control

The recent trend toward total quality management (TQM) has generated a great deal of interest in statistical process control (SPC). This technique has been applied with good success in the discrete part manufacturing industries. In the injection process industries, experiment has been mixed, partly because of misunderstandings about its applicability to chemical process and its interrelation to conventional process control. We introduce SPC here because it is a technique of single-loop control (although the loop is closed by manual interrention). Our aim is to introduce the subject, but, more importantly, to discuss its applicability in the chemical process and, specifically, polymer industries.

In many cases of batch and semibatch polymerizations, the only measurements of the end-use properties are at the end of the batch. As discussed previously, these are often off-line, laboratory analyses. Often the same is true for the product quality variables. An example from the synthetic rubber industry is the Mooney viscosity of the rubber. An example from the synthesis rubber industry is the Mooney viscosity of the rubber. Neither the Mooney viscosity (end-use property) nor its underlying product quality variables (MWD and degree of branching or cross-linking) is measured on-line. In fact, in some cases, the polymer quality variables are not measured at all on a regular basis because release specifications are written in terms of Mooney viscosity. In this situation, closed-loop control of Mooney viscosity is impossible. However, Because the measurement of variables to be controlled (end use or polymer quality) are substantially uncorrelated in time, the use of SPC is appropriate likewise, in continuous polymerizations, the end use and polymer properties variables may be measured very infrequently and, most often, offline. In addition, the laboratory analysis time adds a large delay to the measurement. Under these circumstances, the measurements are substantially uncorrelated in time, and, again, statistic process control may be an appropriate approach to control of polymer quality or end-use properties.

2.5 Measurement of Temperature

In injection molding process, the temperature of the reacting mass is the most importance. The temperature-time profile is essential. Most polymerization are exothermic and require maintenance of reaction temperature for reasons of process safety, if for no other. More typically, however, the reaction temperature influences final polymer properties and, therefore, must be regulate.

In general, temperature measurements for polymerization reactions are made with the same instrumentation that is generally used in the industry. Three classes of instruments are normally used: thermocouples, resistance thermometers, and filled-bulb thermometers. All of these devices display dynamic responses which can be characterized by a first-order lag model without dead time. The time constants for these devices are typically in the range shown in **Table2.3**.

Table2.3 Dynamics of Temperature Measurement

Device	Time constant(sec)
Thermocouple	30-60
RTD	< 5
Filled Bulb	60-120

2.6 Measurement of Pressure

Measurement of pressure is important in many polymerization processes. Typically in exothermic closed reactor systems, pressure is monitored to ensure that the reactor is being safely conducted. Also, in some systems, molecular configuration and reaction rate are pressure dependent. In some special cases where reaction take place in a melt extruder, measurement of pressure at the discharge can be related to viscosity or molecular weight. Each particular polymerization has difference demands on the pressure measuring instruments in term of required precision and noise level. In general, pressure is measured by three basis techniques: liquid columns (characterized by the water or mercury manometer), mechanical sensing elements (diaphragm, bellows, or Bourdon tube), and (27) electrical or electronic methods (strain gauges, thermal conductivity gauges, or ionization gauges). Each of these methods is used for different pressure ranges and situations, but, in general, these instruments are very fast in response. In fact, most of the pressure sensor/transmitter systems which are used in industry have response time of a second or less. Compared to the process lags encountered in most plasticization, the dynamics of pressure measurement can generally be considered insignificant.

2.7 Scanning electron microscopy (28)

The scanning electron microscope provides the microscopist with images that closely approximate what the physiology of the eye and brain expect, since the depth of field for resolved detail in the scanning electron microscopy is very much greater than the spatial resolution in the field of view. That is precisely how our eyes and the visual cortex of our brains have evolved in the order to perceive the three dimensions of the 'real' world. The 'flatness' of the topological and morphological detail that is observed in the light optical or transmission electron microscope is replaced, in the scanning electron microscopy by an image that appears very similar to the play of light and shade over the hills and valleys of the countryside. These feature of the real world look remarkably like the hollows and protrusions of a three-dimensional object viewed in the scanning microscopy. Only two additional features are needs to complete this 'optical illusion'. The first is a true representation of the position of the image detail in depth, normal to the image plane. With a little extra time and effort, scanning electron microscopy (SEM) can also provide this three dimensional, depth information by recording two images from slightly different view points; a technique termed stereoscropic imaging. The second feature missing from the scanning electron microscope image when compared with 'real world' image is the presence of colour. Again, it is possible to use the capacity of the eye to recognize colour by the introduction of colour coding. Colour may be used to enhance contrast, for example when comparing different image during data process. Colour can also be used to code for crystallographic information in the morphological image.

This visual impact of scanning electron microscope image and the ability to reveal details that are displaced along the optic axis, in addition to those resolved in the two dimensional field of view of the image plane, has led to the application of SEM to all branches of science and engineering from the time it was first introduced (late 1950s). It first describe the various imaging signals that are detectable in the scanning electron microscope due to the interaction of a focused beam of high energy electron with a solid sample. The interpretation of the information that can be deried from these different signals is then described, together with some of the special techniques that are available to enhance image contrast and assist in image interpretation.

2.8 Liquids and viscosity

In **table 2.4** is a list of substances in order of increasing viscosity. Clearly, the substance become 'thicker' as we descend the Table, but, of course, it is necessary to be more quantitative than this and we shall want to know where the various polymer systems fit. This will begin to give a clue to the magnitude of the needed to shape them.

Table 2.4 List of substance: increasing viscosity

Substance	'Thickness' or 'consistency'
Air	Gaseous
Water	Fluid
Olive oil	Liquid
Glycerol	Thick liquid
Golden syrup	Syrupy liquid
Pitch	Flowing solid
Glass	Rigid solid

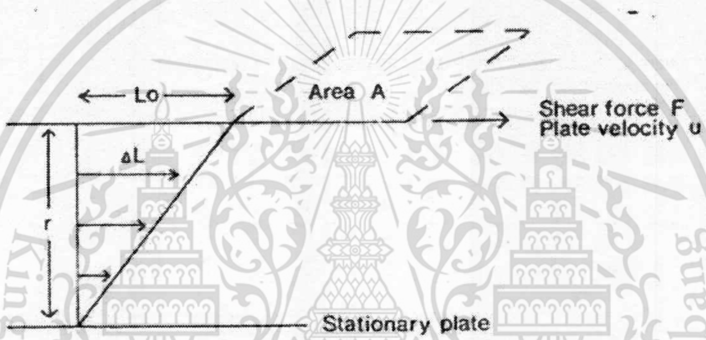

Fig 2.15 Principle of viscosity

Consider two plates (**Fig. 2.15**), separated by distance r. The space between them is occupied by the fluid. One plate moves relatively to the other with velocity U. The movement is resisted by a viscous reaction in the fluid. Since the movement is in shear the reaction is the shear viscosity. It can find the shear stress from the force, F, acting on the moving plate and its area, A.

Shear stress,

$$\tau = F / A \text{ Nm}^{-2} \tag{2.3}$$

The shear rate is found from the velocity U relative to distance, L: it is thus a derivative quantity

Shear rate,

$$\dot{\gamma} = U / L s^{-1} \tag{2.4}$$

$$\tau \propto \dot{\gamma}$$

$$\tau = \eta\dot{\gamma} \tag{2.5}$$

η, the coefficient of shear viscosity, is the proportionality constant between the shear stress and the shear rate. It now have a quantity which can be used to describe the 'thickness' or viscosity of a fluid.

2.8.1 Viscosity and polymer processing

In processing a fluid the 'input' quantity is the shear rate, i.e., the material will be moved, by whatever means is suitable, at an appropriate rate for shaping the article being made. The viscosity may be regarded (for the present) as a material constant property, and a shear stress thus develops in the fluid.

$$\tau = \eta\dot{\gamma} \tag{2.6}$$

The value of the shear stress clearly depends on the rate of shear and the viscosity of the fluid. If the fluid is of low viscosity, e.g., a paint-like or syrupy liquid, the shear stresses needed to distort it will be small.

$$\frac{\tau}{\eta} = \dot{\gamma} \tag{2.7}$$

i.e., quite low values of τ will generate high values of $\dot{\gamma}$, if η is low.

2.8.2 Shear rates of different processed

Before proceeding with a consideration of the shear rates characteristic of different manufacturing processes for polymer products it is important to remember that high rates of shear are not necessarily involved in high processing speeds, i.e., high volume throughput. The shear rate $\dot{\gamma}$ is concerned with the rate of distortion of the fluid elements.

A few examples of shear rates are displayed in **Table 2.5**. The shear rate depends principally on the nature of the shaping, fluid-distorting process, rather than the speed at which that process is run. Much less variation in $\dot{\gamma}$ will result from running the machinery slowly or fast.

Table 2.5 Shear rates of processes

Process	Shear rate (s^{-1})
Compression moulding	1-10
Calendering	10-100
Extrusion	100-1000
Injection moulding	$1000\text{-}10^5$
Reverse roll coating	3×10^3

We can now redraw **Table 2.5** to include some polymer systems, and also insert numerical values for viscosity. **Table 2.6** is the result. In the table the approximate values quoted for viscosities of polymer systems are those which would be met at processing temperature. The outstanding feature to emerge from the Table is the huge spread of values, from the water-like lattices through syrupy liquid resins to the toffee-like melts and tough rubbers. Clearly, we must expect to find a correspondingly wide variation in the shear stresses needed to shape these materials and hence in the processes and machinery required.

Table 2.6 Viscosities of various materials

Substance or system	Viscosity (MPas)	Consistency
Air	10^{-5}	Gaseous
Water	10^{-3}	Fluid
Polymer latex systems	10^{-3}-10^{-2}	Liquid
Olive oil	10^{-1}	Liquid
Paints	10^{-2}-10^{-1}	Creamy
PVC plastisols	$1^{-3}\times10^{-1}$	Paint-like
Glycerol	10	Thick liquid
Resins for resin/glass	50	Syrup
Golden syrup	10^{2}	Syrup
Liquid polyurethanes	10^{2}-10^{3}	Syrup
Polymer melts	10^{2}-10^{6}	Toffee
Rubbers before cure	10^{2}-10^{6}	Stiff plasticine
SMC,DMC (moulding	10^{2}	Dough
compounds)	10^{9}	Flowing solid
Pitch Glass	10^{21}	Rigid solid

2.8.3 Temperature variations of viscosity

It can consider the effect of viscosity variation for liquid by using the free volume concept or by reaction-rate concepts. The latter give a temperature dependence of η (for Newtonian fluids) in the form

$$\eta = B\exp(E/RT) \tag{2.8}$$

where E is an activation energy, R is the gas constant(8.314 $JK^{-1}mol^{-1}$) and T is the absolute temperature. This type of equation is often adequate to describe the variation of viscosity with temperature except over very large changes of temperature. Alternatively, equation (2.9) can be put in a form containing the density (ρ)

$$\nu = \frac{\eta}{\rho} = B' \exp(E / RT) \tag{2.9}$$

Where ν is the kinematic viscosity; this equation, because of the small variation in ρ with temperature, behaves similarly to equation (2.10). Over small ranges of temperature we can also write $\eta = \eta_0 \exp - \alpha(T - T_0)$. This expression is sometimes useful in analytical work. A better description is given by the Walther equation

$$\log_{10} \log_{10}(\nu + \alpha) = m \log_{10} T + b \tag{2.10}$$

Where a, m, and b are constants. This equation has been widely used for lubricating oils; in this case the value of a can be taken as about 0.6 to 0.8 * 10^{-6} m^2/s when ν > 1.5* 10^{-6} m^2/s, thus leaving only two disposable constants.

Another empirical equation that seems more satisfactory than the Walther equation in that it is more accurate over wider ranges of temperature is the Vogel equation.

$$\eta = A_1 \exp B_1 / (T - T_0) \tag{2.11}$$

where A_1, B_1, and T_0 are constants.

2.8.4 Pressure variations of viscosity

Batchinsky (see Vinogradov and Malkin 1977) introduced the free-volumn (V_f) concept, where

$$V_f = V - V_m \tag{2.12}$$

Here V is the specific volumn of the fluid (equal to $1/p$) and V_m is the specific volume of the molecules. The experiments of Doolittle on n-alkanes showed that

$$\eta = A' \exp(CV_m / V_f) \tag{2.13}$$

Where A and C are constants. Often $V_m \sim V$ and these quantites are interchangeable in (2.14)

For isothermal conditions we can write, for a change in density due to pressure (p),

$$V = V_0 (1 - p/K) \tag{2.14}$$

Where V_0 is the specific volume at zero pressure and K is the bulk modulus. Use of (2.14) in (2.15), noting the definition of V_f above, yields the result, when $p << K$,

$$\eta = \eta(0)\exp(p/\beta) \tag{2.15}$$

Where η (0) is the viscosity at zero pressure. This often appears to describe the variation of viscosity with pressure adequately.

2.9 Melt flow index

A convenient, simple form of extrusion capillary rheometer is the melt is the melt is the melt flow indexer, which is used to compare grades within a polymer type. In essence, it comprises a cylinder containing polymer melt which is loaded from above by a piston carrying a weight (**Figure 2.16**). There is a capillary die at the bottom of the cylinder. The procedure is to drive the melt through the die and to measure the output by cutting off sections of extrudate at known time intervals and weighing them. The die dimensions are known, and the driving weight is known, so that a single-point viscosity could be calculated. However, the melt flow index (MFI) of a polymer is quoted directly as the weight expelled, in grams, in 10 min. In BS 2782, the die dimensions specified are:Length, L= 8.00 mm;Diameter, D (a) (for MFI of 1-25) = 2.095 mm,(b) (for MFI of 25-250) = 1.180 mm.

The MFI can vary greatly between grades of a given polymer type, e.g., LDPE or HDPE or PP or PS. The principle difference between grades reflected by MFI is in molecular weight, and the MFI can be regarded as a simple index of this quantity, although it does not, of course give any guide to its absolute value. Low MFI means high molecular weight and vice versa. Thus LDPE of MFI = 20 is a low molecular weight grade. Whereas MFI = 1.0 indicates a high molecular weight polymer.

The MFI must be treated with caution. It is, after all, only a single point determination, at a not very high shear rate. It cannot be used to compare polymer types; thus MFI values for polyethene cannot be compared with those for polypropylene or polystyrene. However, it is widely used by polymer suppliers to compare grades. Difference polymers require different conditions, and standard methods specify a driving weight and a temperature for each polymer type.

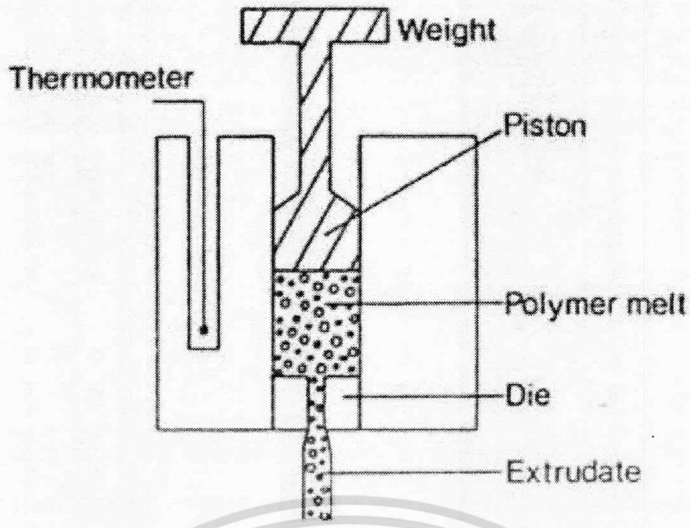

Figure 2.16 MFI apparatus

2.10 Surface modifications

When polymers slide repeatedly over smooth metal surface, their wear rates seldom, if ever, correlate directly with their bulk mechanical properties because surfaces of both polymer and counterface are modified by the sliding process to produce surfaces of both polymer layers or third-bodies. The properties of the third-bodies can be very different from those in bulk.

Insofar as changes to polymer surfaces are concerned, the molecules in the surface later frequently undergo chain scission (29) with a consequent reduction in molecular weight (30). These lower molecular weight constituents may then lead to a surface layer of lower elastic modulus, similar to those produce on elastomers during abrasive wear (31). At high sliding speeds, when interfacial temperatures increase, thermal or oxidative degradation occurs; for thermosetting polymers, this may reduce the ductility of the surface layer. Elevated temperatures also lead to structural modifications, and the disappearance of the spherulites in the surface layers of a number of crystalline thermoplastics has been noted after wear. With PTFE and high density polyethylene, sliding is also known to induce a preferred orientation of the molecular chains (32, 33). Another factor modifying polymer surfaces during sling is the incorporation of material transferred from the counterface (34). Transfer of metal fragments occurs when the subsurface strength is lower than that of the interfacial adhesive bonds and this can arise when conventional finishing treatments leave localized areas of the surface in a weakened state (35)

The two most important modifications to metal counterfaces occurring during sliding against polymers are transfer and abrasion. The successive deposition of transferred fragments gradually builds up a more-or-less uniform film on the counterface which can vary in thickness from a few nm to a few µm, depending upon the type of polymer, the initial counterface roughness, and the conditions transition temperatures and highly cross-linked structures usually tend to shear at the original sliding interface. Most thermoplastics do exhibit transfer above their T_gs, although it should be noted that the relevant T_g may differ from that of the bulk materials because of the high stresses and shear rates involved in the sliding process (36). The fragments transferred from crystalline thermoplastics are usually commensurate in size with the individual areas of real contact, but there are two notable exceptions. PTFE and high density polyethylene, which have already been noted as having low friction because of their smooth molecular profiles, transfer as extremely thin highly oriented films < 10 nm thick. This anomalous behavior, however, is restricted to a comparatively narrow range of sliding conditions and particularly to low speeds of sliding. At high speeds, molecular relaxation to permit chain orientation is inhibited and the transfer behavior becomes more normal, ie, lumpy particles rather than thin films.

The adhesion of transferred polymer fragments to a metal counterface is usually relatively weak (ie, van der Waals forces), but can increase appreciably when the sliding conditions initiate polymer degradation. The latter aspect has been extensively studied and becomes very significant for filled and reinforced polymer . There may also be an element of mechanical keying of the transferred fragments into the surface depressions on the counterface. Reductions in wear associated with transfer film formation result from two main causes: The sliding interface ultimately becomes that of polymer against polymer, which reduce the work of adhesion leading to lower adhesive forces. This is particularly important for PTEE and high density polyethylene when there is preferential chain orientation.(3) Filling of the counterface depression by transfer reduces the surface roughness and, in turn, the magnitude of the local contact stresses. Steady-state wear rates thus become much less sensitive to the initial counterface roughness.

2.11 Thermal Insulation

Cellular plastics, especially polystyrenes, polyurethanes, polyisocyanurates, phenolics, and fire-resistant polymers are widely used as thermal insulation materials and in insulation systems. They were developed initially for severe environmental applications, but their prime use

Much of the inefficiency of injection molding is related to its intermittent rather than continuous operation. Since there is a significant basic power consumption during the entire cycle, even during periods when little energy is actually being used, cycle time is very important; usually, the shorter the cycle time the higher the overall energy efficiency. Use of multiple, stacked-mold cavities and hot runners increases throughput per cycle and decreases the cycle time, respectively, thus improving efficiency.

For a given cycle time, the efficiency can be increased by reducing losses in the motor and hydraulic system. The load varies significantly during a molding cycle and selecting a motor on the basis of the peak load is wasteful because an electric motor operating without load still draws 40-50% of its rated power (43). The root-mean-square (rms) cycle power requirement rather than the peak load should determine motor size; motors can often operate at 200% torque overload over 25% of the cycle without damage (44). Schemes for supplying mechanical power for both plastication-injection and clamping include (44) one hydraulic motor for plastication-injection and a second hydraulic motor for clamping; a single hydraulic motor for both operations; and a hydraulic motor for plastication-injection with a mechanical clamping system. Although the last scheme gives the minimum power consumption, it cannot be used for certain applications. When hydraulic clamping is required, a single hydraulic motor is recommended. The use of two pumps is less efficient, because only one is in use at one time, while the other is idling pump can draw several watts; cycle settings must be optimized (44). As much as 50% of the power flowing from the motor to the hydraulic pumps is dissipated in the hydraulic system and removed as heat. This is a main source of inefficiency, and recent improvements have reduced these losses. The hydraulic pressure and flow rate have measured as functions of time during the injection-molding cycle. The results have led to several conclusions about maximizing efficiency. The accumulator should not be loaded during the injection phase and reduction injection pressure does not save energy if this pressure is supplied by an accumulator. The most important conclusion is that a variable flow-rate pump should be used. Variable displacement pumps consume less energy. Variable volume pumps do not need the throttling valves required for traditional fixed volume pumps. As many as five variable volume pumps can be couple together if a microprocessor-based controller is used. Although the use of variable volume pumps may not always significantly increase efficiency, they offer advantages in most cases.

2.12 Literature review

Rapid heating and cooling assist in injection molding process are interested in Weld- line Elimination Technology (Wellness Technology) and Heating and Cooling Technology.

The core for these technologies is heat transfer. In the process, the material's properties are related between Glass transition (Tg) and Heat distortion temperature (HDT).

- Shia – Chang Chen[Effect of cavity surface coating on mold temperature variation and the quality of injection mold parts, International Communications in Heat and Mass Transfer, 36(2009)1030 - 1033]

His experiment shown ABS injection with Dumbell shape that used Gate position at the top and the bottom (see in **Figure2.17**). In the process is installed mold temperature control system that is Infrared heating combined with surface coating. It is increasing temperature from 50 °C to 120 °C in 2 – 5 sec. But in real case, the temperature is increasing from 50 °C to 120 °C in 17 sec that use TiN and PTFE in heating combined with surface coating. The part in this experiment that is ABS is not weld – line.

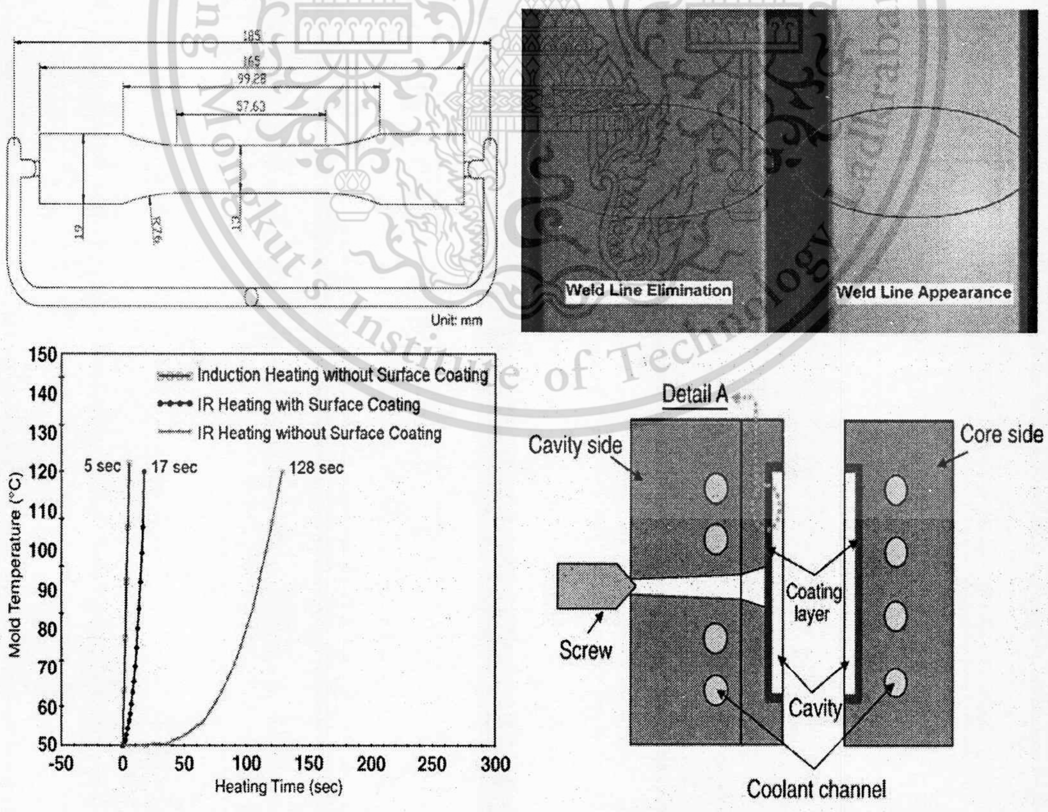

Figure2.17 TiN and PTFE in heating combined with surface coating

● Guilong Wang [Research of thermal response simulation and mold structure optimization for rapid heat cycle molding processes respectively with stream Heating and electric heating, Materials and Design, 31 (2010) 382 - 395]

Rapid heat cycle molding (RHCM) is special technique that is increasing mold temperature is higher than Heat Distortion Temperature. Melting plastic is injected into mold that is heat exchange from plastic to mold's surface. There is a solidification that is a cause of gloss's quality. When mold's surface temperature is not enough temperature level, the product's surface is not smooth. The problem is solved by increasing pack pressure. In this case, the mold's surface is polished by diamond wax. The product is high gloss.

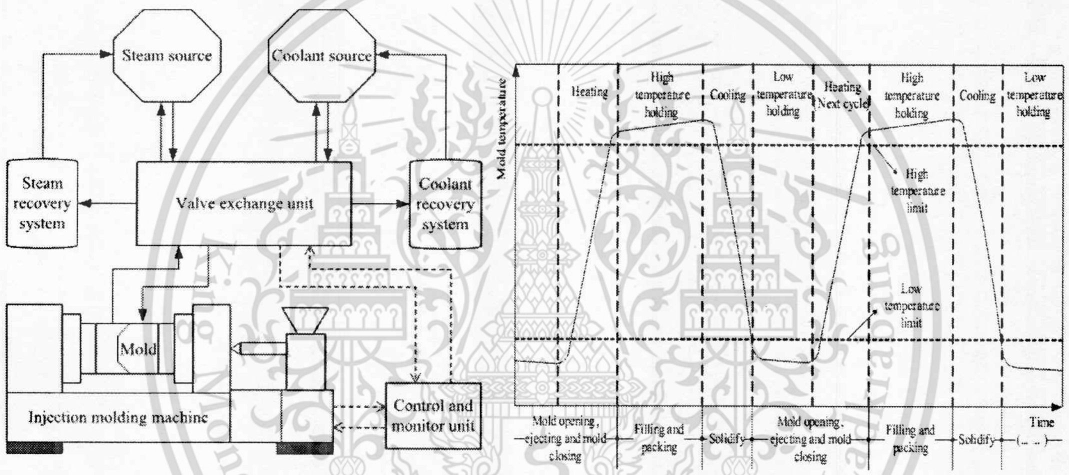

(a)

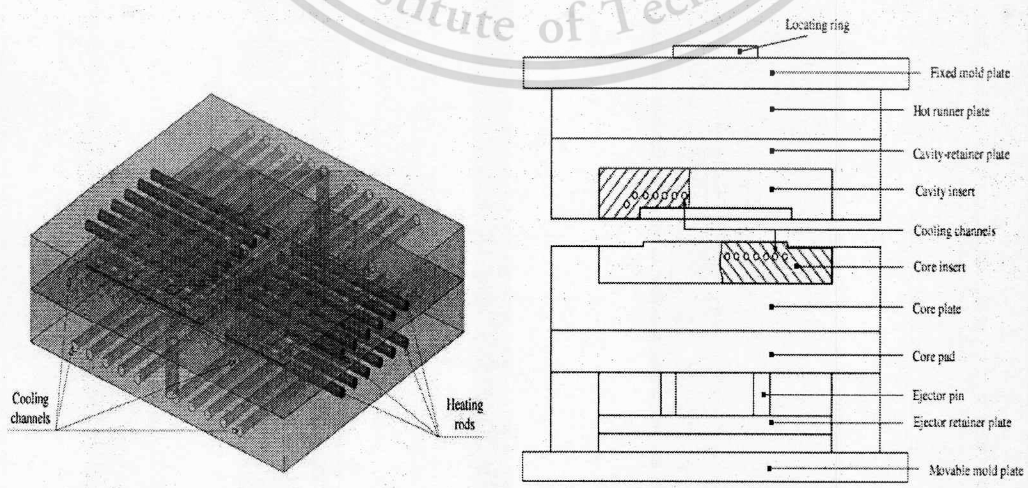

(b)

Figure2.18 (a.) RHCM (Rapid heat cycle molding) and (b.) Mold Layout

Table2.7 Thermal conductivity of material

	Material	Density (kg/m^3)	Heat capacity (J/kg °C)	Thermal conductivity (W/m °C)
Retainer plate	AISI 1045	7850	486	49.8
Insulation layer	Bakelite	1400	1420	0.40
Cavity/core	AISI P20	7850	460	34
	AMPCO 940	8710	380	208
Heating rods	$MgO-SiO_2$	2700	1100	5.5

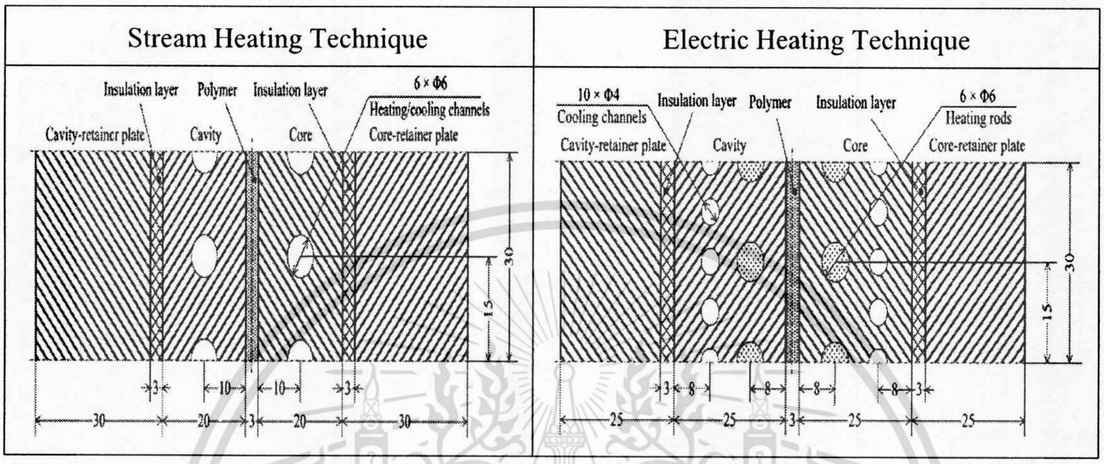

Figure2.19 Mold Layout

Table2.8 Cycle time in heating and cooling

	Case 1	Case 2	Case 3	Case 4	Case 5	Case 6	Case 7	Case 8
Heating time (s)	12.1	10.2	11.5	7.2	15.6	23.5	15.4	17.1
Cooling time (s)	20.7	17.8	21.1	17.6	27.4	18.9	27.6	18.7
Total (s)	32.8	28.0	32.6	24.8	43.0	42.4	43.0	35.8

From **Figure2.20** is shown energy consumption. Stream Technique is saver than Electric Heat Technique (Electric Heating ; Stream Heating = 70kJ;25kJ). Moreover Stream Heating Technique is safety that pressurized stream is pressure level at 10 Bar, when hot water (180°C) flow into mold. If you use boiler, it is hard maintenance. But in Electric Heating used heating bar that conduct heat into mold's surface. In cycle time, heating and cooling in mold's surface temperature is 120°C. Stream Heating is more advantage in core insert that can be use AISI P20 (k = 34 W/m.C) or AMPCO 940 (k = 208 W/m.C)

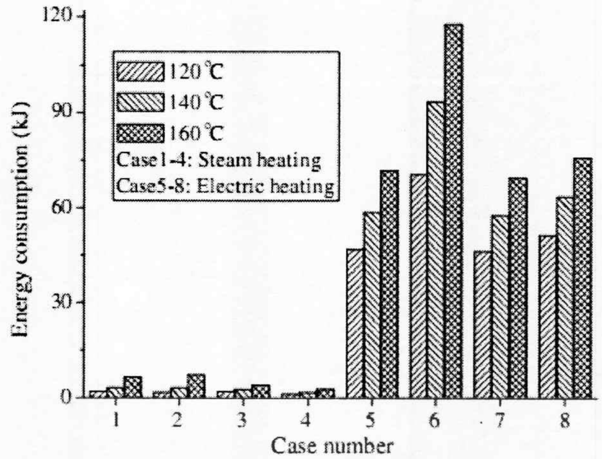

Figure2.20. Energy consumption in Electric Heating and Stream Heating

●3D Weldless Technology by MITSUBISHI CORPORATION TECHNOS, Japan [2] and RTC- Rapid Temperature Cycling by Gas Injection Worldwide Ltd , UK [3]

This technology is controlling stream at 4 – 10 bar that is increasing temperature at 120°C - 180°C. It assists in injection molding. The melt plastic flows into mold well and in cooling time, there are rapid cool down temperature for part's ejection. The hot water is from boiler and cool water is form cooling tower. It is high cost and hard maintenance.

●(WO/2001/038062) A METHOD FOR OBTAINING A THERMOPLASTIC RESIN INJECTION-MOLDED PRODUCT HAVING A HIGH-QUALITY APPEARANCE [1]

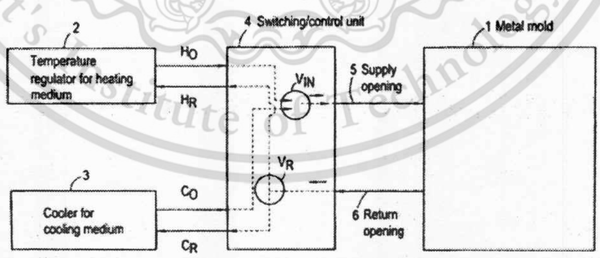

Figure2.21. control system of WO/2001/038062

CHAPTER 3

EXPERIMENTAL PROCEDURES

3.1 Material

In this study, it is investigating in the effect of surface's gloss and surface's roughness in injection molding parameters. Materials used two types of polymers as:

3.1.1 Amorphous polymer

In this study are three grades of amorphous polymers that are Acrylonitrile butadiene styrene (ABS KU901, ABS SP200 and ABS GA300). ABS KU901 that is supported by IRPC/Polimaxx company is a high heat resistance grade of ABS resin for injection molding process. It is specially designed for automotive parts (instrument panel) and electrical appliance (rice cooker, coffee maker, microwave part and etc). ABS SP200 that is supported by IRPC company is specially designed for motorcycle components, especially for electroplating and painting articles. ABS GA300 is a high flow grade of ABS resin for injection molding process with featuring of high gloss and easy flow ability. It is suitable for air conditioner, toys, sanitary ware, cosmetic packaging, and etc. These amorphous polymers was different melt flow index (MFI) because this investigation was focused on the major and minor effects of surface's gloss and surface's roughness by various injection molding parameters such as mold temperature, barrel temperature, injection speeds, pack pressure, and packing time. The characteristics and technical data of amorphous used in this study are shown in **Table 3.1**.

Table3.1 The characteristics and technical data of amorphous (A) KU901, (B) SP200, (C) GA300

(A) KU901

ABS KU901				
Physical Properties:	VALUE	UNIT	TEST METHOD	TEST CONDITION
Melt Flow Index	6	g/10min.	ASTM D1238	10 kg/220°C
Izod Notched Impact	13	Kg-cm/cm	ASTM D256	¼", 23°C
Tensile Strength at Yield	500	kg/cm2	ASTM D638	23°C
Flexural Strength at Yield	720	kg/cm2	ASTM D790	23°C
Flexural Modulus	2.4	×104kg/cm2	ASTM D790	23°C
Rockwell Hardness	112	R-Scale	ASTM D785	¼", 23°C
Heat Distortion Temperature	104	°C	ASTM D648	¼", 18.6 kg/cm2
Heat Distortion Temperature	114	°C	ASTM D648	¼", 4.6 kg/cm2
Flammability	HB (1.5)	-	UL-94	

(B) SP200

ABS SP200				
Physical Properties:	VALUE	UNIT	TEST METHOD	TEST CONDITION
Melt Flow Index	17	g/10min.	ASTM D1238	10 kg/220°C
Izod Notched Impact	36	Kg-cm/cm	ASTM D256	1/4", 23°C
Tensile Strength at Yield	420	kg/cm2	ASTM D638	23°C
Flexural Strength at Yield	570	kg/cm2	ASTM D790	23°C
Flexural Modulus	2.05	×104kg/cm2	ASTM D790	23°C
Rockwell Hardness	109	R-Scale	ASTM D785	1/4", 23°C
Heat Distortion Temperature	84	°C	ASTM D648	1/4", 18.6 kg/cm2
Heat Distortion Temperature	90	°C	ASTM D648	1/4", 4.6 kg/cm2
Flammability	HB (1.5)	-	UL-94	1.5 mm, 3.1 mm thickness

(C) GA300

ABS GA300				
Physical Properties:	VALUE	UNIT	TEST METHOD	TEST CONDITION
Melt Flow Index	30	g/10min.	ASTM D1238	10 kg/220 °C
Izod Notched Impact	22	Kg-cm/cm	ASTM D256	1/4", 23 °C
Tensile Strength at Yield	480	kg/cm2	ASTM D638	23 °C
Flexural Strength at Yield	670	kg/cm2	ASTM D790	23 °C
Flexural Modulus	2.3	×104kg/cm2	ASTM D790	23 °C
Rockwell Hardness	112	R-Scale	ASTM D785	1/4", 23 °C
Heat Distortion Temperature	86	°C	ASTM D648	1/4", 18.6 kg/cm2
Heat Distortion Temperature	94	°C	ASTM D648	1/4", 4.6 kg/cm2
Flammability	HB (1.5)	-	UL-94	

3.1.2 Crystal polymer

In this study are two grades of amorphous polymers that are **acetal** (POM M90 and POM M 270). The commercial name of (POM M90 and POM M270) are Duracon M90-44 and Duracon M270-44 that supplied by Polyplastics company. These crystal polymers were different melt flow index (MFI) because this investigation was focused on the major and minor effects of surface's gloss and surface's roughness by various injection molding parameters such as mold temperature, barrel temperature, injection speeds, pack pressure, and packing time. The characteristics and technical data of crystal used in this study is shown in **Table 3.2**.

Table3.2 The characteristics and technical data of crystal polymers (A)POM M90, (B)POM M270

(A) POM M90

POM M90			
Physical Properties:	VALUE	UNIT	TEST METHOD
Melt Flow Index	9	g/10min.	ASTM D1238
Izod Notched Impact	6	kJ/m2	ISO 179/1eA
Tensile Strength	62	MPa	ISO 527-1,2
Flexural Strength	87	MPa	ISO 178
Flexural Modulus	2500	MPa	ISO 178
Heat Distortion Temperature	95	°C	ASTM D648
Flammability	HB	-	UL-94

(B) POM M270

POM M270			
Physical Properties:	VALUE	UNIT	TEST METHOD
Melt Flow Index	27	g/10min.	ASTM D1238
Izod Notched Impact	5.3	kJ/m2	ISO 179/1eA
Tensile Strength	63	MPa	ISO 527-1,2
Flexural Strength	88	MPa	ISO 178
Flexural Modulus	2550	MPa	ISO 178
Heat Distortion Temperature	100	°C	ASTM D648
Flammability	HB	-	UL-94

3.2. Equipment

3.2.1 Equipment for Specimen Preparation is injection molding process

3.2.1.1 Hopper

Before injection molding process, the materials have to drying granulated plastic. In this study, ABS is dried at 80°C for 4 hours. The hopper shows in **Figure3.1** and the specification shows in **Table3.3**.

Figure3.1 Hopper

Table3.3 The specification of hopper

Model	**HD – 50T**
NO.	**844**
Source	**380 V. 3PH**
Ampere	**6.4A**
Error tolerance	**-3°C/100°C**

3.2.1.2 Chiller

For injection molding process, chiller used for temperature control. It is working with injection molding machine. In this study, the chiller is manipulated at 13°C. The chiller is shown in **Figure3.2** and the specification is shown in **Table3.4**.

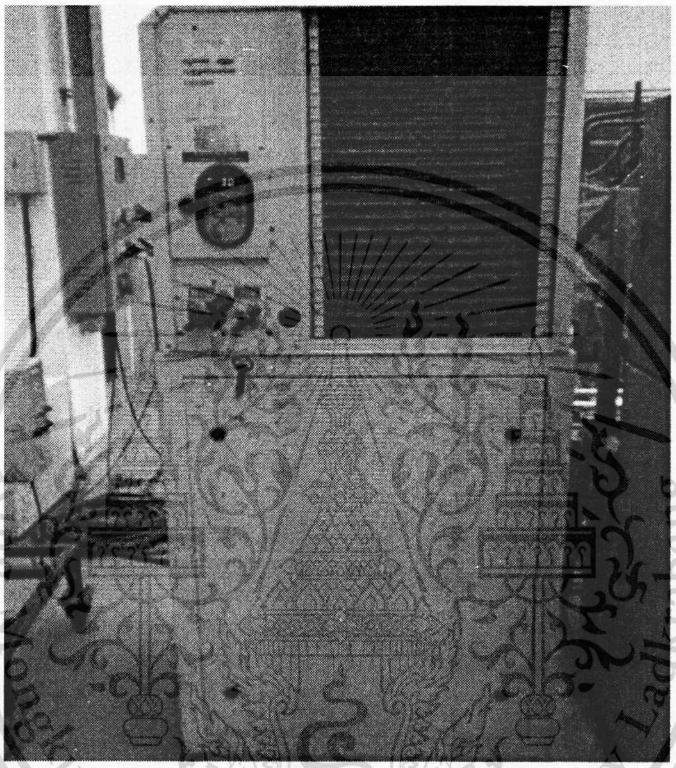

Figure3.2 Chiller Carrier – 38LB060SC

Table3.4 The specification of chiller

Model	**Carrier – 38LB060SC**
Power supply	**380 V. 3PH 50 Hz**
Rated Load	**9.2 Amp.**
Fan Motor	**220 V. 1PH 1/5 HP**
Cooling Capacity	**60,000 BTU/H**
Refrigerant	**R-22**

3.2.1.3 Injection Molding Machine

The Injection molding machine is Fanuc Roboshot s - 2000i 100B that shown in **Figure3.3** and the specification is shown in **Table3.5**.

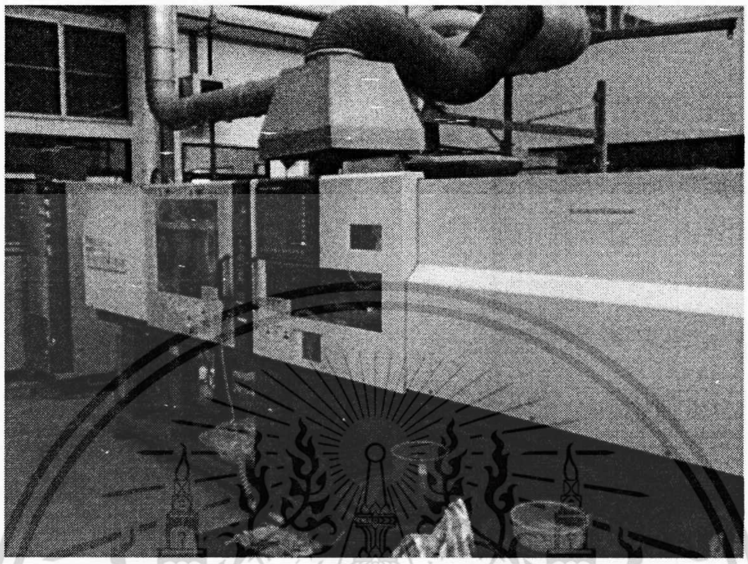

Figure3.3 Injection molding machine Roboshot S – 2000i 100B

Table3.5 The specification of injection machine

	Item	Unit	ROBOSHOT S-2000*i* 100B
Clamping unit	Tonnage	kN	1000 (100 tonf)
	Maximum and Minimum die height	mm	450 / 150
	Clamping stroke	mm	350
	Tie bar spacing (HxV)	mm	460 x 410
	Platen size (HxV)	mm	660 x 610
	Ejector point	point	5
	Ejector force	kN	25 (2.5 tonf)
	Ejector stroke	mm	100
Injection unit	Injection specification	-	Injection speed 200mm/s
	Screw diameter	mm	32
	Maximum injection volume	cm^3	103
	Maximum injection pressure (High pressure filling mode)	MPa	220

4.1.1 Laboratory Develop HC System (Heating and Cooling)

The heating and cooling control system is shown in **Figure3.4** (Appendix A).

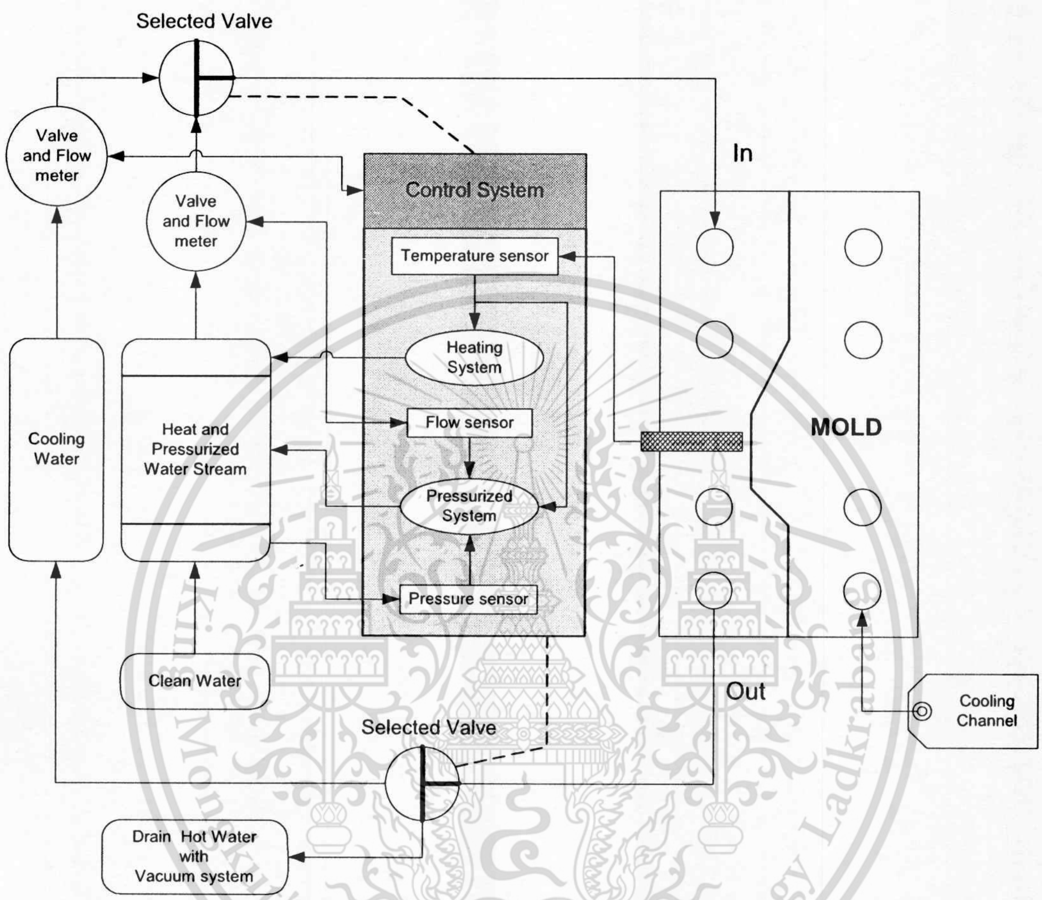

Figure3. 4 Controlling equipment and heating and cooling control system

3.2.1.5 Temperature control

Temperature control use for conventional injection molding. The parameter in process is mold surface temperature that the temperature are 40°C, 60°C, and 80°C. In this study used ToolTemp™ Mold temperature control, which the temperature range is 30 °C - 100 °C. ToolTemp™ Mold temperature control is shown in **Figure3.5**.

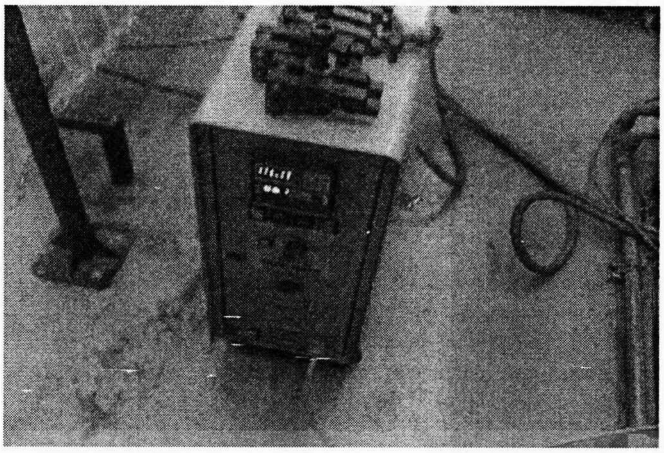

Figure 3.5 ToolTemp™ Mold temperature control

3.2.1.6 Mold

Mold in this study is designed by MTEC. It is installed two thermocouples and a pressure sensor. The mold is released heat by water. The material of conducted heat is BeCu. The mold is shown in **Figure 3.6**.

(a.) **(b.)**

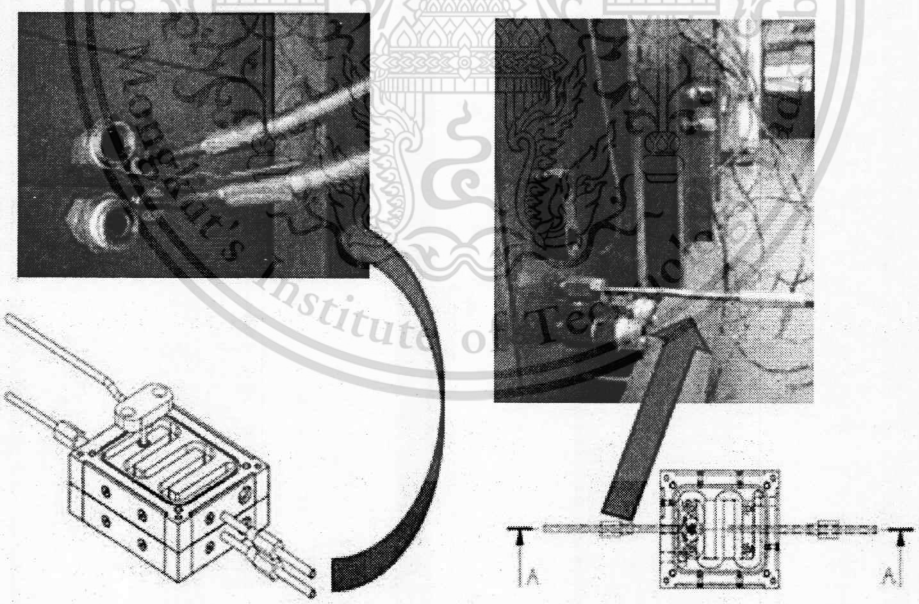

(c.) **(d)**

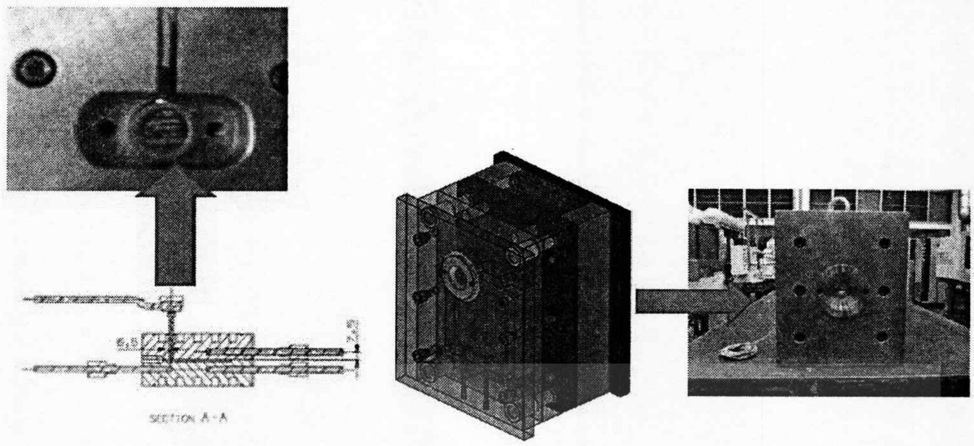

Figure3.6(a) two thermocouples at water flow out,(b) a thermocouple at water flow in, (c) a pressure sensor position, (d) mold in injection process

Mold for preparing specimen is a rectangle part that the dimension is 50x70x2 mm. The dimension of part and the real part is shown in **Figure3.7**.

(a) **(b)**

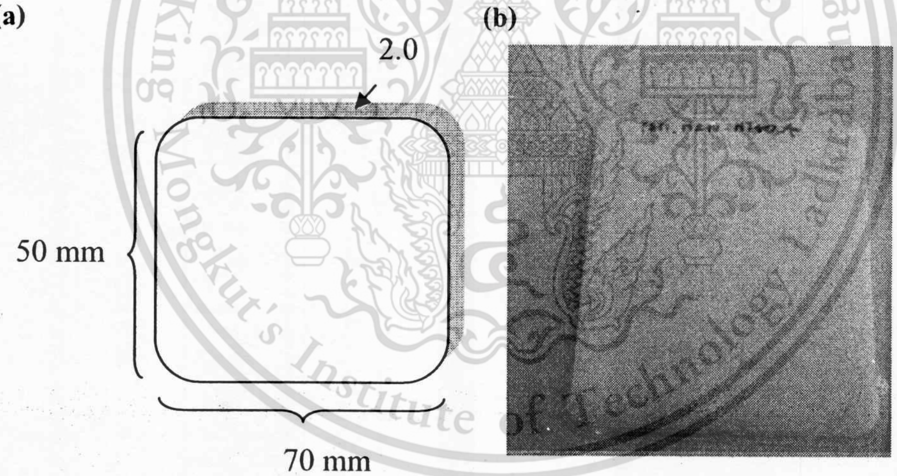

Figure 3.7 (a) the dimension of part, (b) the specimen part

3.2.1.7 Thermocouple

In this work is measured temperature by three thermocouple that is Misumi type K. the thermocouple model is MSFK1.6 – 170 - F2.5 – Y. Thermocouple is shown in **Figure 3.8** (Appendix B).

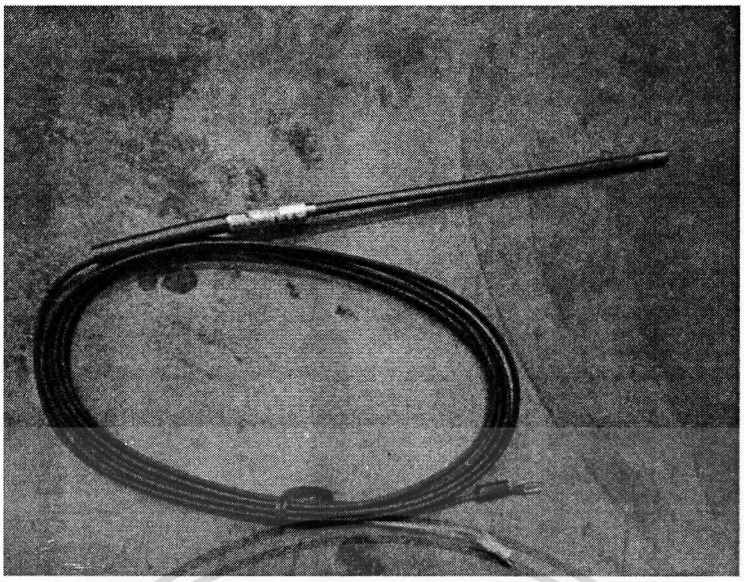

Figure3.8 Thermocouple

3.2.1.8 Pressure sensor

This study is measured pressure by load cell that is Bongshin – CBFS. The model is shown in **Figure 3.9** (Appendix B).

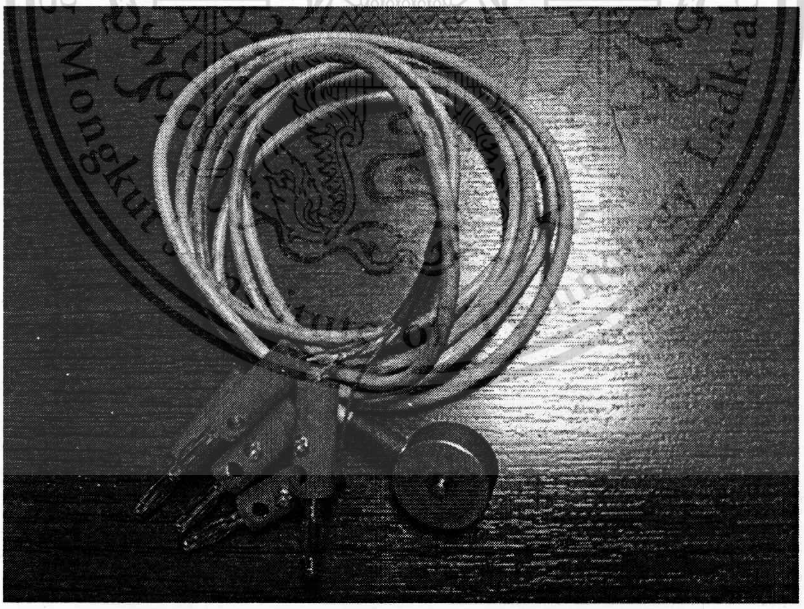

Figure3.9 Load cell Bongshin – CBFS

3.2.1.9 Data logger

In injection mold process, is measured data by three thermocouples and a load cell that is a pressure sensor. There is a data logger for correcting data from process. Data logger has three channels for temperature data and one channel for pressure data. Data logger is shown in **Figure3.10** (Appendix C).

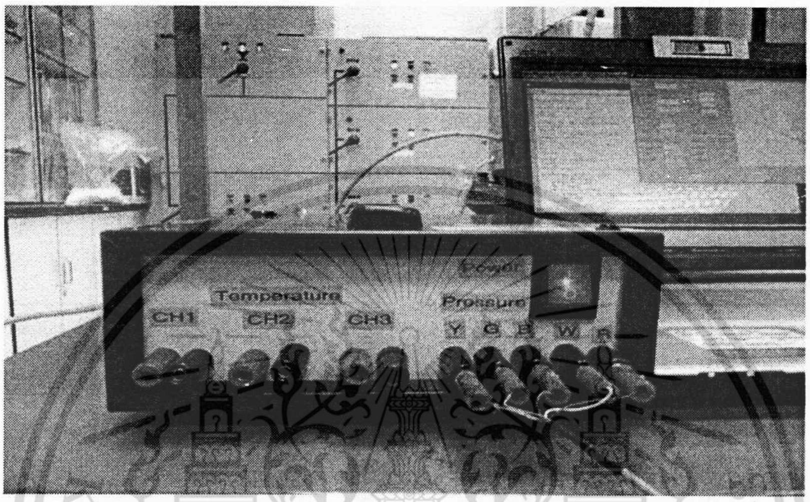

Figure3.10 data logger

3.2.1.10 Software

Software in this study, is developed for correcting data from data logger. The software is made from Microsoft Visual Basic 6.0 and showed in Figure3.11 (**Appendix C**).

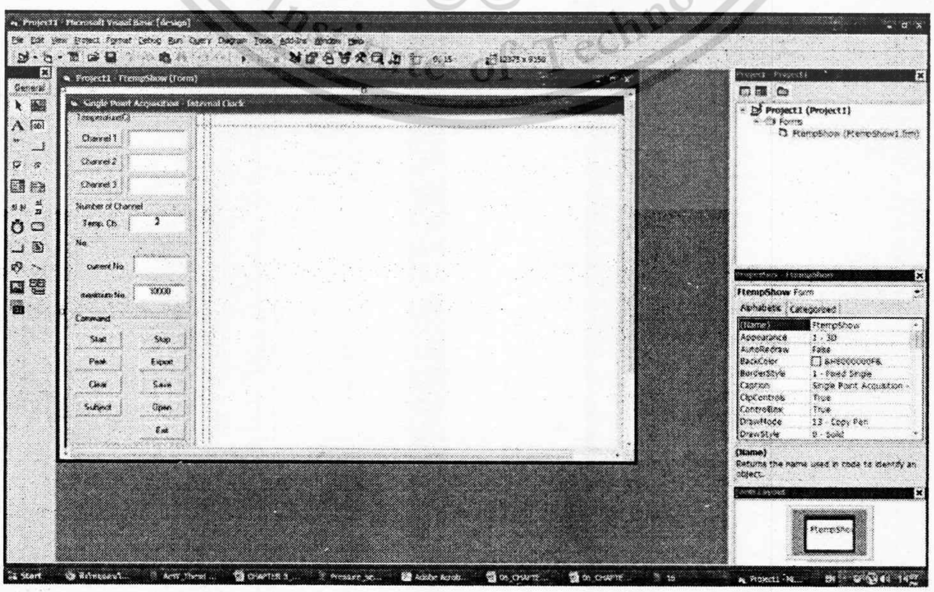

(a)

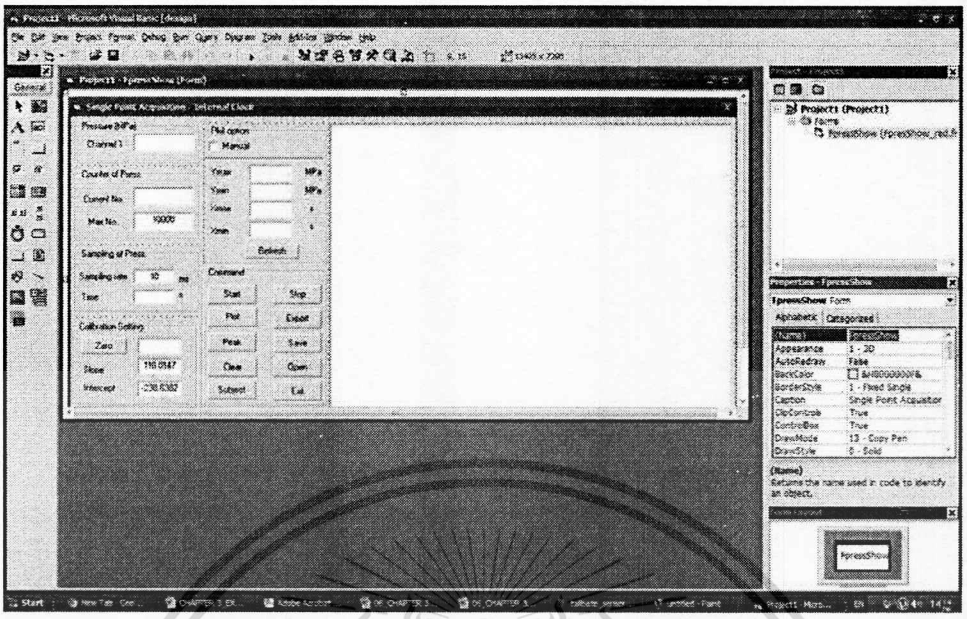

(b)

Figure 3.11 (a) Correcting temperature data software, (b) correcting pressure data software

3.3 Process

There are two parts of this work is conventional injection molding and injection molding via rapid heating and cooling control. Conditions in injection molding have five parameters that are mold temperature, barrel temperature, injection speed, packing pressure and packing time. In **Table 3.6** is shown injection molding parameters.

Table 3.6 The conditions in injection molding (a) ABS conditions in conventional injection molding, (b) POM conditions in conventional injection molding, (c) ABS conditions in injection molding via rapid heating and cooling control, (d) POM conditions in injection molding via rapid heating and cooling cycle

(a)

Material			ABS
Std. Conditon			ABS-H230-MT60-HP450-HPT5-V30
Parameters	Value	unit	Conditions
Barrel Temperature	220	^{o}C	ABS -H220-MT60-HP450-HPT5-V30
	230	^{o}C	ABS -H230-MT60-HP450-HPT5-V30
	240	^{o}C	ABS -H240-MT60-HP450-HPT5-V30
Mold Temperature	20	^{o}C	ABS -H230-MT20-HP450-HPT5-V30
	40	^{o}C	ABS -H230-MT40-HP450-HPT5-V30
	60	^{o}C	ABS -H230-MT60-HP450-HPT5-V30
	80	^{o}C	ABS -H230-MT80-HP450-HPT5-V30
Packing Pressure	100	Mpa	ABS -H230-MT60-HP100-HPT5-V30
	200	Mpa	ABS -H230-MT60-HP200-HPT5-V30
	300	Mpa	ABS -H230-MT60-HP300-HPT5-V30
	450	Mpa	ABS -H230-MT60-HP450-HPT5-V30
	500	Mpa	ABS -H230-MT60-HP500-HPT5-V30
Packing Time	1	s	ABS -H230-MT60-HP450-HPT1-V30
	3	s	ABS -H230-MT60-HP450-HPT3-V30
	5	s	ABS -H230-MT60-HP450-HPT5-V30
	7	s	ABS -H230-MT60-HP450-HPT7-V30
	9	s	ABS -H230-MT60-HP450-HPT9-V30
Injection speed	10	mm/s	ABS -H230-MT60-HP450-HPT5-V10
	20	mm/s	ABS -H230-MT60-HP450-HPT5-V20
	30	mm/s	ABS -H230-MT60-HP450-HPT5-V30
	50	mm/s	ABS -H230-MT60-HP450-HPT5-V50
	70	mm/s	ABS -H230-MT60-HP450-HPT5-V70

(b)

Material			POM
Std. Conditon			POM-H230-MT60-HP300-HPT3-V30
Parameters	Value	unit	Conditions
Melt Temperature	220	°C	POM -H220-MT60-HP300-HPT3-V30
	230	°C	POM -H230-MT60-HP300-HPT3-V30
	240	°C	POM -H240-MT60-HP300-HPT3-V30
Mold Temperature	20	°C	POM -H230-MT20-HP300-HPT3-V30
	40	°C	POM -H230-MT40-HP300-HPT3-V30
	60	°C	POM -H230-MT60-HP300-HPT3-V30
	80	°C	POM -H230-MT80-HP300-HPT3-V30
Packing Pressure	100	Mpa	POM -H230-MT60-HP100-HPT3-V30
	200	Mpa	POM -H230-MT60-HP200-HPT3-V30
	300	Mpa	POM -H230-MT60-HP300-HPT3-V30
	500	Mpa	POM -H230-MT60-HP450-HPT3-V30
	700	Mpa	POM -H230-MT60-HP700-HPT3-V30
Packing Time	1	s	POM -H230-MT60-HP300-HPT1-V30
	3	s	POM -H230-MT60-HP300-HPT3-V30
	5	s	POM -H230-MT60-HP300-HPT5-V30
	7	s	POM -H230-MT60-HP300-HPT7-V30
	9	s	POM -H230-MT60-HP300-HPT9-V30
Injection speed	10	mm/s	POM -H230-MT60-HP300-HPT3-V10
	20	mm/s	POM -H230-MT60-HP300-HPT3-V20
	30	mm/s	POM -H230-MT60-HP300-HPT3-V30
	50	mm/s	POM -H230-MT60-HP300-HPT3-V50
	70	mm/s	POM -H230-MT60-HP300-HPT3-V70

(c)

Material			ABS
Std. Conditon			ABS-H230-MT120-HP450-HPT5-V30
Parameters	Value	unit	Conditions
Mold Temperature	100	^{o}C	H230-HP450-HPT5-V30-MT100
Mold Temperature	110	^{o}C	H230-HP450-HPT5-V30-MT110
Mold Temperature	120	^{o}C	H230-HP450-HPT5-V30-MT120
Packing Time	1	s	MT120-HP450-V30-H230-HPT1
Packing Time	3	s	MT120-HP450-V30-H230-HPT3
Packing Time	5	s	MT120-HP450-V30-H230-HPT5
Packing Time	7	s	MT120-HP450-V30-H230-HPT7
Packing Time	9	s	MT120-HP450-V30-H230-HPT9

(d)

Material			POM
Std. Conditon			POM-H220-MT120-HP300-HPT3-V30
Parameters	Value	unit	Conditions
Mold Temperature	100	^{o}C	H220-HP300-HPT3-V30-MT100
Mold Temperature	110	^{o}C	H220-HP300-HPT3-V30-MT110
Mold Temperature	120	^{o}C	H220-HP300-HPT3-V30-MT120
Packing Time	1	s	MT120-HP300-V30-H220-HPT1
Packing Time	3	s	MT120-HP300-V30-H220-HPT3
Packing Time	5	s	MT120-HP300-V30-H220-HPT5
Packing Time	7	s	MT120-HP300-V30-H220-HPT7
Packing Time	9	s	MT120-HP300-V30-H220-HPT9

3.4 Experiment

3.4.1 Properties Testing

3.4.1.1 Gloss Measurement

In gloss measurement, object's surface is measured at 20, 60 and 85 angle, that shown in **Figure 3.12**. The standard in gloss measurement is shown in **Table3.7**.

Table3.7 Standard in gloss measurement

Reference standard	ASTMD523, ISO2813, JISZ8741
Level of object's surface	Angle
Medium's gloss	60
Low's gloss	85
High's gloss	20
45 angle for ceramic's surface is measured by ASTM C346	
75 angle for paper's surface is measured by TAPPIT 480	

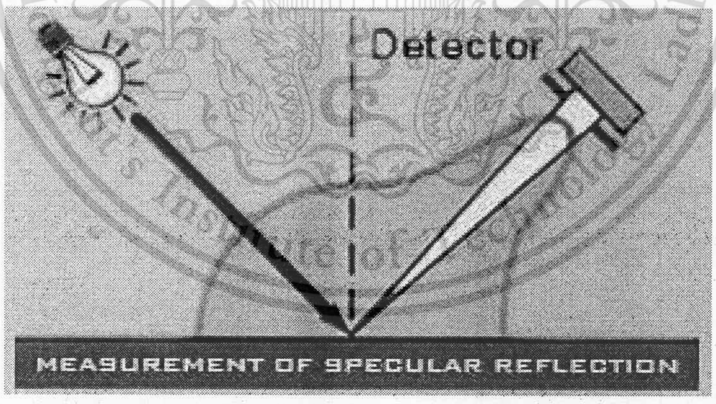

Figure3.12 Measure the gloss's surface

The injection specimens, are completely tested by gloss properties. There are four procedures for gloss measuring.

- The specimens are cleaned by micro cotton (showed in **Figure 3.13**).

Figure 3.13 Clean the specimen.

- In this experiment used ETB – 0833 Gloss meter that is concerned by ISO 2813. The specific of model is shown in **Table3.8**.

Table3.8 The specification of ETB – 0833 Gloss meter

Specification	Detail
Measure range	0-200 GU
Stability	<± 0.4 GU/30 Min
Value error	<± 1.2 GU
Power	1.5V
Projecting angle	20, 60,85
Environment temperature	0-40^{o}C
Relative humidity	$\leq$ 85 %

- Gloss meter is calibrated by the instruction of gloss meter's calibration. The calibration of gloss meter is shown in **Figure 3.14**.

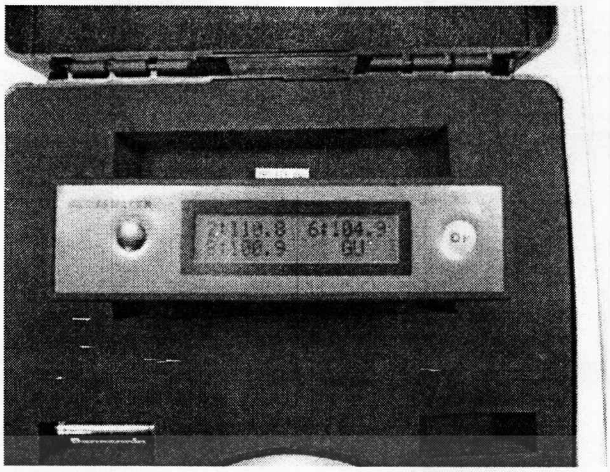

Figure 3.14 Glossmeter and calibration's value before gloss measurement

- Gloss meter is measuring the specimens. Then the gloss meter shows measuring value (shown in **Figure 3.15**).

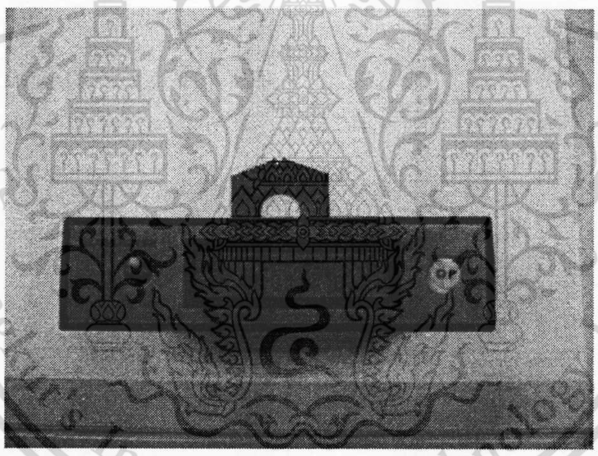

Figure 3.15 Gloss meter with measurement value

3.4.1.2 Roughness Measurement

The surface roughness was performed with Mitutoyo Surftest sv-3000. **Figure 3.16** shown sv – 3000. The roughness average (R_a) is universally recognized (see in **Figure 3.17**). The value was calculated according to Equation (3.1).

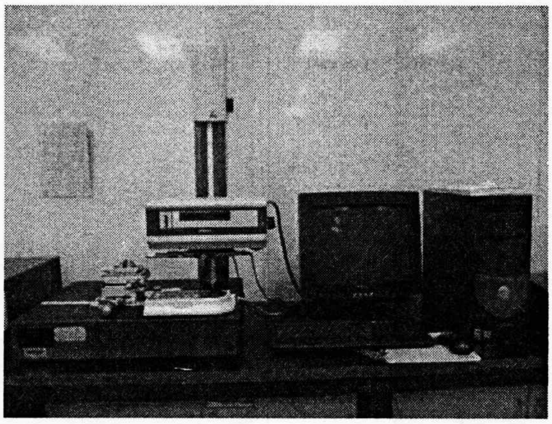

Figure 3.16 Mitutoyo Surftest sv-3000

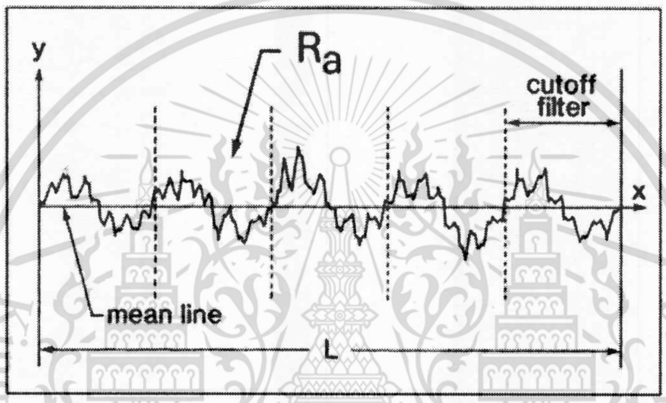

Figure3.17 Ra Roughness Analytical Function

$$R_a = \frac{1}{L} \int_{x=0}^{x=L} |y| dx \tag{3.1}$$

R_a is the arithmetic average deviation from the mean line within the assessment **length** (L) and y is profile deviation.

The specimens are tested by roughness properties. There are four procedures **for** measuring.

- Put the part on the measurement position (see in **Figure 3.18**).

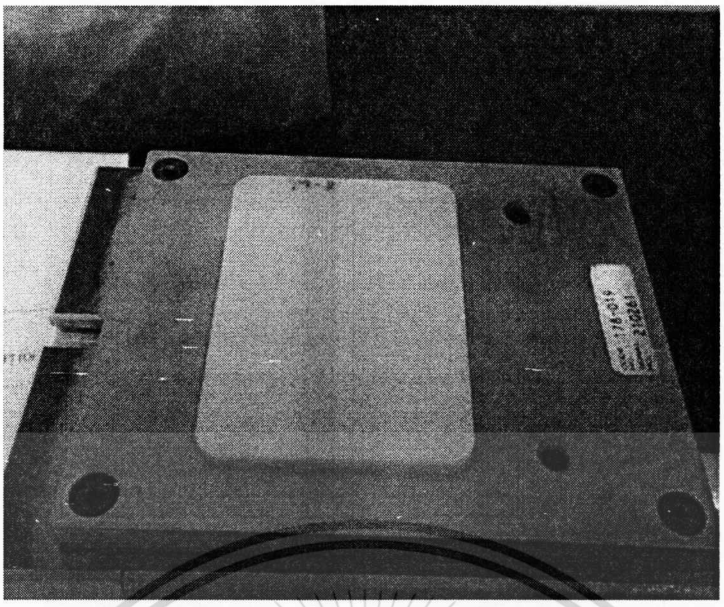

Figure 3.18 Measurement position

- Set the range of measuring is 3 mm. in input's software.
- Command start measurement by computer programming (see in **Figure 3.19**).

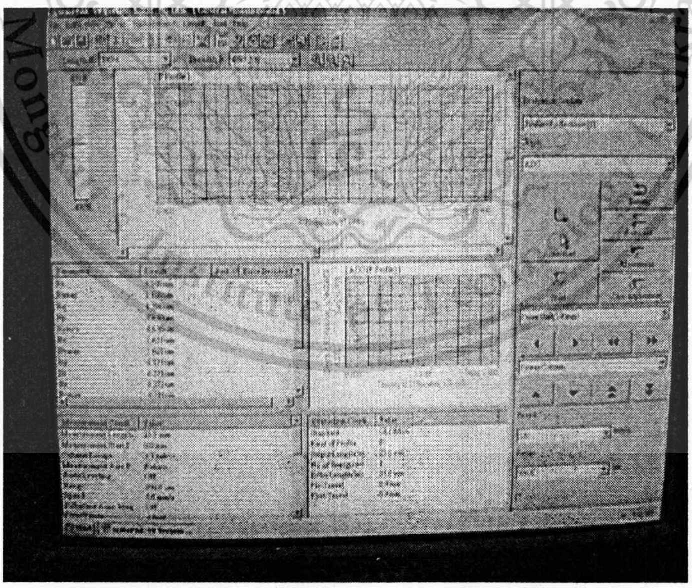

Figure3.19 Start measurement by computer

- Save the measurement data by computer

3.4.1.3 Scanning Electron Microscope(SEM)

The characterization of the surface structure of the specimens was observed using the scanning electron microscopy (SEM) JEOL JSM – 5410 in **Figure 3.20**. There are three procedures for scanning electron microscopy (SEM).

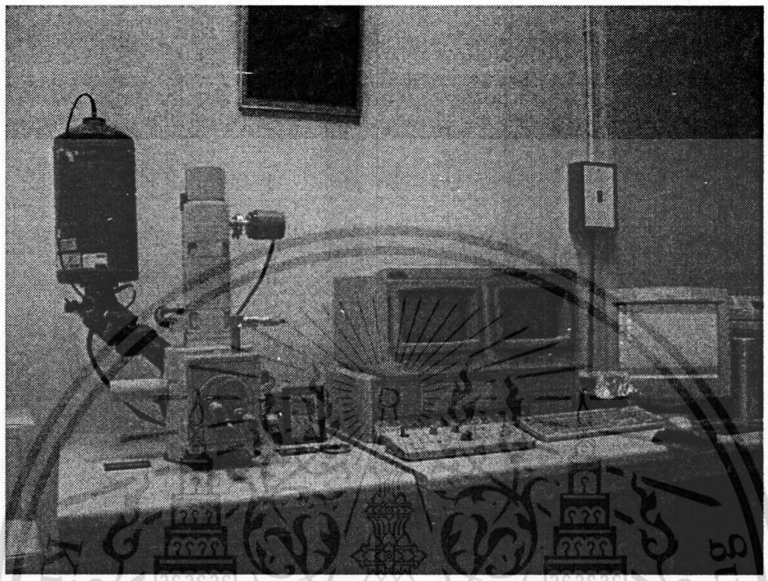

Figure 3.20 Scanning electron microscopy (SEM) JEOL JSM-5410

A. The samples were cut by the sonic cutter (see in **Figure 3.21**). In **Figure 3.22** is a cut sample.

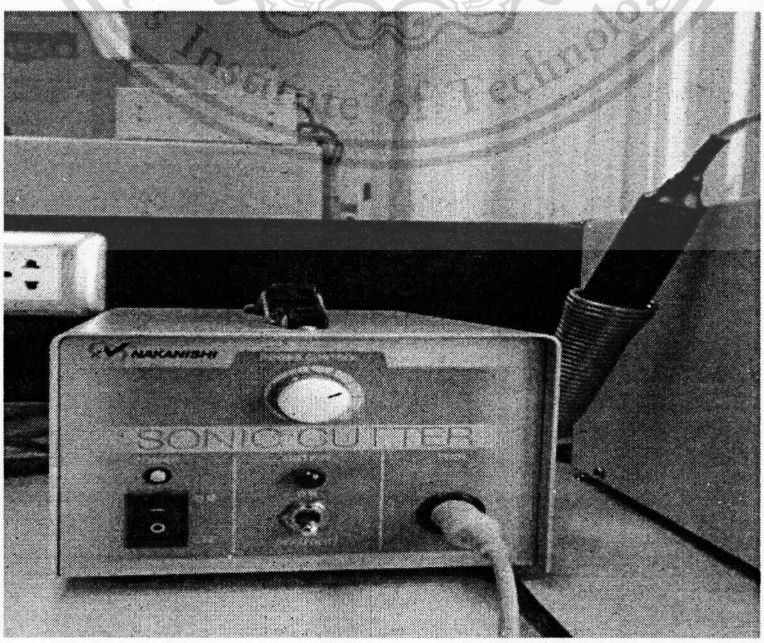

Figure 3.21 Sonic cutter

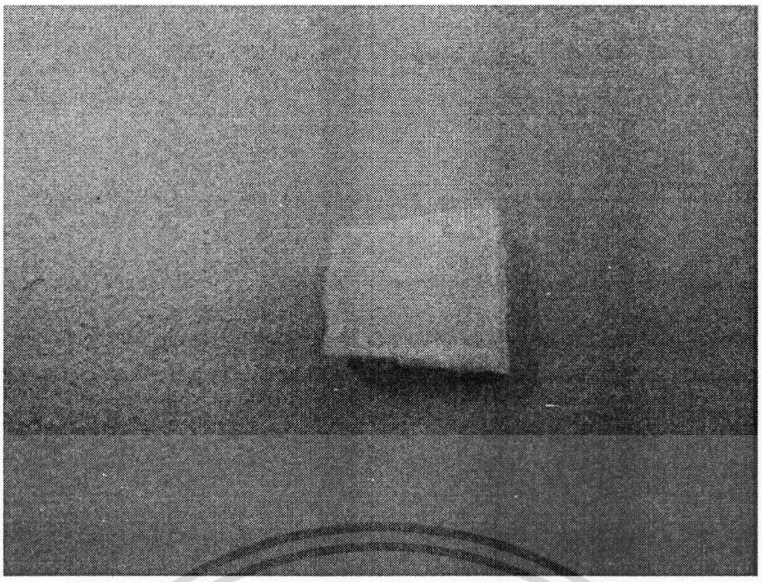

Figure 3.22 A cut sample

B. The fracture surface were gold coated to make them conducting by using JEOL JFC – 1200 fine coater in **Figure 3.23**. In **Figure 3.24** are gold surface samples.

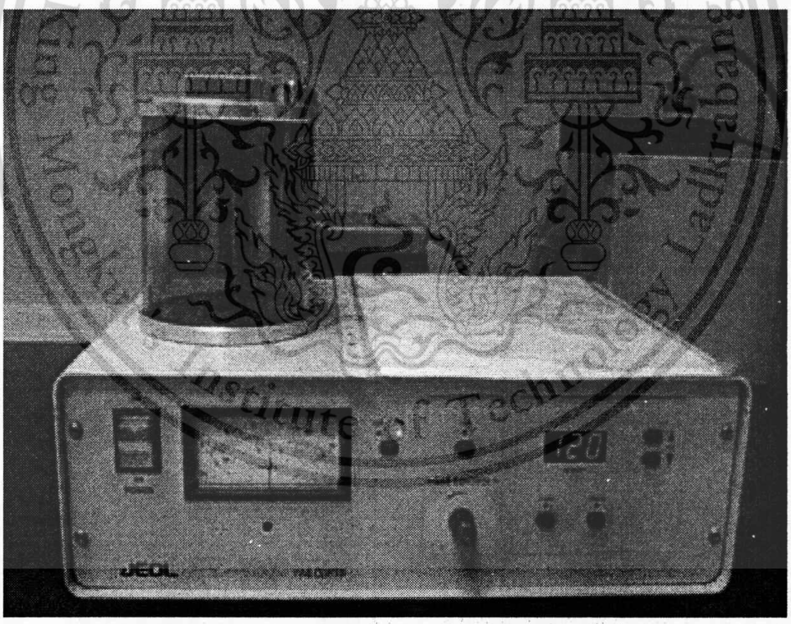

Figure 3.23 Fine coater JEOL JFC-1200

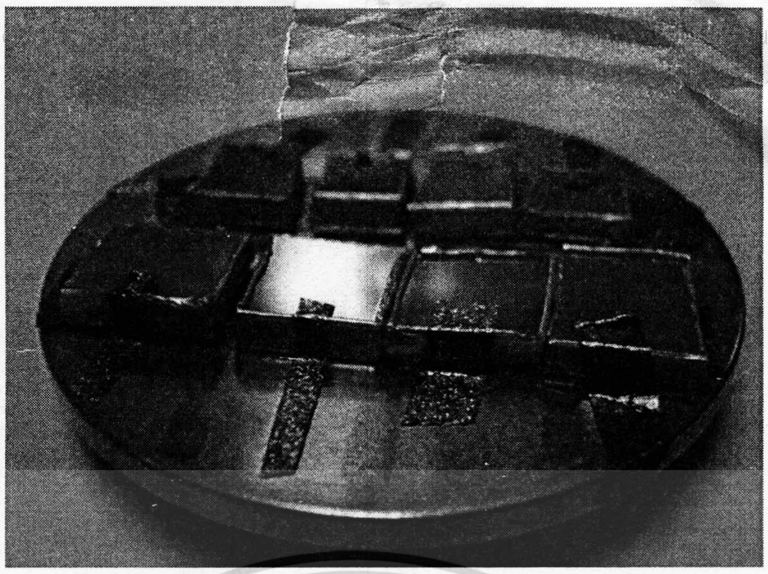

Figure3.24 Gold surface samples

C. In this study is studied in micro structure that is the surface's **area**. The SEM's result is a micro structure's picture which understanding the surface roughness's acknowledgement (see in **Figure3.25**).

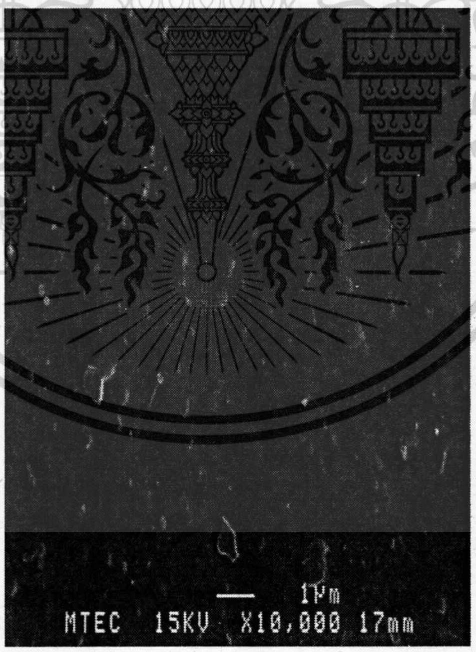

Figure3.25 Observed area of Scanning Electron Microscope

3.4.1.4 Capillary rheometer test

Rheology is the study of the flow of complex liquids in both sample and complex flow geometries. When most flows of practical are complex flows, it is usually not possible to perform general and quantitatively accurate measurements of the fluids's behavior in these flows due to their highly complex dynamics and kinematics. Thus, in this case used the Bohlin instrument capillary rheometer model RH2000 (see in **Figure 3.26**). The result will be understand the rheology properties of materials. The sample for testing was taken inside the barrel of extrusion assembly and forced down into the capillary using a plunger. The melt was extruded through the capillary at plunger speeds. The measurements were calculating the viscosities at the different melt flow rates and temperatures. The shear viscosity is represented in Equation (3.2).

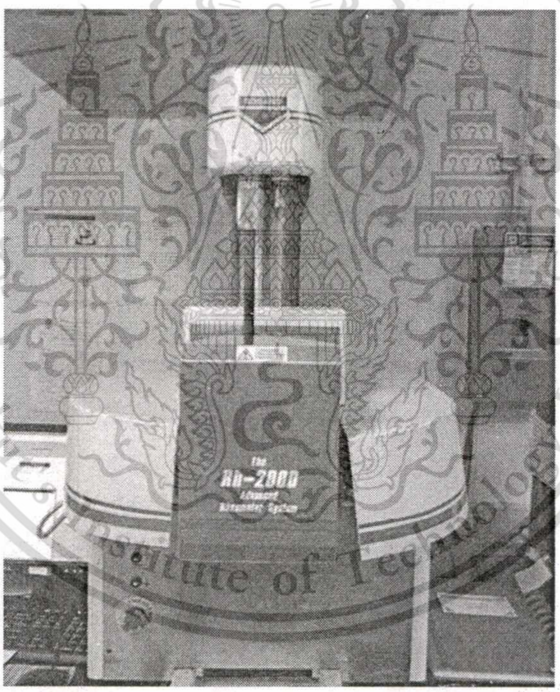

Figure 3.26 Capillary rheometer model RH2000

$$\eta = \tau / \dot{\gamma} \tag{3.2}$$

$$\tau_w = \frac{RP_c}{2L}$$

$$\dot{\gamma} = \frac{4Q}{\pi R^3}$$

Where: τ_w is wall shear stress

$\dot{\gamma}_w$ is wall shear strain

R is Diameter of capillary die

L is Length of capillary die

P_c is Pressure

Q is Flow volume

3.4.2 Energy consuming

In this case is considered on heat consuming in injection molding. The heat energy is assumed in Equation (3.3).

$$E_h = M_p \int_{T_1}^{T_2} C_m dT + \int_0^{t_i} p\dot{v}dt + M_p \int_{T_3}^{T_4} C_p dT \tag{3.3}$$

Where E_h is energy consuming

M_p is mass of plastic

C_m is specific heat capacity of mold

p is injection pressure

$\dot{v}$ is volumetric injection rate

C_p is specific heat capacity of plastic

The solution can be show in Appendix D.

CHAPTER 4

RESULTS AND DISCUSSION

4.1 Gloss result

Guoqun Zhao [45] is investigated the correlation between cavity surface temperature just before filling and the surface gloss of the molded parts for ABS/PMMA/nano-C_aCO_3 and FRPP. The result reported the surface gloss of the molded part can be greatly improved by increasing the cavity surface temperature just before filling. As the cavity surface just before filling rise from 25 °C to 183 °C, the surface gloss of the part for ABS/PMMA/nano-C_aCO_3 and FRPP can be increased from 46% to 88% and from 0% to 71%. The experimental results show that the injection molded resin forced plastic parts can also have very smooth and glossy surfaces as long as the cavity surface temperature just before filling is high enough.

In this experiment is investigated in gloss's measurement that in this case studied the relationship between gloss's measurement and injection parameters. The injection parameters are mold temperature (see in **4.1.1**), barrel temperature (see in **4.1.2**), packing pressure (see in **4.1.3**), packing time (see in **4.1.4**), and injection speed (see in **4.1.5**).

4.1.1 Effect of mold temperature

4.1.1.1 ABS

From experiment, in **Figure 4.1** is the effect of mold temperature in injection molding with ABS, that are ABS KU901, ABS SP200, and ABS GA300. In this case, the temperature between 20 °C and 80 °C used conventional injection molding. However, the temperture between 100 °C and 120 °C used injection molding via rapid heating and cooling system. It is used heating and cooling technique bacause the product is stability part and can eject it.

From the **Figure 4.1**,when The mold temperature is increasing, the surface's gloss will be increased. In the ABS KU901, the surface's gloss is rising from 92.82 GU to 102.46 GU. Then in the ABS SP200, the surface's gloss is rising from 94.03 GU to 103.42 GU. And the last is ABS GA300, the surface's gloss is rising from 86.71 GU to 103.46 GU.

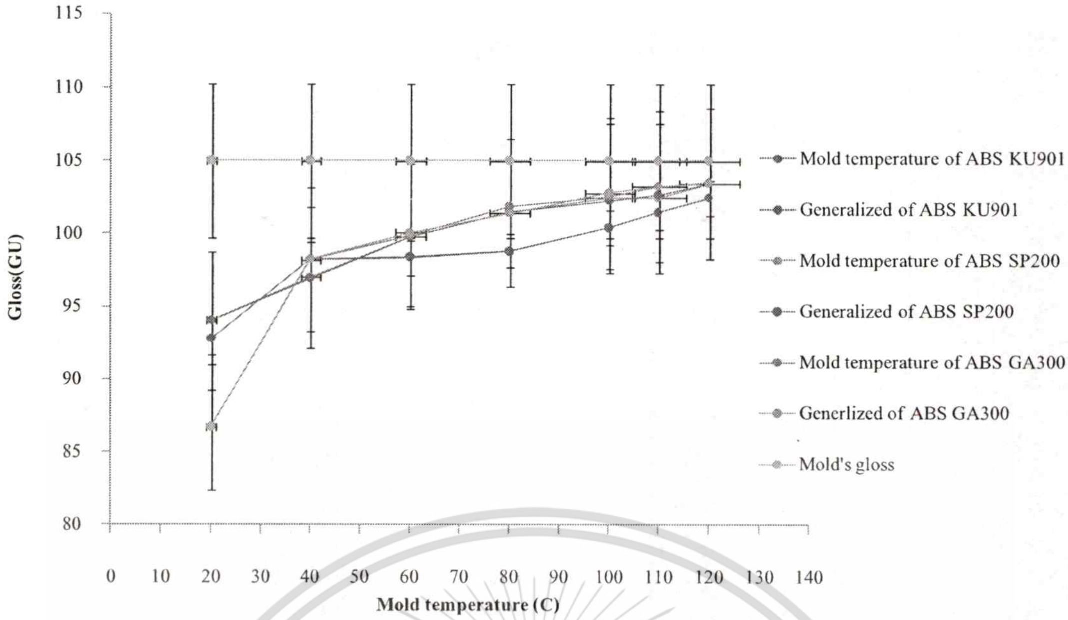

Figure4.1 Effect of mold temperature in Injection molding with ABS(surface's gloss)

Where;

$$y=\begin{cases}0.27x+89.42; x=[20,40]\\ 0.01575x+97.52167; x=[60,80]\\ 0.1025x+90.17167; x=[100,110,120]\end{cases}, \text{Generlized of ABS KU901}$$

$$y=\begin{cases}0.14375x+91.18667; x=[20,40,60]\\ 0.036929x+98.56357; x=[80,100]\\ 0.093x+92.26; x=[110,120]\end{cases}, \text{Generlized of ABS SP200}$$

$$y=\begin{cases}0.5755x+75.2; x=[20,40]\\ 0.06825+95.9733; x=[60,80]\\ 0.023x+100.7; x=[100,110,120]\end{cases}, \text{Generlized of ABS GA300}$$

The reson of this result is temperature variations of viscosity. It can consider the effect of viscosity variation for liquid by using the free volume concept or by reaction-rate concepts. The latter give a temperature dependence of η (for Newtonian fluids) in the form

$$\eta = B\exp(E/RT) \tag{4.1}$$

where E is an activation energy, R is the gas constant(8.314 $JK^{-1}mol^{-1}$) and T is the absolute temperature.

It has a relationship between the viscosity and temperature is invariant direction. Then the result is also related with this relation.

4.1.1.2 POM

From experiment, in **Figure 4.2** is the effect of mold temperature in injection molding with POM that are POM M90 and POM M270. In POM M90 experiment, the surface's gloss is rapidly increased from 41.11 GU to 94.76 GU. In POM M270, the surface's gloss is increased form 83.47 GU to 96.35 GU.

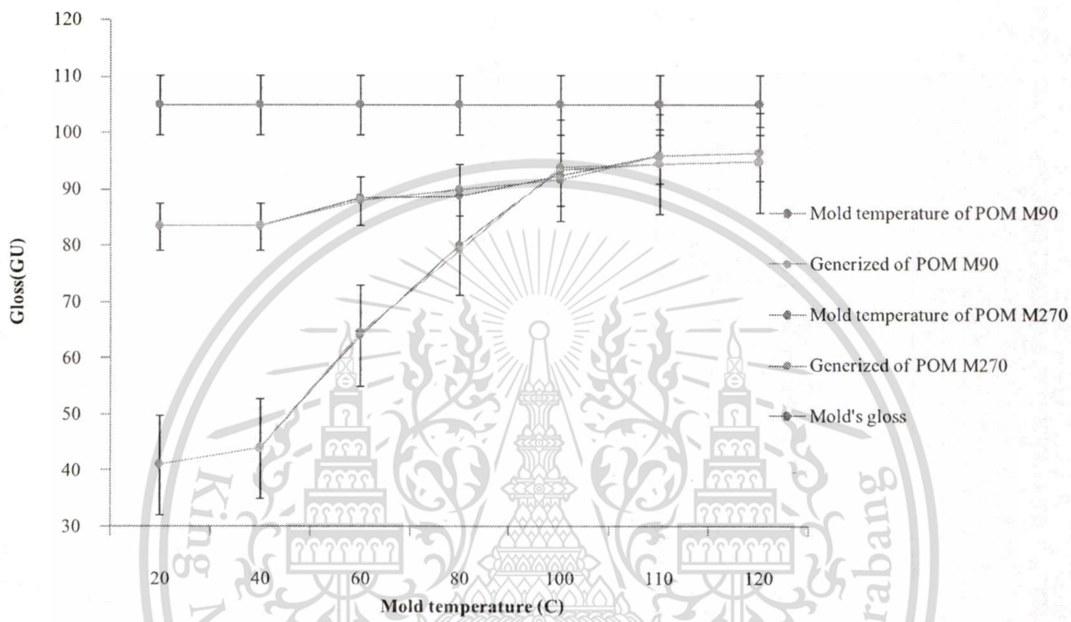

Figure4.2 Effect of mold temperature in injection molding with POM(surface's gloss)

Where;

$$y=\begin{cases}0.148x+38.15; x=[20,40]\\0.73175x+20.6533; x=[60,80,100]\\0.031x+91.04; x=[110,120]\end{cases}, \text{Generlized of POM M90}$$

$$y=\begin{cases}0.01x+83.47; x=[20,40]\\0.09425x+82.33667; x=[60,80,100]\\0.057x+89.51; x=[110,120]\end{cases}, \text{Generlized of POM M270}$$

In the effect of mold temperature conditions in injection molding with ABS and POM, there are the relationship between mold temperature and surface's gloss. In this case, the surface's gloss will be increase the gloss's value, when the mold temperaturature is increased. The relation is direct variation.

It has a relationship between the viscosity and temperature is invariant direction. Then the result is also related with this relation.

4.1.2 Effect of barrel temperature

4.1.2.1 ABS

In the **Figure 4.3** is the effect of barrel temperature in injection molding with ABS SP200. The barrel temperature conditions are three values that are 220°C, 230°C, and 240°C. The barrel temperature at 230°C is gloss's measured 99.78 GU(60°). From the **Figure 4.3**, the condition at 230°C is better gloss's value than the condition at 220°C(98.8 GU(60°) but in the condition at 230°C and the condition at 240°C, there are the same gloss's value about 99.8 GU(60°). The mold's gloss that is the estimated experiment is shown in red line in **Figure 4.3.**

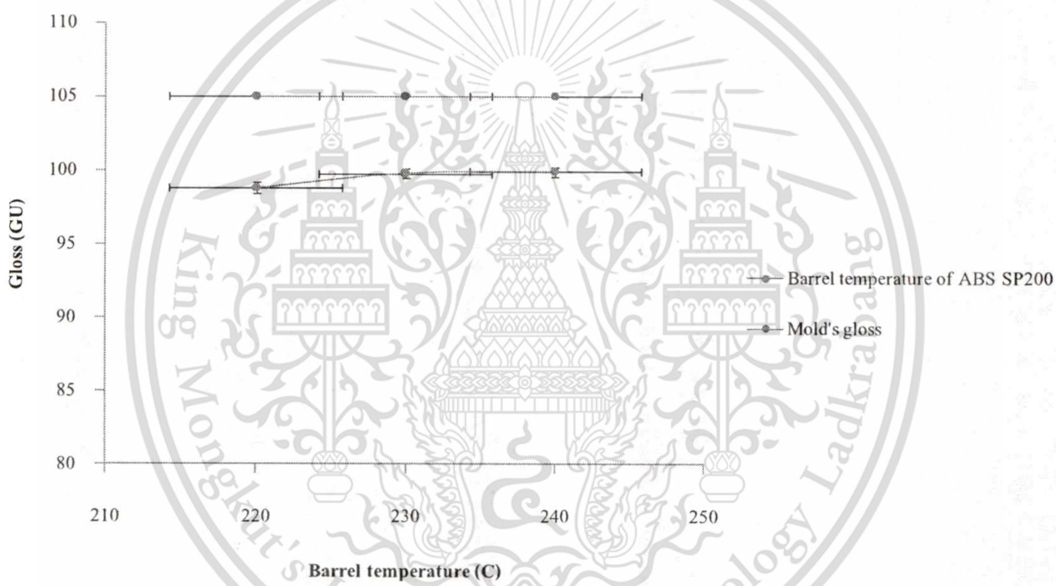

Figure4.3 Effect of barrel temperature on Injection molding with ABS (surface's gloss)

4.1.2.2 POM

In the **Figure 4.4** is the effect of barrel temperature in injection molding with POM that are POM M90 and POM M270. The barrel temperature conditions are three values that are 220°C, 230°C, and 240°C. In POM M90, the barrel temperature at 220°C, 230°C, and 240°C are the same gloss's value 78.4 GU. In POM M270, are the same gloss's value 87.88 GU. The mold's gloss that is the estimated experiment is shown in red line in **Figure 4.4.**

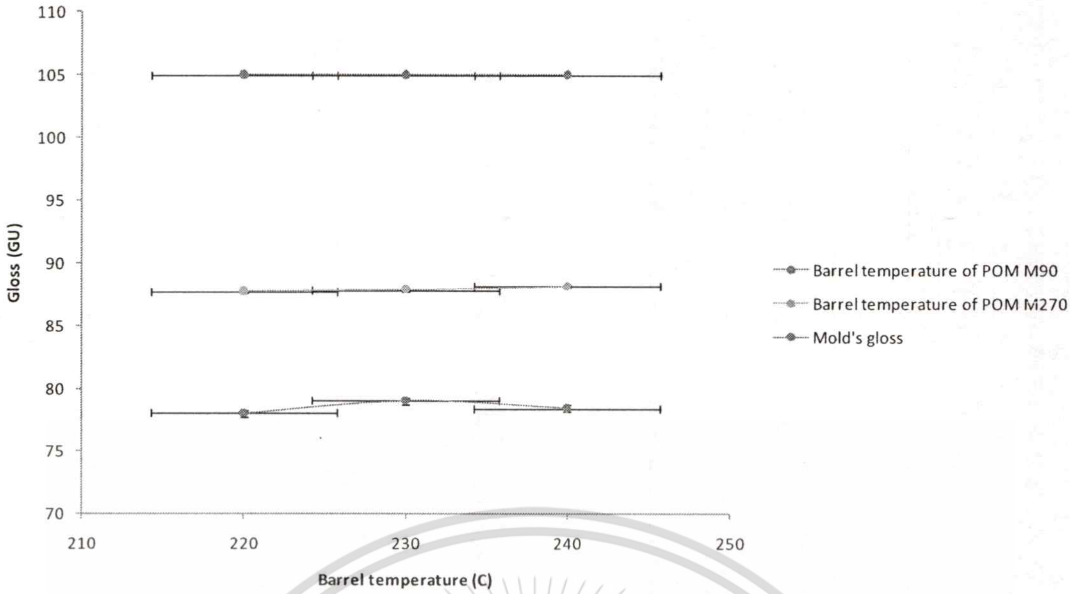

Figure4.4 Effect of barrel temperature in injection molding with POM (surface's gloss)

The effect of barrel temperature in injection molding with ABS and POM, the suface's gloss are stable, when the barrel temperature are increased.

4.1.3 Effect of packing pressure

4.1.3.1 ABS

In **Figure 4.5** is shown the effect of packing pressure in injection molding and the estimated mold's gloss value(105 GU(60°)). The packing pressure conditions are five values that are 100 bar, 200 bar, 300 bar, 450 bar, and 500 bar. In the **Figure4.5**, the packing pressure is 100 bar, the gloss's value is 99.76 GU(60°) that is the highest value in this case. The trend of case is reduce surface's gloss, when there are increased packing pressure. The surface's gloss is decreased because the packing pressure is related with viscosity in indirect variance.

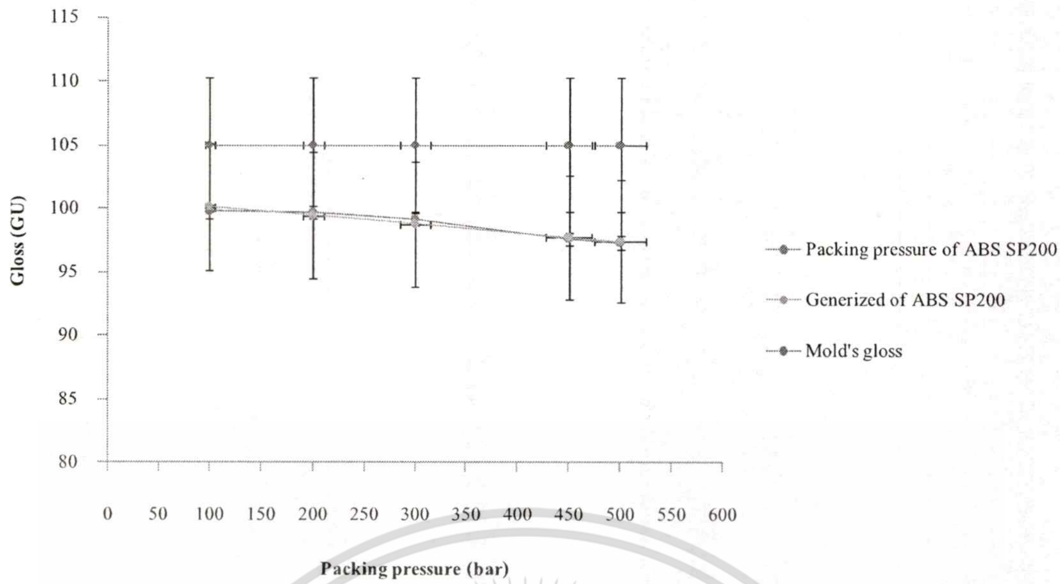

Figure4.5 Effect of packing pressure in injection molding with ABS (surface's gloss)

Where;

$y = -0.00673x + 100.791; x = [100, 200, 300, 450, 500]$, Generlized of ABS SP200

The reson of this result is packing pressure variations of viscosity. It can consider the effect of viscosity variation for liquid by using the free volume concept or by reaction-rate concepts. The latter give a temperature dependence of η (for Newtonian fluids) in the form

$$\eta = \eta(0)\exp(p/\beta) \tag{4.2}$$

From the equation 4.2, the relation between η and packing pressure is direct variant. Then from the packing result, it also related with the viscosity.

4.1.3.2 POM

In **Figure 4.6** is shown the effect of pack pressure in injection molding and the estimated mold's gloss value(105 GU(60°)). The pack pressure conditions are five values that are 100 bar, 200 bar, 300 bar, 400 bar, and 500 bar. In the M90, the surface's gloss is decreased from 73.35 GU(60°) to 69.51 GU(60°). In the POM M270, the surface's gloss is stable at 88.15 GU(60°). The surface's gloss is decreased because the packing pressure is related with viscosity in indirect variance (equation 4.2).

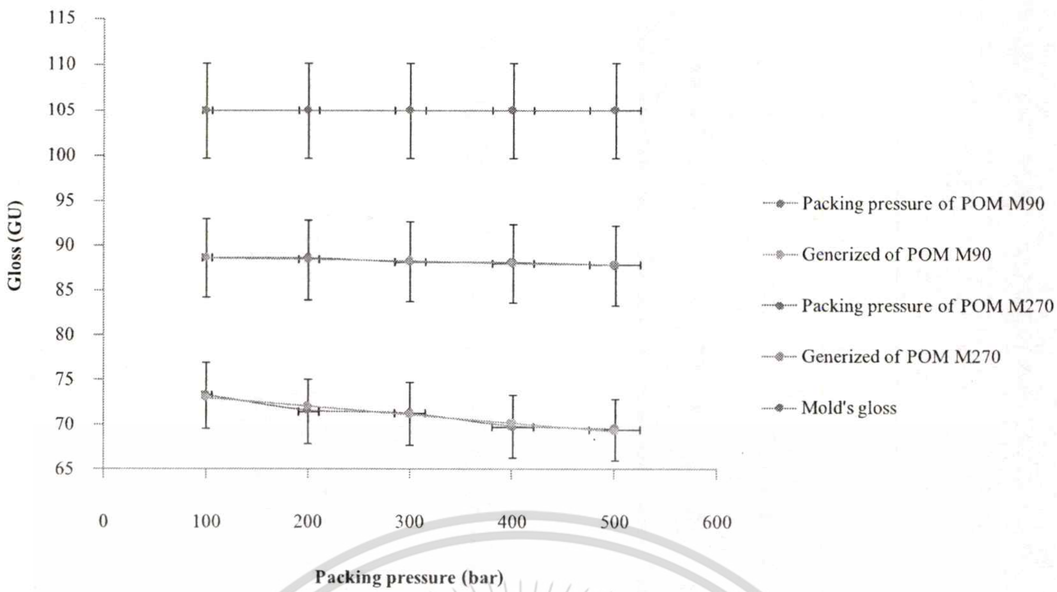

Figure4.6 Effect of packing pressure in injection molding with POM(surface's gloss)

Where;

$y = -0.00941x + 73.943; x = [100, 200, 300, 400, 500]$, Generlized of POM M90

$y = -0.00212x + 88.874; x = [100, 200, 300, 400, 500]$, Generlized of POM M270

From the equation 4.2, the relation between η and packing pressure is direct variant. Then from the packing result, it also related with the viscosity.

4.1.4 Effect of packing time

4.1.4.1 ABS

In **Figure 4.7** is shown the effect of packing time in injection molding and estimated mold's gloss value. In this case, used special technique in injection molding that is heating and cooling control system. The packing time conditions are four values that are 3 sec, 5 sec, 7 sec and 9 sec. The pack pressure of conventional injection is ABS SP200, when the packing time is 1 sec, the gloss's value is 98.2 GU(60°) that is the lowest gloss's value in this case. The packing time at 3 sec, 5 sec, 7 sec and 9 sec are equal value about 99.56 GU(60°).

In injection molding via heating and cooling system, when the packing time is 3 sec, the gloss's value of ABS KU901 is 101.61 GU(60°). The surface's gloss of ABS SP200 is 100.49 GU(60°) and ABS GA300 is 100.28 GU(60°). The packing time at 5 sec, 7 sec and 9 sec are equal value about 102.3 GU(60°)(ABS KU901), 102.45 GU(60°)(ABS SP200), and 102.46 GU(60°)(ABS GA300).

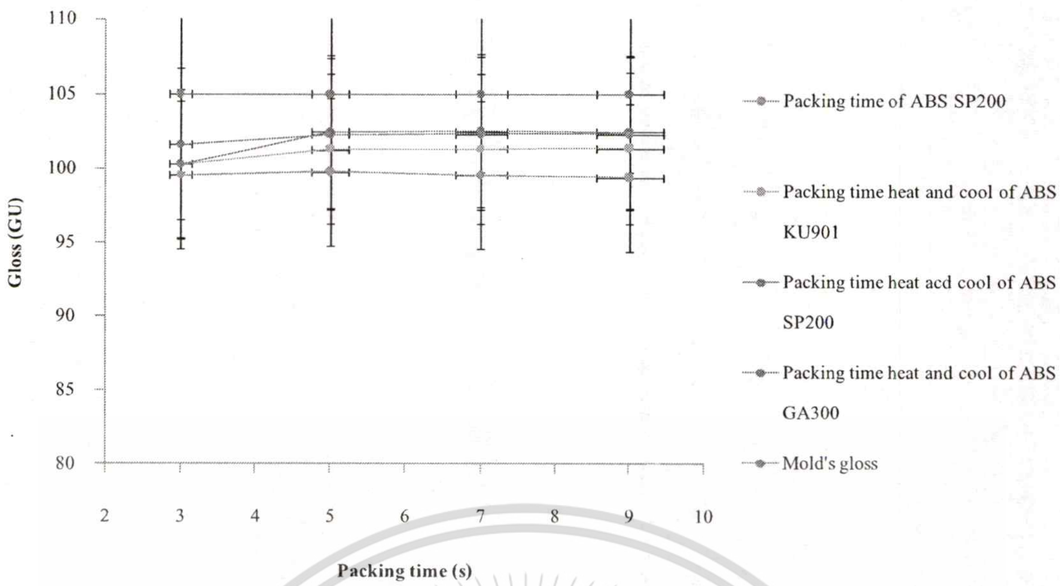

Figure4.7 Effect of packing time in injection molding with ABS(surface's gloss)

4.1.4.5 POM

In **Figure 4.8** is shown the effect of pack pressure time in injection molding with POMs that are POM M90 and POM M270. In this study is the effect of pack pressure time in injection molding via heating and cooling control system. In the **Figure 4.8**, the pack pressure time conditions are five values that are 1 sec, 3 sec, 5 sec, 7 sec and 9 sec.

In conventional injection at POM M90, the surface's gloss is little increased from 68.65 GU(60°) to 74.47 GU(60°). In POM M270, the surface's gloss is stable at 88 GU(60°).

In the injection molding via heating and cooling system, POM M90 is increased surface's gloss value from 94.56 GU(60°) to 96.41 GU(60°). POM M270 is increased surface gloss value from 96.28 GU(60°) to 97.25 GU(60°).

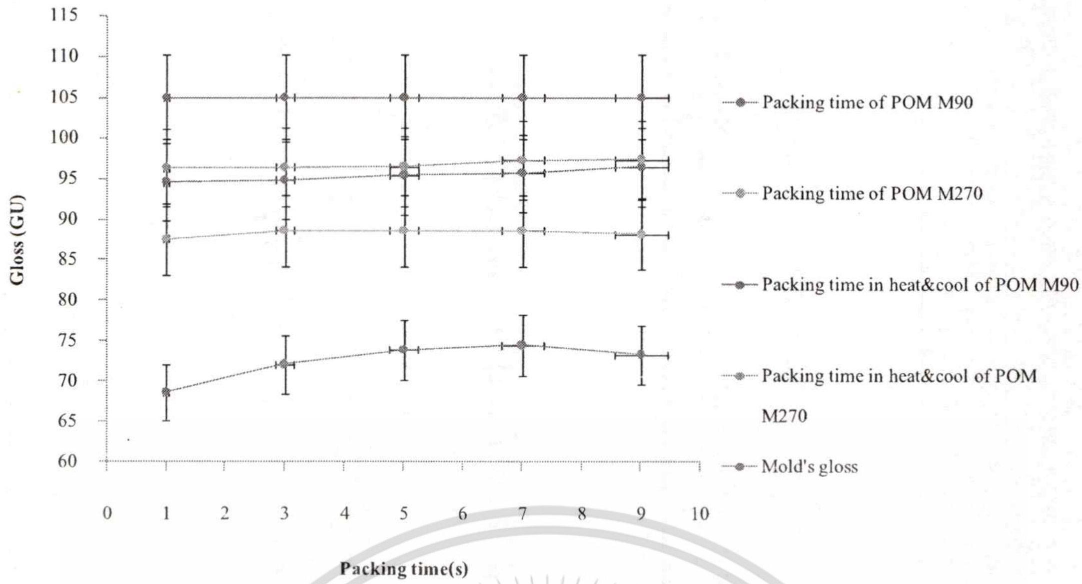

Figure4.8 Effect of packing time in injection molding with POM(surface's gloss)

4.1.5 Effect of injection speed

4.1.5.1 ABS

In **Figure 4.9** is shown the effect of injection speed in injection molding with ABS SP200. The injection speed condition are six values that are 10 mm/s, 20 mm/s, 30 mm/s, 40 mm/s 50 mm/s, and 70 mm/s. The gloss's value is increased from 97.96 GU(60°) to 101.16 GU(60°) when the injection speed is manipulated up.

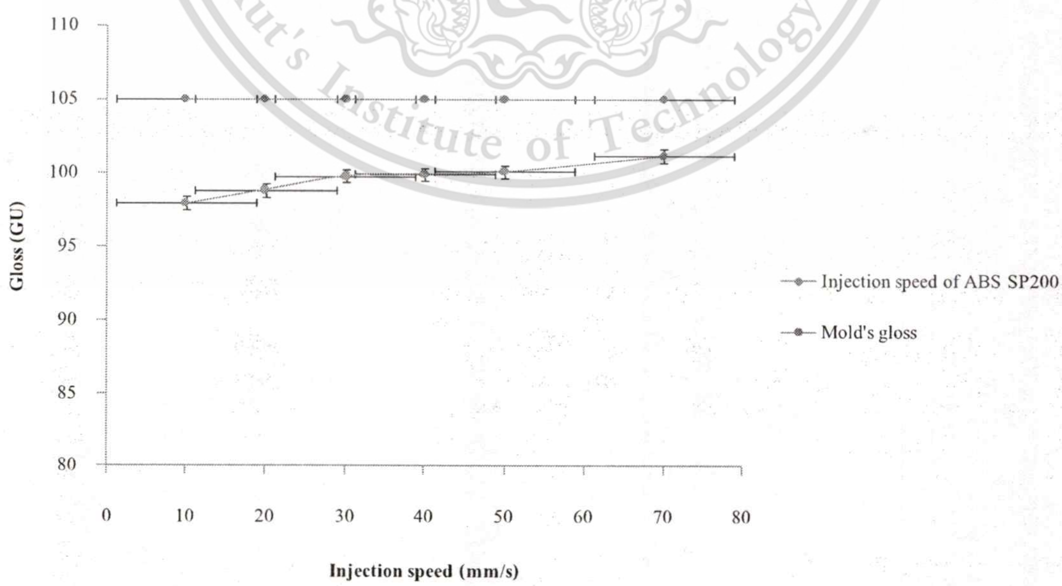

Figure4.9 Effect of pack injection speed in injection molding with ABS SP200(surface's gloss)

4.1.5.2 POM

In **Figure 4.10** is shown the effect of injection speed in injection molding with POMs, that are POM M90 and POM M270. The injection speed condition are five values that are 10 mm/s, 20 mm/s, 30 mm/s, 50 mm/s, and 70 mm/s. The gloss's value (POM M90) is increased from 62.38 GU(60°) to 71.8 GU(60°) and the gloss's value (POM M270) is increased from 78.9 GU(60°) to 88.77 GU(60°) when the injection speed is manipulated up.

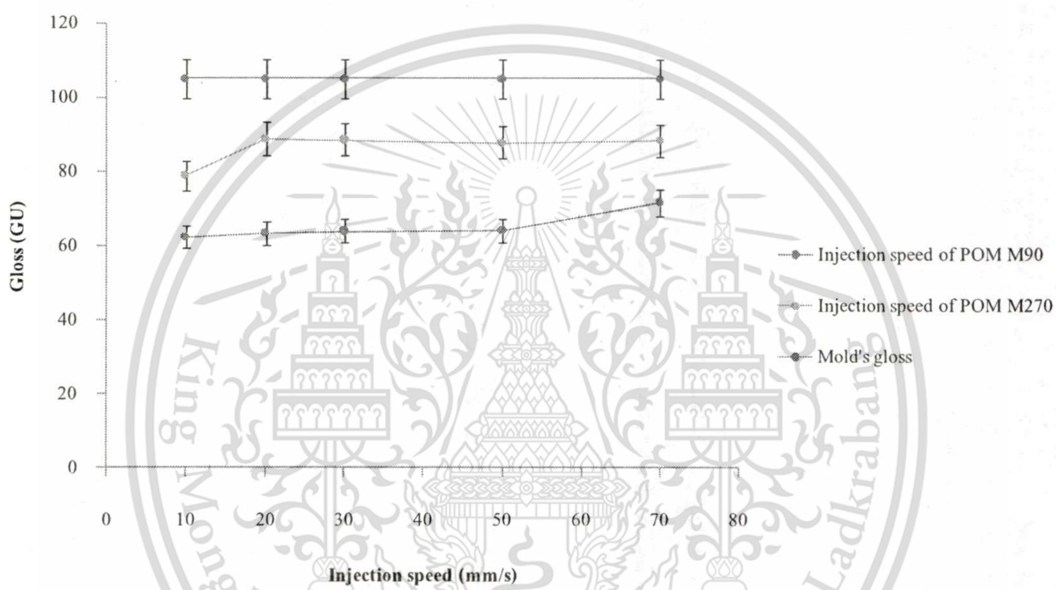

Figure4.10 Effect of pack injection speed in injection molding with POM(surface's gloss)

4.2 Roughness result

Kuo-Ming Tsai [46] suggested that the Taguchi experiment on roughness of products. The result represented that the control factors only had a minor effect on roughness of products. The optimum combination of process parameters are a barrel temperature of 230°C, screw speed of 10 m/min, injection speed of 70 mm/s, injection pressure of 100 MPa, packing pressure of 120 MPa, packing time of 4s, mold temperature of 60°C and cooling time of 20 s. A mold with a rougher insert products a rougher surface finish of products, however the process parameters have only limited effects.

In this experiment is investigated in surface's roughness that in this case studied the relationship between surface's roughness and injection parameters. The injection parameters are mold temperature (see in **4.2.1**), barrel temperature (see in **4.2.2**), packing pressure (see in **4.2.3**), packing time (see in **4.2.4**), and injection speed (see in **4.2.5**).

4.2.1 Effect of mold temperature

4.2.1.1 ABS

In **Figure 4.11** is shown the effect of mold temperature in injection molding with ABSs, that are ABS KU901, ABS SP200, and ABS GA300. The mold temperature conditions are seven conditions that that are 20 °C, 40 °C, 60 °C, 80 °C, 100 °C, 110 °C, and 120 °C. Especially, there is used injection molding via heating and cooling system in 100 °C, 110 °C, and 120 °C because the products are stability part and can eject them.

The surface's roughness of ABS is rapidly decreased the roughness value, when the mold temperature is increasing from 20 °C to 120 °C. The ABS KU901, the surface's roughness is decreased from 0.135 μm to 0.025 μm. The ABS SP200, the surface's roughness is decreased from 0.114 μm to 0.025 μm. The ABS GA300, the surface's roughness is decreased from 0.077 μm to 0.023 μm.

In this result, it has the relationship between mold temperature and surface's roughness. The relation is reverse variation.

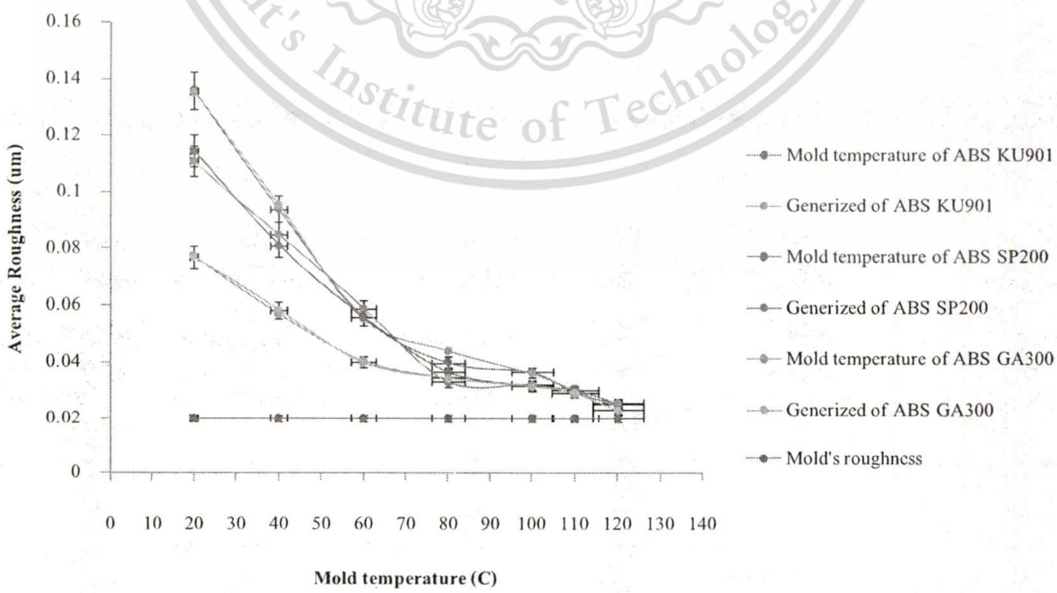

Figure4.11 Effect of mold temperature in injection molding with ABS(surface's roughness)

Where;

$$y=\begin{cases}-0.002x+0.175; x=[20,40,60]\\ -0.00048+0.082556; x=[80,100]\\ -0.00057x+0.092556; x=[110,120]\end{cases}\text{, Generlized of ABS KU901}$$

$$y=\begin{cases}-0.00072x+0.23133; x=[20,40]\\ -0.00282x+0.31633; x=[60,80]\\ -0.00037x+0.094222; x=[100,110,120]\end{cases}\text{, Generlized of ABS SP200}$$

$$y=\begin{cases}-0.00093x+0.09522; x=[20,40,60]\\ -0.00015x+0.04633; x=[80,100]\\ -0.0066x+0.095; x=[110,120]\end{cases}\text{, Generlized of ABS GA300}$$

From this equation 4.1, the relationship between viscosity and temperature is indirect variant. Then the result is also related with the relationship.

4.2.1.4 POM

In **Figure 4.12** is shown the effect of mold temperature in injection molding with POMs that are POM M90 and POM M270. The mold temperature conditions are seven conditions that that are 20 $^{\circ}$C, 40 $^{\circ}$C, 60 $^{\circ}$C, 80 $^{\circ}$C, 100 $^{\circ}$C, 110 $^{\circ}$C, and 120 $^{\circ}$C. Especially, there is used injection molding via heating and cooling system in 100 $^{\circ}$C, 110 $^{\circ}$C, and 120 $^{\circ}$C because the products are stability part and can eject them.

The surface's roughness of POM is rapidly decreased the roughness value. The POM M90, the roughness value is decreased from 0.217 μm to 0.091 μm. The POM M270, the roughness value is decreased from 0.35 μm to 0.036 μm.

In this result, it has the relationship between mold temperature and surface's roughness. The relation is reverse variation.

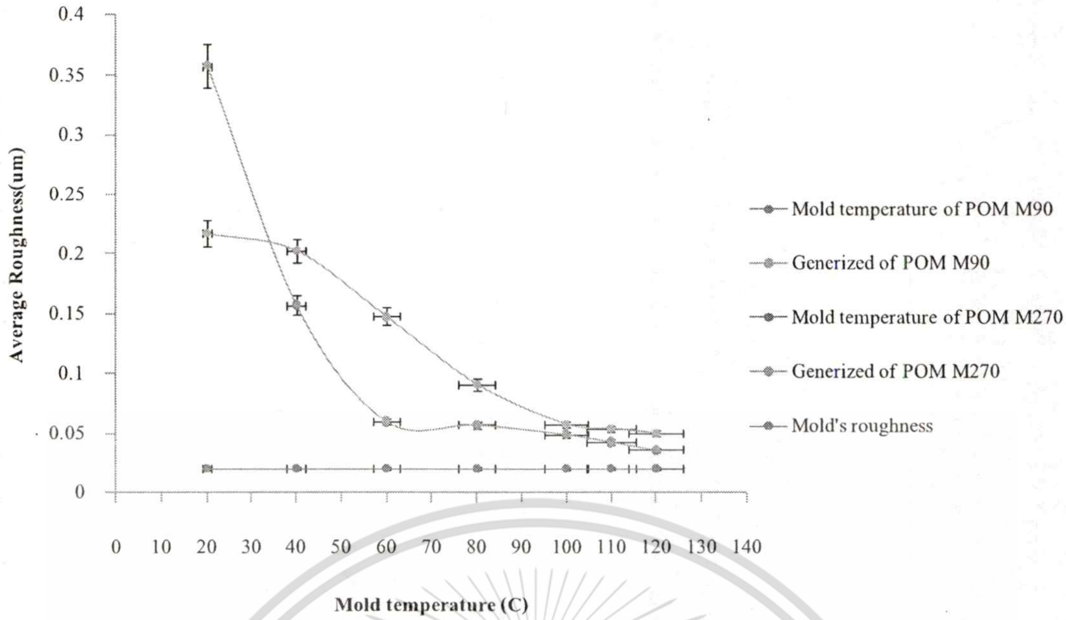

Figure4.12 Effect of mold temperature in injection molding with POM(surface's roughness)

Where;

$$y=\begin{cases} -0.00072x+0.23133; x=[20,40] \\ -0.00282x+0.31633; x=[60,80] \\ -0.00037x+0.094222; x=[100,110,120] \end{cases}, \text{Generlized of POM M90}$$

$$y=\begin{cases} -0.01003x+0.558333; x=[20,40] \\ -0.00015x+0.069; x=[60,80] \\ -0.00065x+0.114056; x=[100,110,120] \end{cases}, \text{Generlized of POM M270}$$

From this equation 4.1, the relationship between viscosity and temperature is indirect variant. Then the result is also related with the relationship.

4.2.2 Effect of barrel temperature

4.2.2.1 ABS

In Figure 4.13 is shown the effect of barrel temperature in injection molding with ABS SP200. The barrel temperature conditions are three conditions that are 220 °C, 230 °C, and 240 °C. In the conditions between 220 °C and 240 °C, the surface's roughness is decreased from 0.064 µm to 0.046 µm.

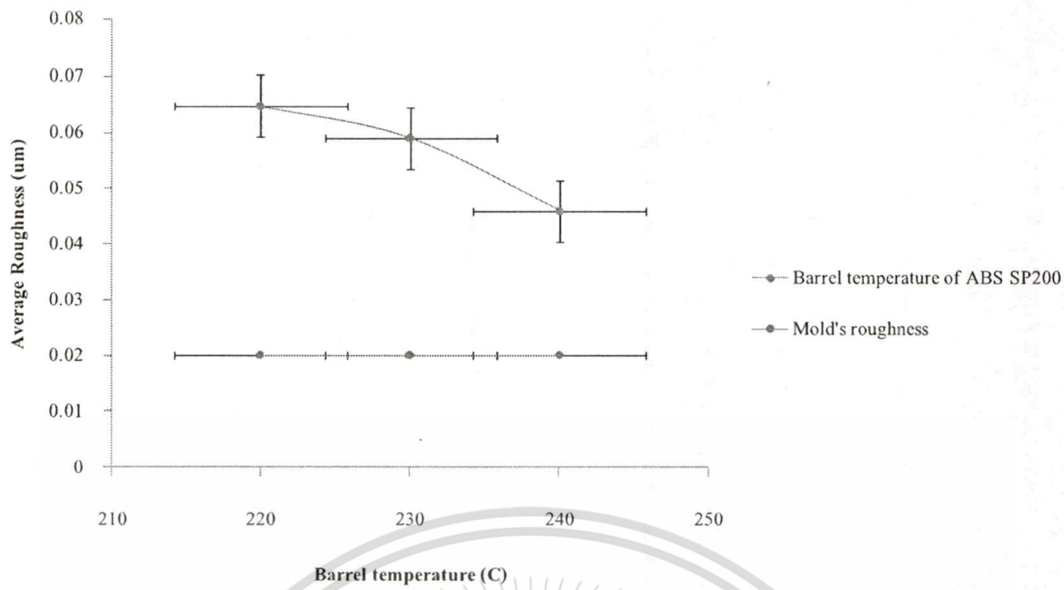

Figure4.13 Effect of barrel temperature in injection molding with ABS(surface's roughness)

4.2.2.2 POM

In Figure 4.14 is shown the effect of barrel temperature in injection molding with POMs that are POM M90 and POM M270. The barrel temperature conditions are four conditions that are 210 °C, 220 °C, 230 °C, and 240 °C. In the POM M90, the surface's roughness is decreased from 0.135 μm to 0.124 μm. In the POM M270, the surface's roughness is decreased from 0.085 μm to 0.047 μm.

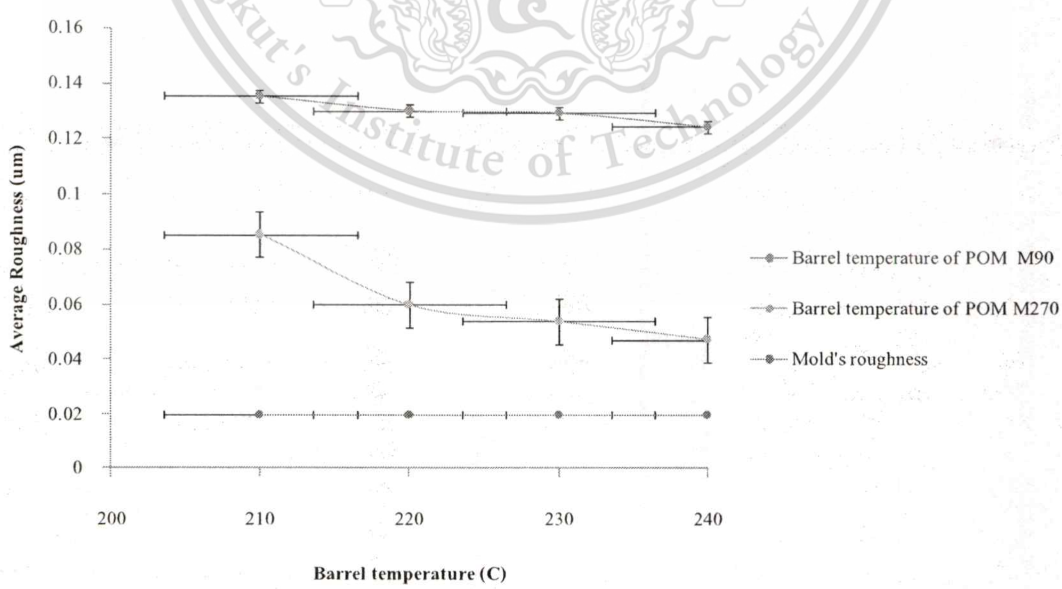

Figure4.14 Effect of barrel temperature in injection molding with POM(surface's roughness)

4.2.3 Effect of packing pressure

4.2.3.1 ABS

In **Figure 4.15** is shown the effect of packing pressure in injection molding with ABS SP200. The packing pressure conditions are five values that are 100 bar, 200 bar, 300 bar, 450 bar and 500 bar. In the ABS SP200, the surface's roughness is increased from 0.048 μm to 0.079 μm. The surface's roughness is increased because the packing pressure is related with viscosity in indirect variance (equation 2.15).

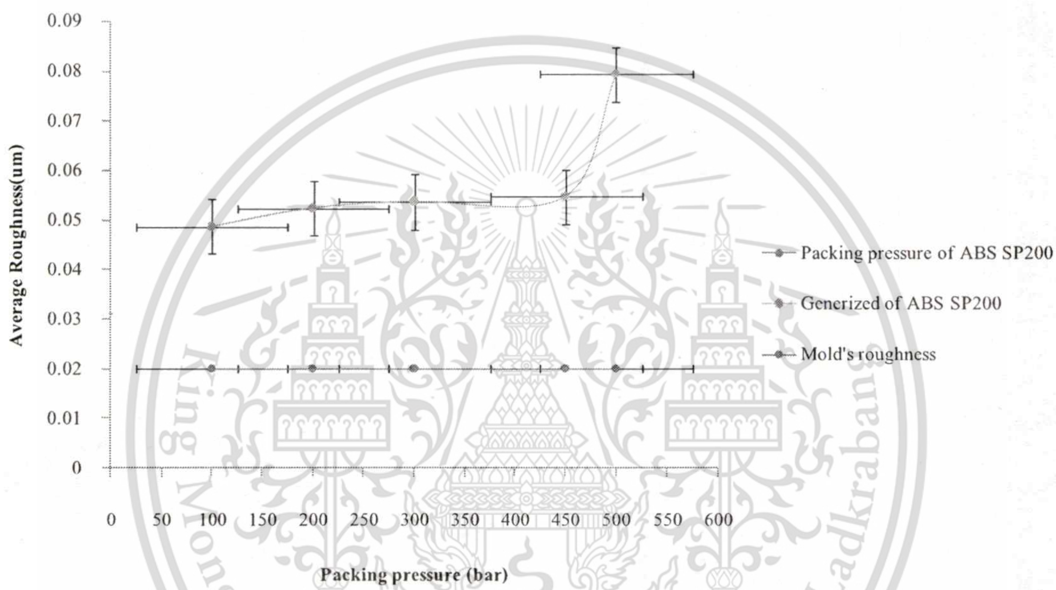

Figure4.15 Effect of packing pressure in injection molding with ABS(surface's roughness)

Where;

$$y=\begin{cases} 0.0000367x+0.045; x=[100,200] \\ 0.00000667x+0.051667; x=[300,450] \\ 0.000493x-0.16733; x=[450,500] \end{cases}, \text{ Generlized of ABS SP200}$$

From this equation 4.2, the relationship between viscosity and packing pressure is direct variant. Then the result is also related with the relationship.

4.2.3.2 POM

In **Figure 4.16** is shown the effect of packing pressure in injection molding with POMs that are POM M90 and POM M270. The packing pressure conditions are five values that are 100 bar, 200 bar, 300 bar, 400 bar and 500 bar. In POM M90, the roughness value is rapidly increased from 0.115 μm to 0.217 μm. In POM M270, the roughness value is rapidly increased from 0.039

μm to 0.17 μm. The surface's roughness is increased because the packing pressure is related with viscosity in indirect variance (equation 2.15).

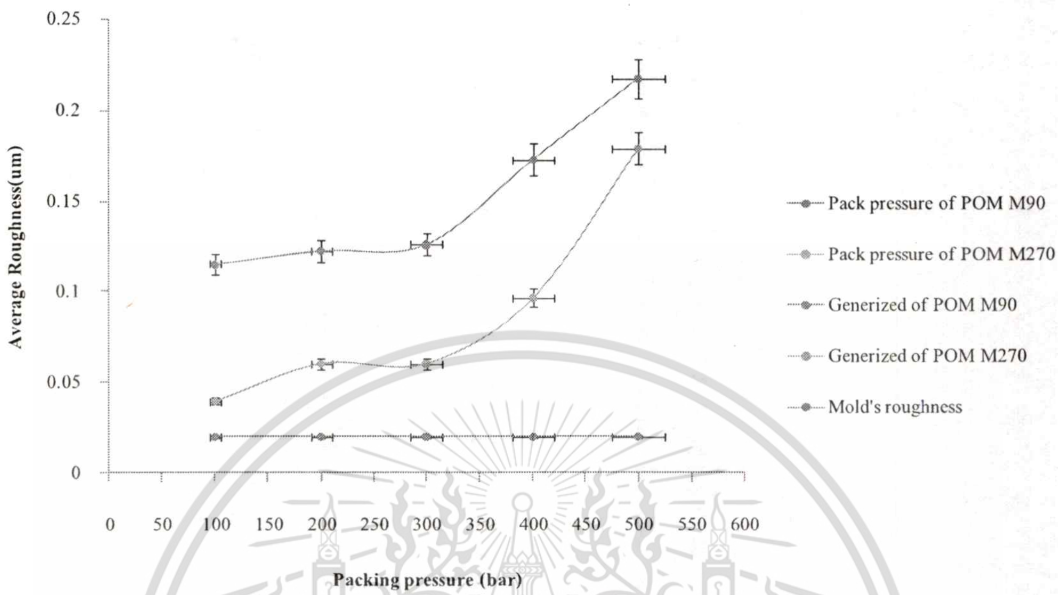

Figure4.16 Effect of packing pressure in injection molding with POM(surface's roughness)

Where;

$$y=\begin{cases} 0.0000733x+0.107667; x=[100,200] \\ 0.000467x-0.014; x=[300,400] \\ 0.000823x-0.233; x=[400,500] \end{cases}, \text{Generlized of POM M90}$$

$$y=\begin{cases} 0.000207x+0.018667; x=[100,200] \\ 0.000363x-0.049; x=[300,400] \\ 0.000823x-0.0233; x=[400,500] \end{cases}, \text{Generlized of POM M270}$$

From this equation 4.2, the relationship between viscosity and packing pressure is direct variant. Then the result is also related with the relationship.

4.2.4 Effect of packing time

4.2.4.1 ABS

In **Figure 4.17** is shown the effect of packing time in injection molding with ABS that are ABS KU901, ABS SP200, and ABS GA300. The conventional injection molding (ABS SP200), the roughness value is decreased from 0.093 μm to 0.035 μm. In this condition, it has a special technique that is injection molding via heating and cooling control system. The packing time conditions are four values that are 3 sec, 5 sec, 7 sec, and 9 sec.

In ABS KU901, the roughness value is decreased from 0.093 µm to 0.035 µm. In ABS SP200, the roughness value is decreased from 0.031 µm to 0.024 µm. In ABS GA300, the roughness value is decreased from 0.029 µm to 0.023 µm.

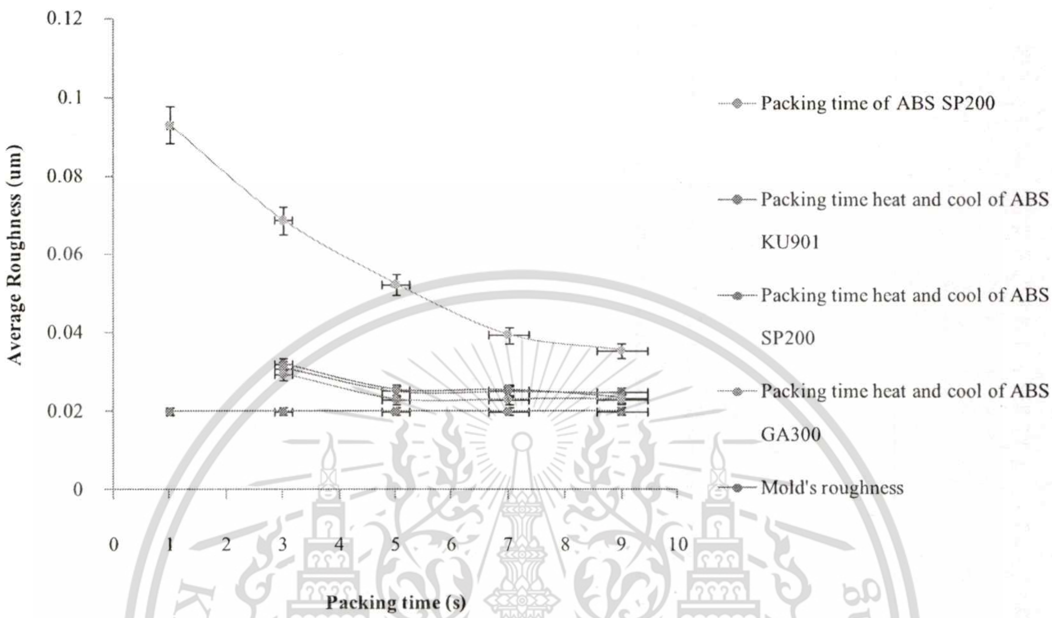

Figure4.17 Effect of packing time in injection molding with ABS(surface's roughness)

4.2.4.2 POM

In **Figure 4.18** is shown the effect of packing time in injection molding with POM that are POM M90 and POM M270. The conventional injection molding (POM M90), the roughness value is decreased from 0.145 µm to 0.070 µm. In POM M270, the roughness value is decreased from 0.082 µm to 0.045 µm.

In this case was used injection molding via heating and cooling system. The roughness value of POM M90 is decreased from 0.056 µm to 0.044 µm. POM M270 is decreased from 0.04 µm to 0.026 µm.

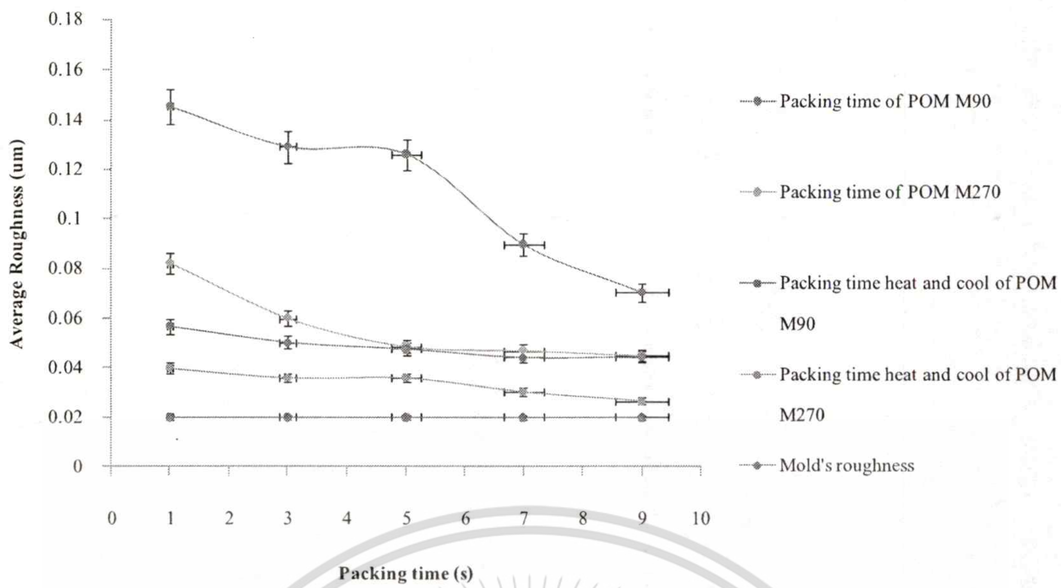

Figure4.18 Effect of pack pressure time in injection molding with POM(surface's roughness

4.2.5 Effect of injection speed

4.2.5.1 ABS

In **Figure 4.19** is shown the effect of injection speed in injection molding with ABS SP200. The injection speed conditions are five conditions that are 10 mm/s, 20 mm/s, 30 mm/s, 50 mm/s and 70 mm/s. In the injection speed between 10 mm/s and 70 mm/s, the surface's roughness is decreased from 0.09 μm to 0.036 μm.

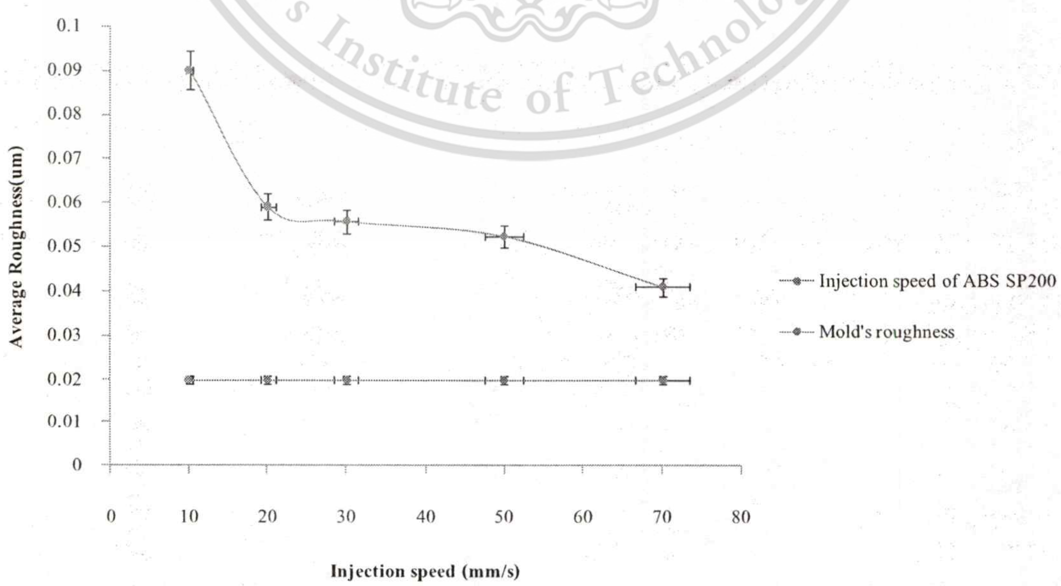

Figure4.19 Effect of injection speed in injection molding with ABS SP200(surface's roughness)

4.2.5.2 POM

In **Figure 4.20** is shown the effect of injection speed in injection molding with POMs that are POM M90 and POM M270. The injection speed conditions are five conditions that are 10 mm/s, 20 mm/s, 30 mm/s, 50 mm/s and 70 mm/s. In the injection speed between 10 mm/s and 30 mm/s, the surface's roughness of POM M90 is decreased from 0.33 μm to 0.23 μm. In POM M270, the surface's roughness is decreased from 0.14 μm to 0.06 μm. In the injection speed between 30 mm/s and 70 mm/s, the surface's roughness of POM M90 is stabled at 0.22 μm. And the POM M270, the surface's roughness is stabled at 0.06 μm.

The trend of this relation can be explained by melt flow index. The POM M270 is higher melt flow index than POM M90 (**4.3**). Although, the surface's roughness of POM M270 is lower than POM M90.

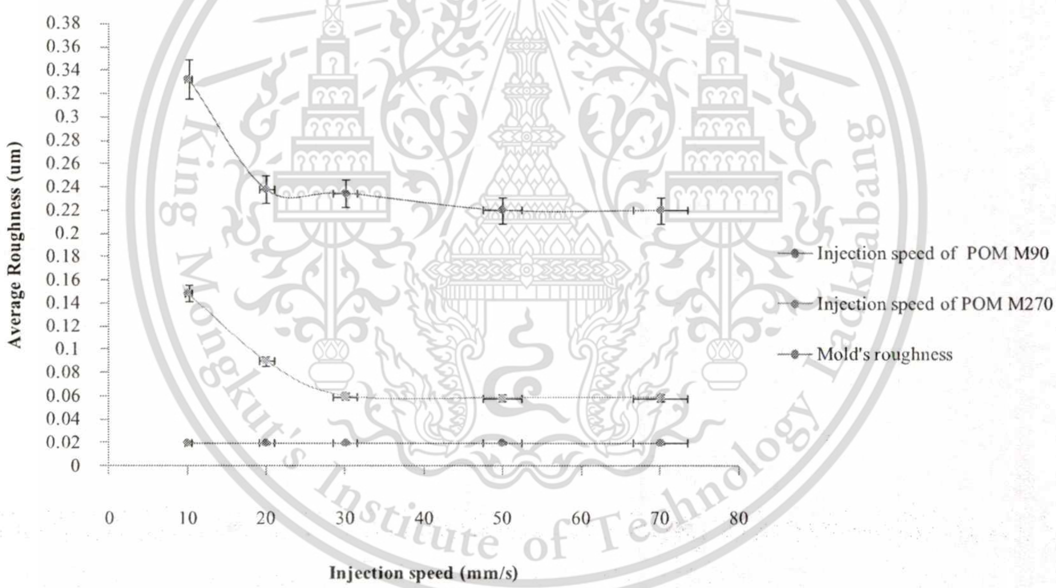

Figure4.20 Effect of injection speed in injection molding with POM(surface's roughness)

4.3 Scanning Electron Microscopy

Guogun zhao [45] studied the micro surface image of the part molded with different cavity surface temperature just before filling for ABS/PMMA/nano-$CaCO_3$ and FRPP. It can be clearly seen that there are a lot of nano-$CaCO_3$ and also many glass fibres exposed on the part surface for

FRPP. The concluded that exposed particles and fibres should be responsible for the roughness part surface.

From the **4.1** and **4.2** are studied in the effect of parameters injection molding for finishing surface. The main parameters are mold temperature and pack pressure are effected in surface's gloss and surface's roughness. The micro surface images of the parts are presented in **4.3.1**, that is the effect of mold temperature in injection molding and in **4.3.2** is the effect of pack pressure in injection molding.

4.3.1 Effect of mold temperature

4.3.1.1 ABS

From **4.1.1** and **4.2.1** were studied the effect of mold temperature. The surface's gloss was increased values and the surface's roughness was decreased values, when the mold temperature was increased. In this part shown the micro surface images of the ABS parts, that represented in **Figure 4.21**(ABS KU901), **Figure 4.22**(ABS SP200), and **Figure 4.23**(ABS GA300). It can be clearly seen that there are a lot butadiene on low mold temperature. However, the butadiene on surface was decreased in high mold temperature. There are related with the previous study that is surface finishing. The relation in gloss is direct-change and the relation in roughness is indirect-change.

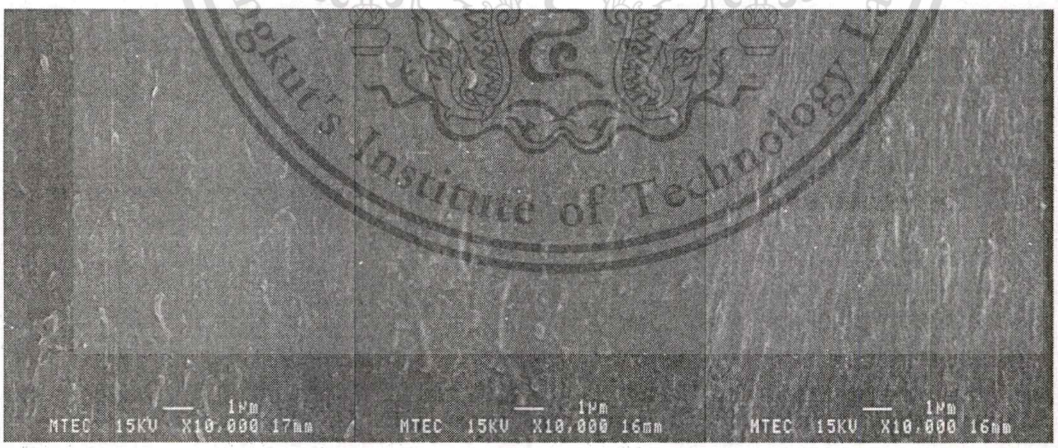

(a) (b) (c)

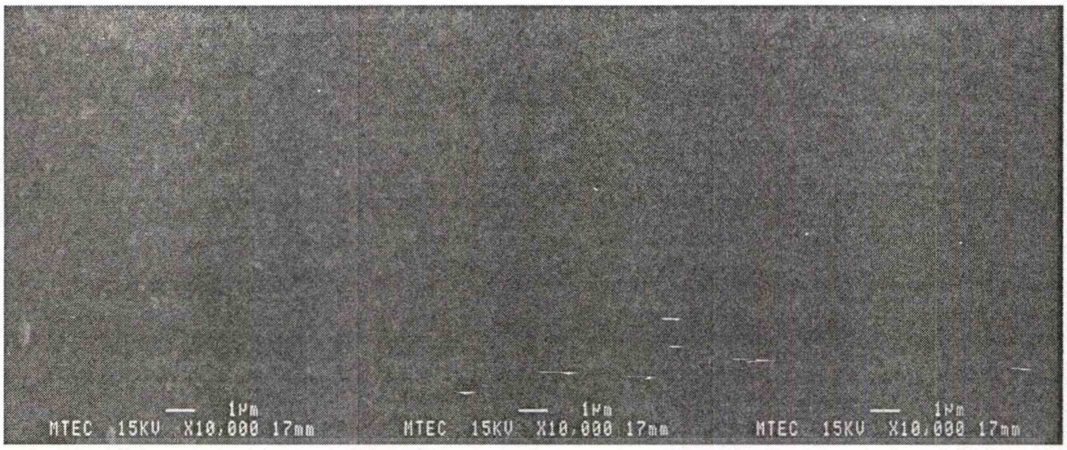

(d) (e) (f)

Figure 4.21 The SEM micrograph of mold temperature in ABS KU901 (a) 20°C, (b) 40 °C, (C) 60 °C, (d)100 °C, (e) 110 °C, and (f) 120 °C

(a) (b) (c)

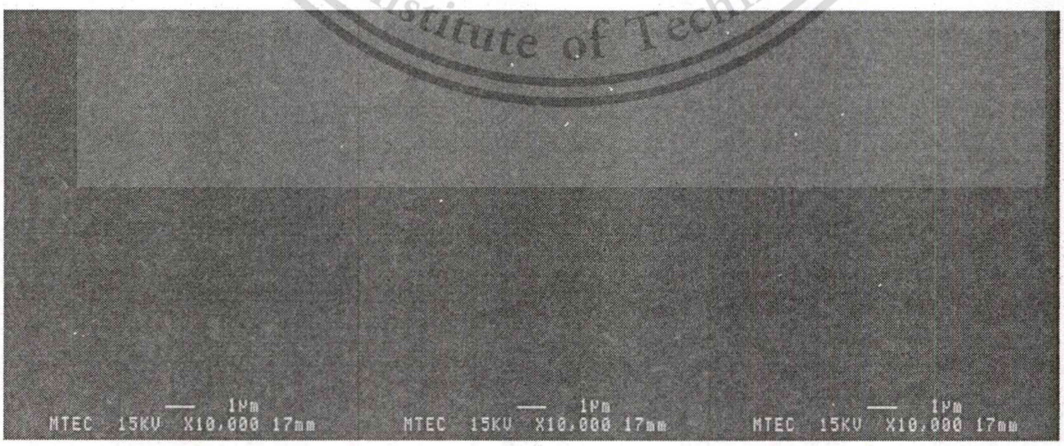

(d) (e) (f)

Figure 4.22 The SEM micrograph of mold temperature in ABS SP200 (a) 20°C, (b) 40 °C, (C) 60 °C, (d)100 °C, (e) 110 °C, and (f) 120 °C

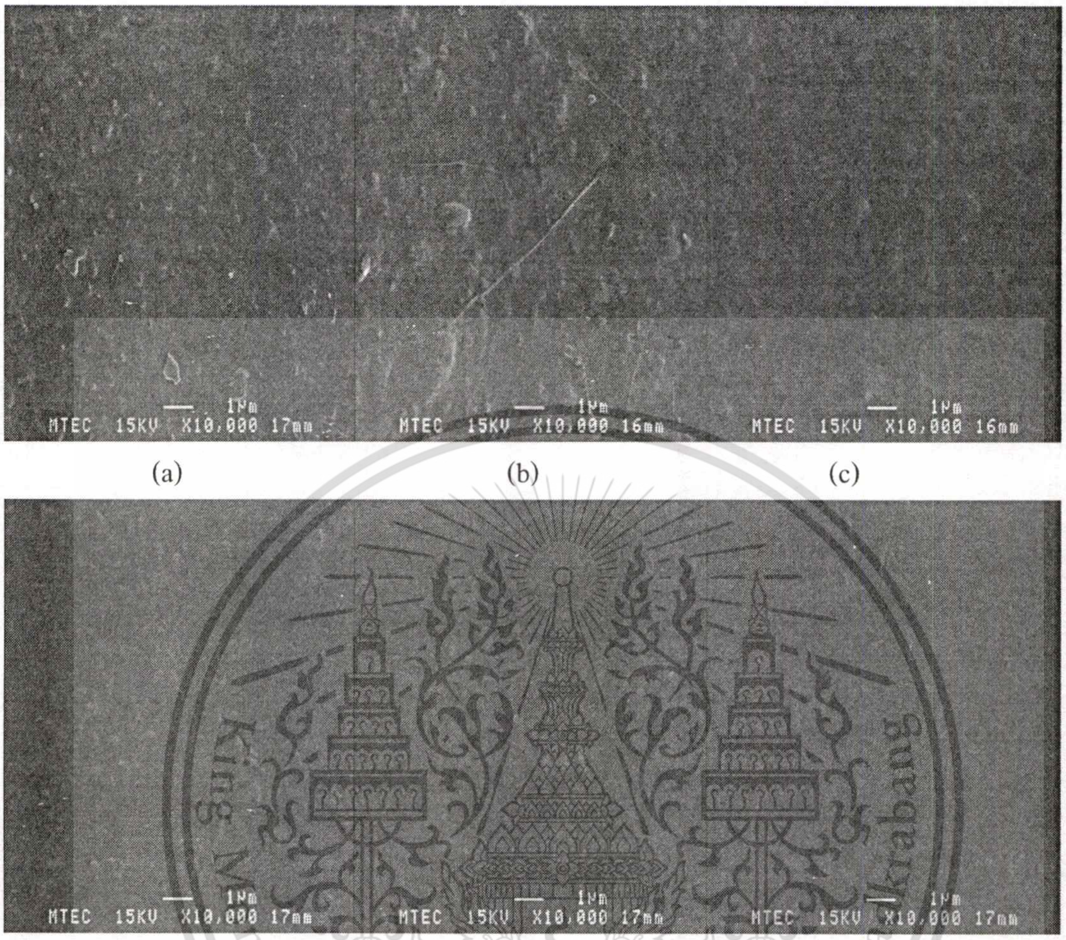

(a) (b) (c)

(d) (e) (f)

Figure 4.23 The SEM micrograph of mold temperature in ABS GA300 (a) 20°C, (b) 40°C, (C) 60°C, (d)100°C, (e) 110°C, and (f) 120°C

From the SEM micrographs are image analyzed by image processing method. The image processing uses image processing software is ImageJ. The software can detect amount of white dot is uncompleted melt plastic. On uncompleted melt plastic area has defect of part is the roughness's effect. In **Figure 4.24** to **Figure 4.26** are the SEM analysis micrograph of mold temperature in ABS KU901, ABS SP200, and ABS GA300, respectively. And in **Figure 4.27** is the relationship between the amount of white dot and mold temperature of ABS. Although, there are the indirect variant relationship.

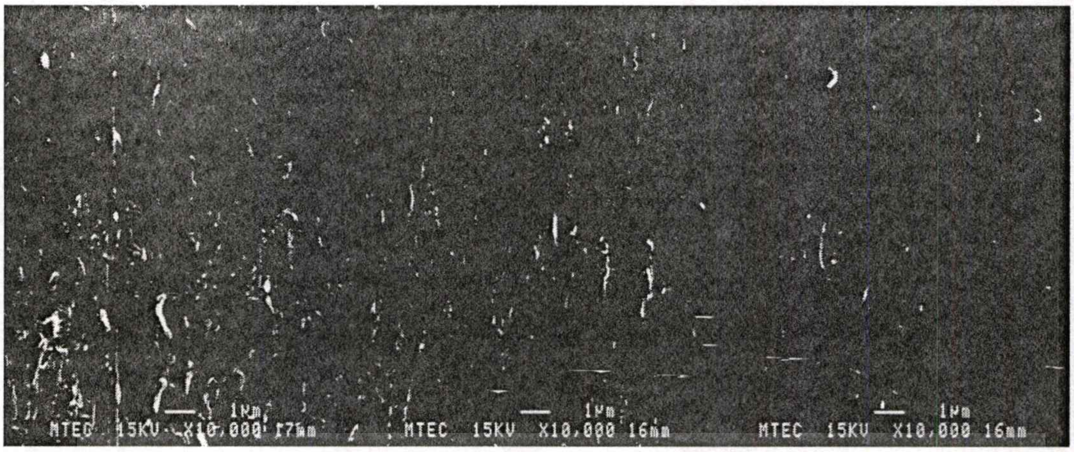

(a) (b) (c)

(d) (e) (f)

Figure 4.24 The SEM analysis micrograph of mold temperature in ABS KU901 (a) 20°C, (b) 40 °C, (c) 60 °C, (d) 100 °C, (e) 110 °C, and (f) 120 °C

(a) (b) (c)

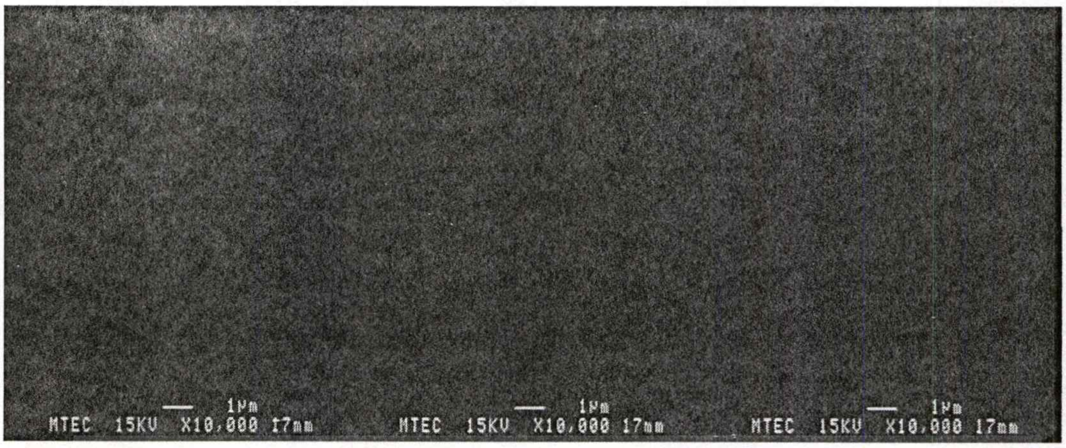

(d) (e) (f)

Figure 4.25 The SEM analysis micrograph of mold temperature in ABS SP200 (a) 20°C, (b) 40 °C, (c) 60 °C, (d) 100 °C, (e) 110 °C, and (f) 120 °C

(a) (b) (c)

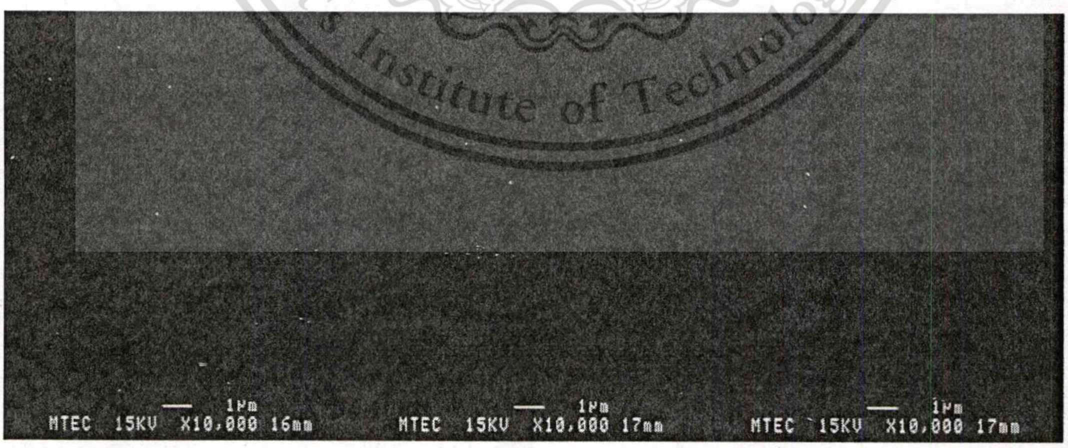

(d) (e) (f)

Figure 4.26 The SEM analysis micrograph of mold temperature in ABS GA300 (a) 20°C, (b) 40 °C, (c) 60 °C, (d) 100 °C, (e) 110 °C, and (f) 120 °C

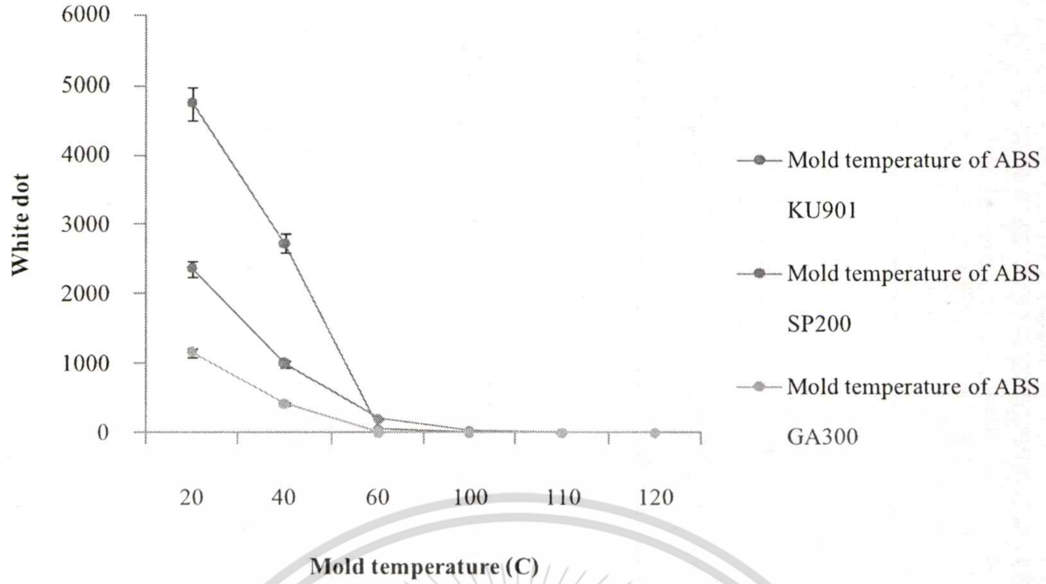

Figure 4.27 The relationship between white dot and mold temperature of ABS

4.3.1.2 POM

From **4.1.1** and **4.2.1** were studied the effect of mold temperature. The surface's gloss was increased values and the surface's roughness was decreased values, when the mold temperature was increased. In this part shown the micro surface images of the POM parts, that represented in **Figure 4.24**(POM M90) and **Figure 4.25**(POM M270). In low temperature, the micro graphs shown many crystalline gains were not diffused on surface's plat. But in high temperature, the micro graphs shown crystalline gains were completely diffused on surface's plate. There are related with the previous study that is surface finishing. The relation in gloss is direct-change and the relation in roughness is indirect-change.

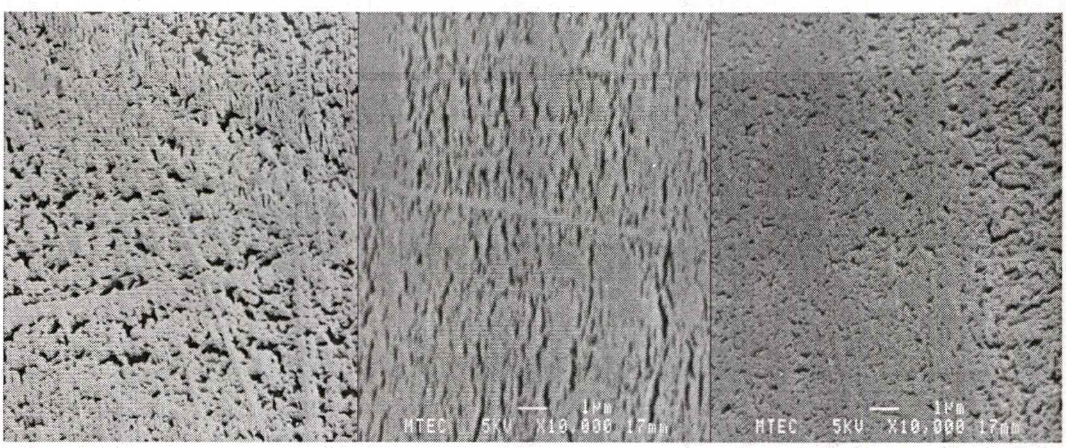

(a) (b) (c)

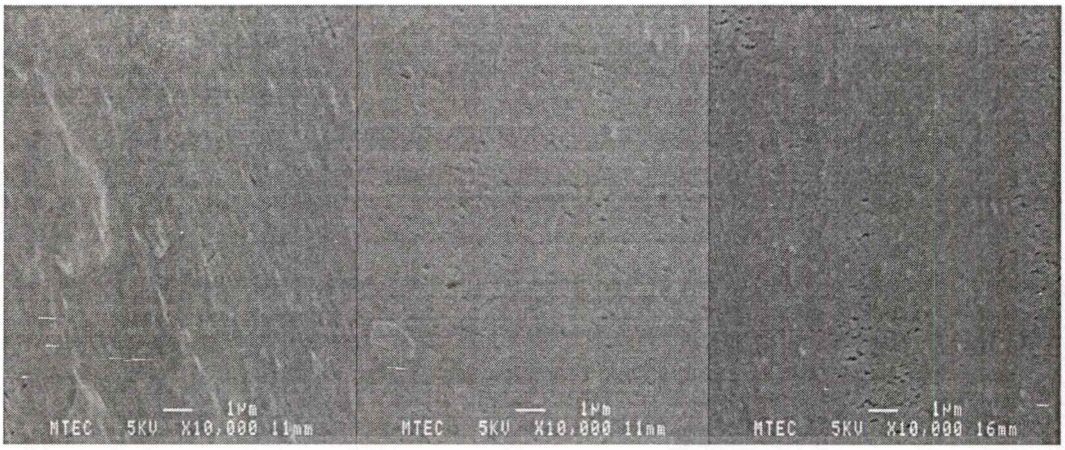

(d) (e) (f)

Figure 4.28 The SEM micrograph of mold temperature in POM M90 (a) 20°C, (b) 40°C, (c) 60°C, (d)100°C, (e) 110°C, and (f) 120°C

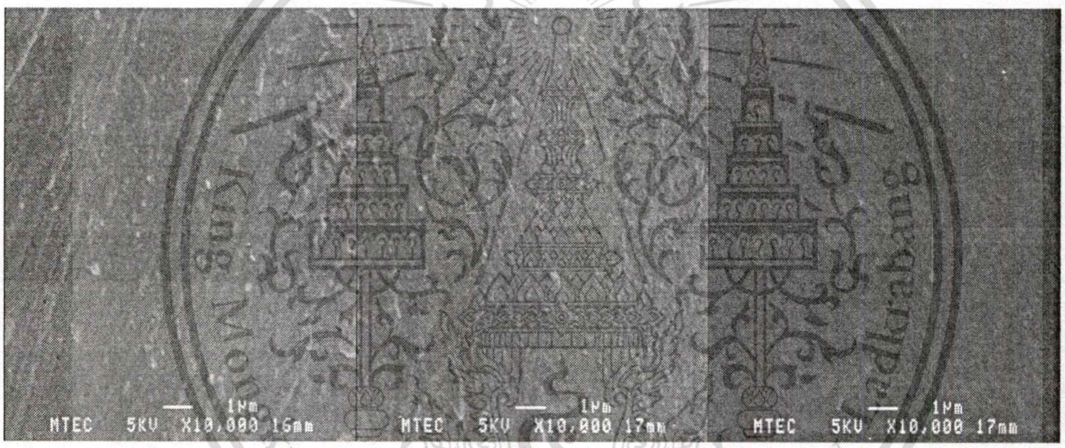

(a) (b) (c)

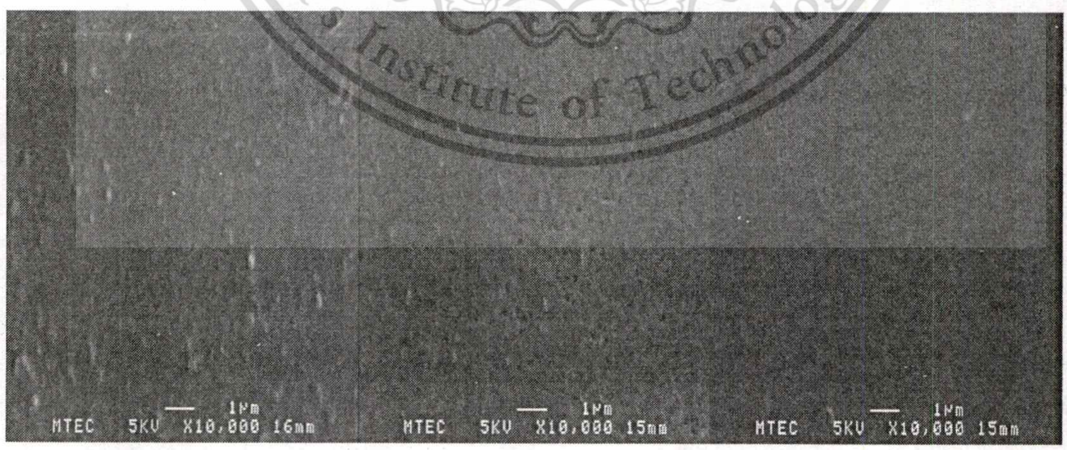

(d) (e) (f)

Figure 4.29 The SEM micrograph of mold temperature in POM M270 (a) 20°C, (b) 40°C, (c) 60°C, (d)100°C, (e) 110°C, and (f) 120°C

From the SEM micrographs are image analyzed by image processing method. The image processing uses image processing software is ImageJ. The software can detect amount of white dot is uncompleted melt plastic. On uncompleted melt plastic area has defect of part is the roughness's effect. In **Figure 4.30** to **Figure 4.31** are the SEM analysis micrograph of mold temperature in POM M90 and POM M270. And in **Figure 4.32** is the relationship between the amount of white dot and mold temperature of POM. Although, there are the indirect variant relationship.

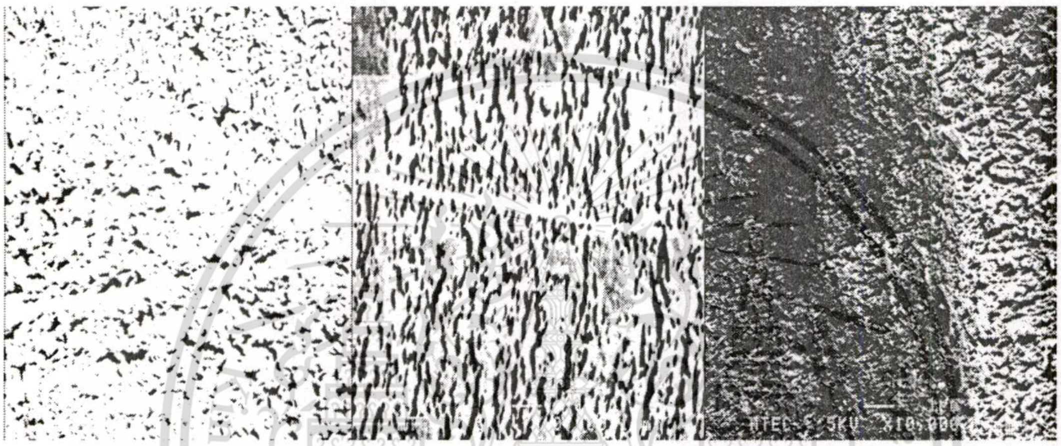

(a) (b) (c)

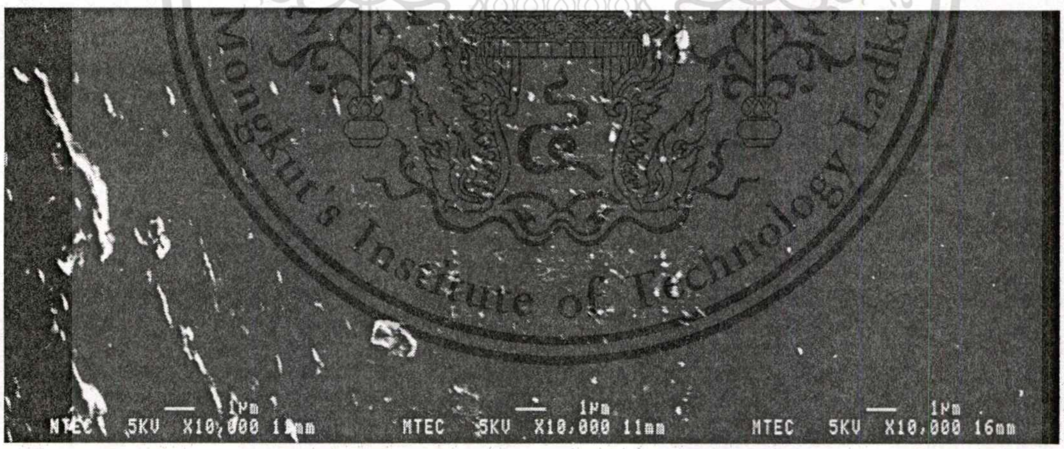

(d) (e) (f)

Figure 4.30 The SEM analysis micrograph of mold temperature in POM M90 (a) 20°C, (b) 40°C, (c) 60°C, (d)100°C, (e) 110°C, and (f) 120°C

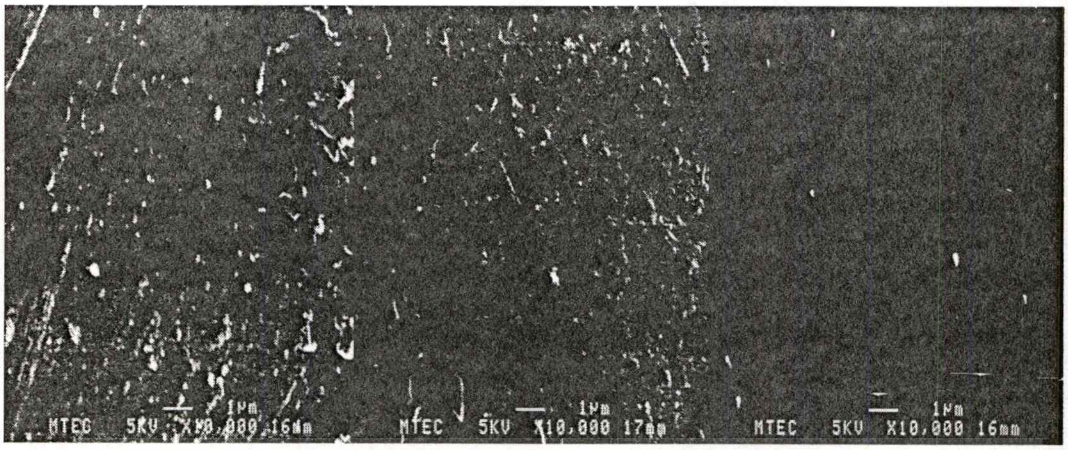

(a) (b) (c)

(d) (e) (f)

Figure 4.31 The SEM analysis micrograph of mold temperature in POM M270 (a) 20°C, (b) 40 °C, (c) 60 °C, (d)100 °C, (e) 110 °C, and (f) 120 °C

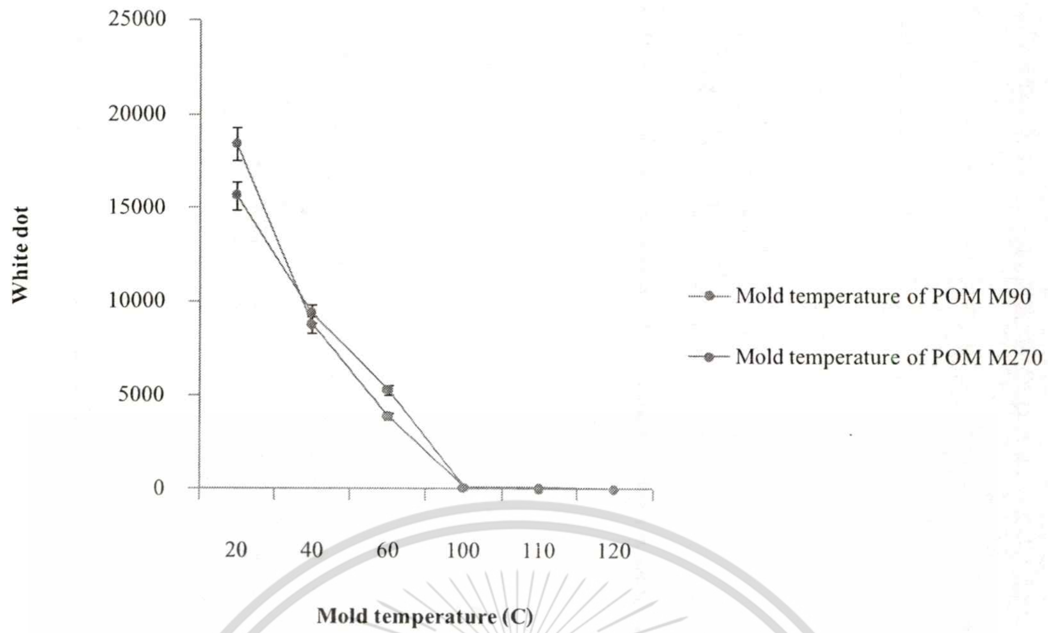

Figure 4.32 The relationship between white dot and mold temperature of POM

4.3.2 Effect of packing pressure

4.3.2.1 ABS

From **4.1.3** and **4.2.3** were studied the effect of pack pressure. The surface's gloss was increased values and the surface's roughness was decreased values, when the pack pressure was increased. In this part shown the micro surface images of the ABS parts, that represented in **Figure 4.26**(ABS SP200). It can be clearly seen that there are a lot butadiene and large particle size of butadiene on low pack pressure. However, the butadiene on surface was increased and large particle size in high pack pressure. There are related with the previous study that is surface's gloss and surface's roughness. The relation in gloss is indirect-change and the relation in roughness is direct-change.

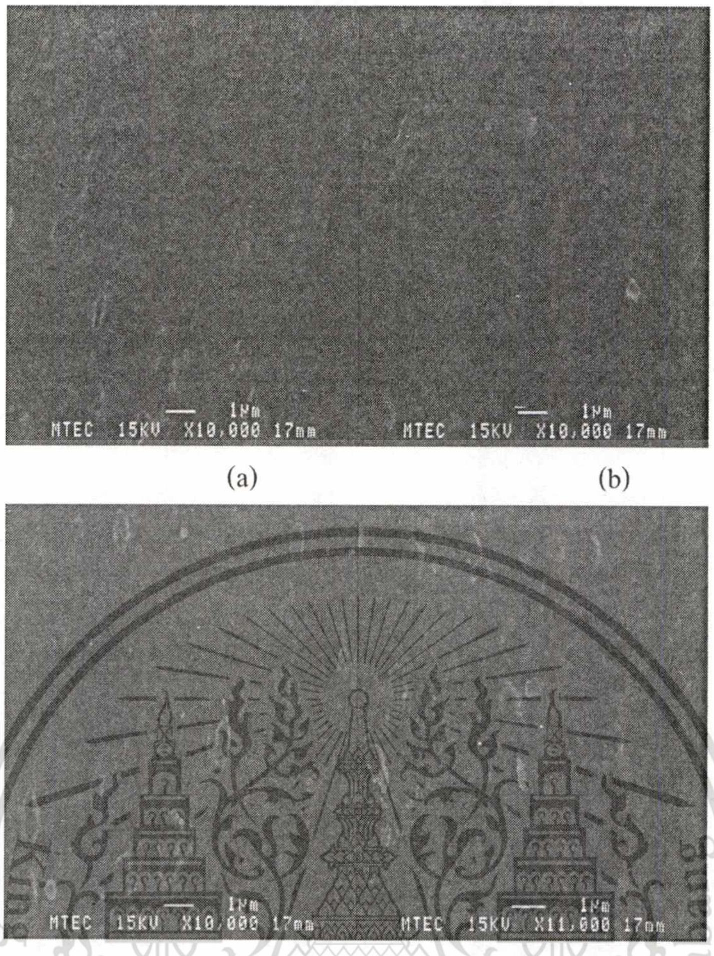

Figure 4.33 The SEM micrograph of packing pressure in ABS SP200 (a) 100 bar, (b) 200 bar, (c) 300 bar, and (d) 450 bar

From the SEM micrographs are image analyzed by image processing method. The image processing uses image processing software is ImageJ. The software can detect amount of white dot is uncompleted melt plastic. On uncompleted melt plastic area has defect of part is the roughness's effect. In **Figure 4.34** is the SEM analysis micrograph of packing pressure in ABS SP200. And in **Figure 4.35** is the relationship between the amount of white dot and packing pressure of ABS. Although, there is the direct variant relationship.

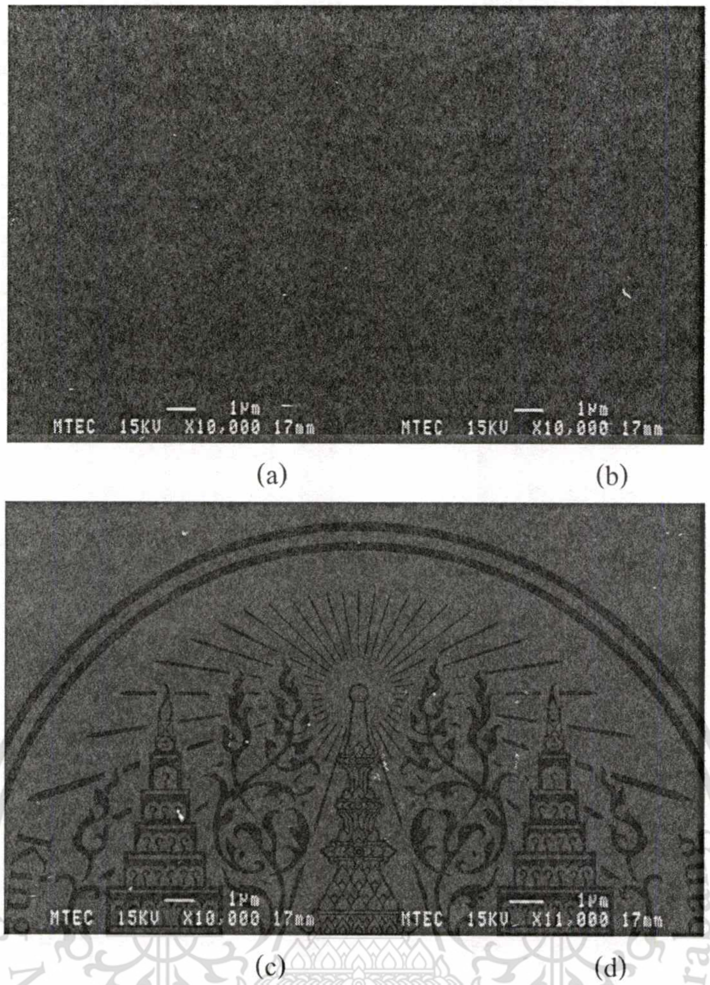

Figure 4.34 The SEM analysis micrograph of packing pressure in ABS SP200 (a) 100 bar, (b) 200 bar, (c) 300 bar, and (d) 450 bar

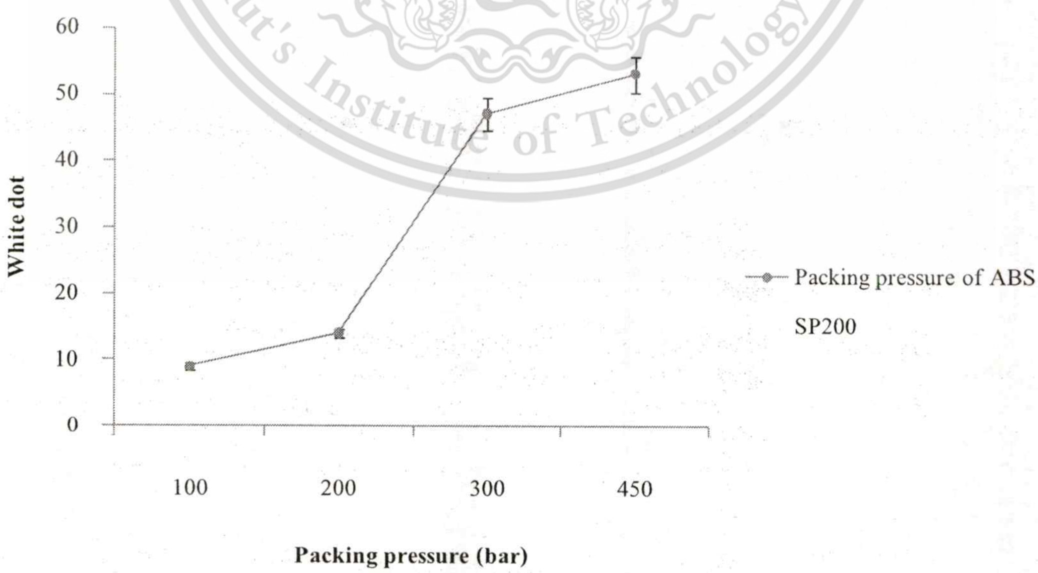

Figure 4.35 The relationship between white dot and packing pressure of ABS SP200

4.3.2.2 POM

From **4.1.3** and **4.2.3** were studied the effect of packing pressure. The surface's gloss was increased values and the surface's roughness was decreased values, when the pack pressure was increased. In this part shown the micro surface images of the POM parts, that represented in **Figure 4.27**(POM M90) and **Figure 4.28**(POM M270). It can be clearly seen that there are a lot of crack crystalline gains and large particle size of gains in high packing pressure. But in low packing pressure is reducing particle size of gains and it is completely the crystalline gains in high pack pressure. There are related with the previous study that is surface's gloss and surface's roughness. The relation in gloss is indirect-change and the relation in roughness is direct-change.

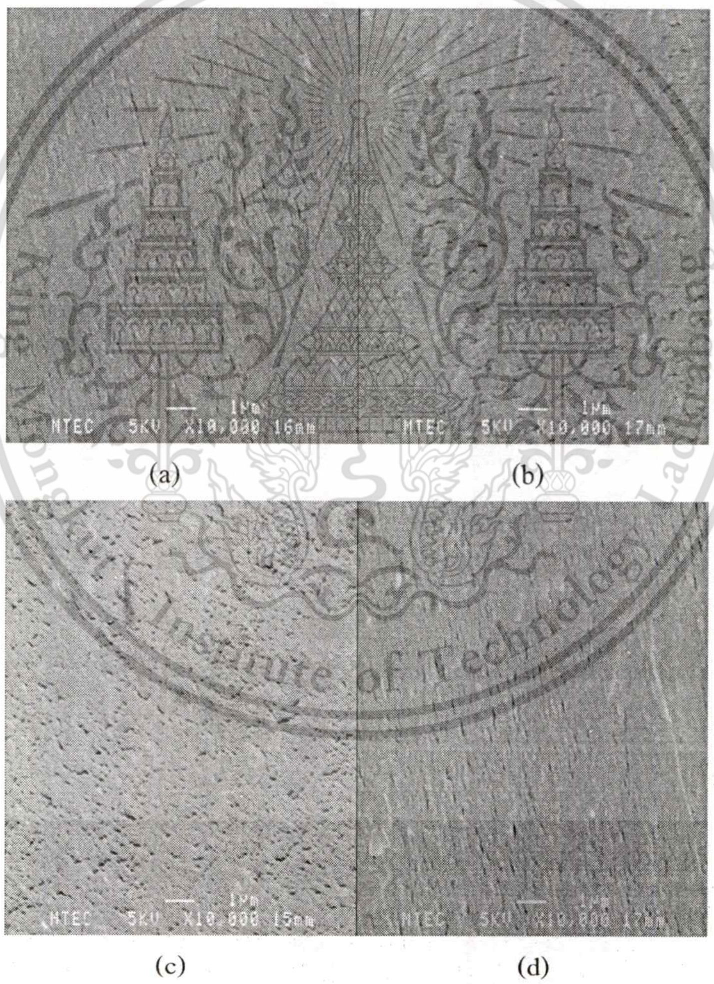

Figure 4.36 The SEM micrograph of packing pressure in POM M90 (a) 100 bar, (b) 200 bar, (c) 300 bar, and (d) 400 bar

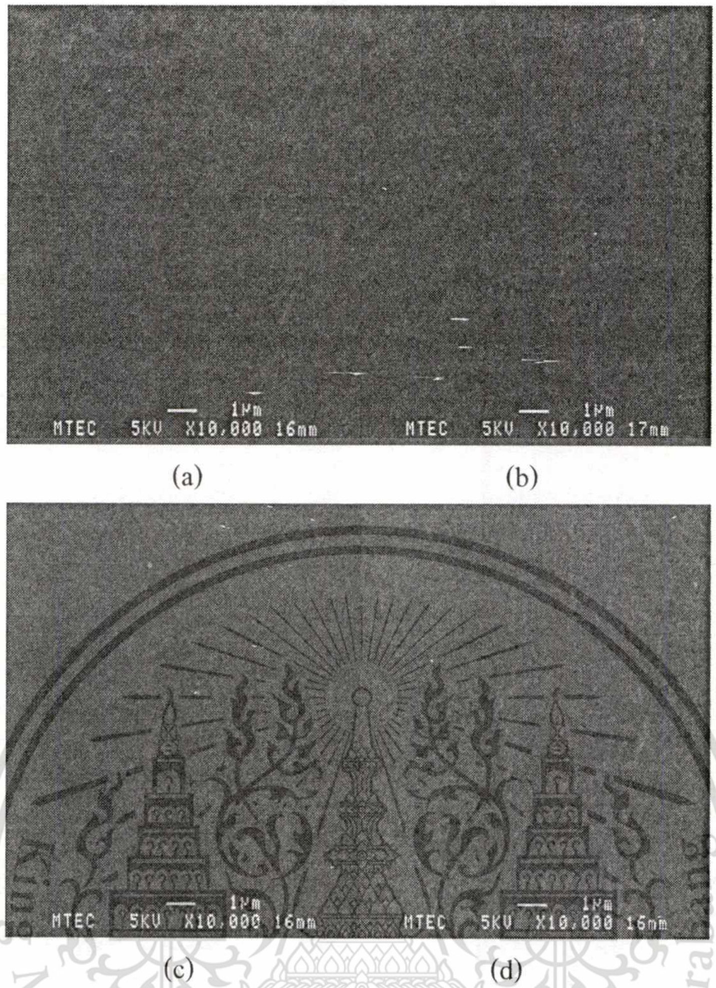

Figure 4.37 The SEM micrograph of packing pressure in POM M270 (a) 100 bar, (b) 200 bar, (c) 300 bar, and (d) 400 bar

From the SEM micrographs are image analyzed by image processing method. The image processing uses image processing software is ImageJ. The software can detect amount of white dot is uncompleted melt plastic. On uncompleted melt plastic area has defect of part is the roughness's effect. In **Figure 4.38** to **Figure 4.39** are the SEM analysis micrograph of packing pressure in POM M90 and POM M270. And in **Figure 4.40** is the relationship between the amount of white dot and packing pressure of POM. Although, there are the direct variant relationship.

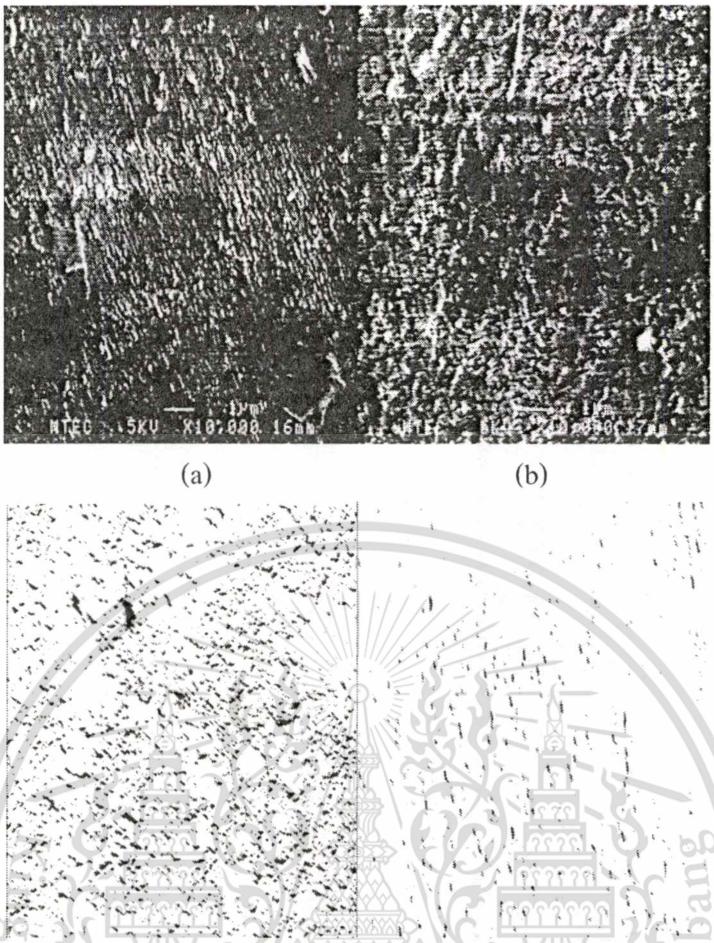

(a) (b)

(c) (d)

Figure 4.38 The SEM analysis micrograph of packing pressure in POM M90 (a) 100 bar, (b) 200 bar, (c) 300 bar, and (d) 400 bar

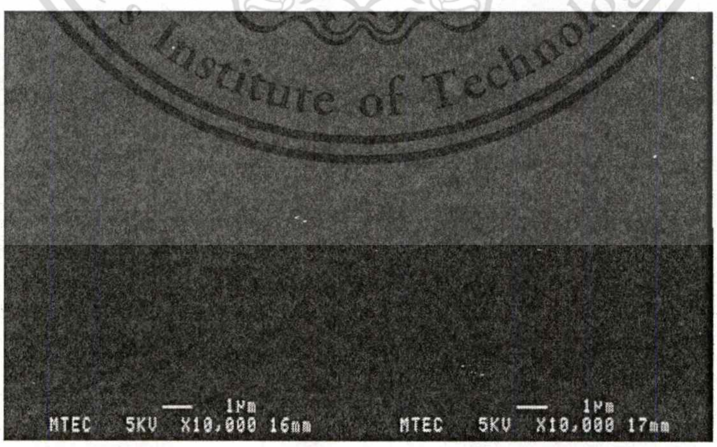

(a) (b)

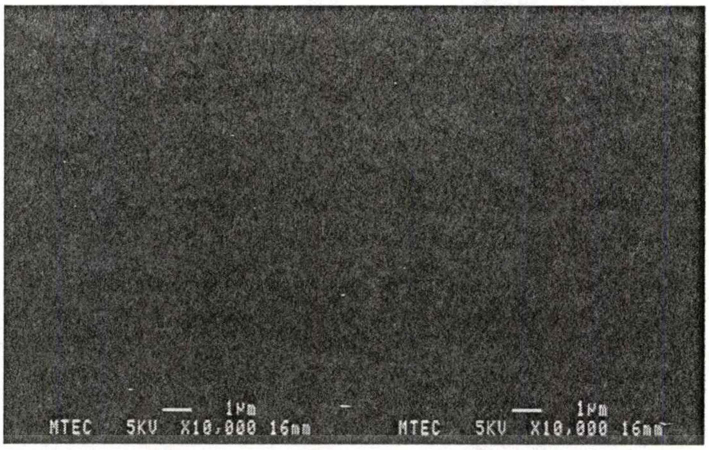

(c) (d)

Figure 4.39 The SEM analysis micrograph of packing pressure in POM M270 (a) 100 bar, (b) 200 bar, (c) 300 bar, and (d) 400 bar

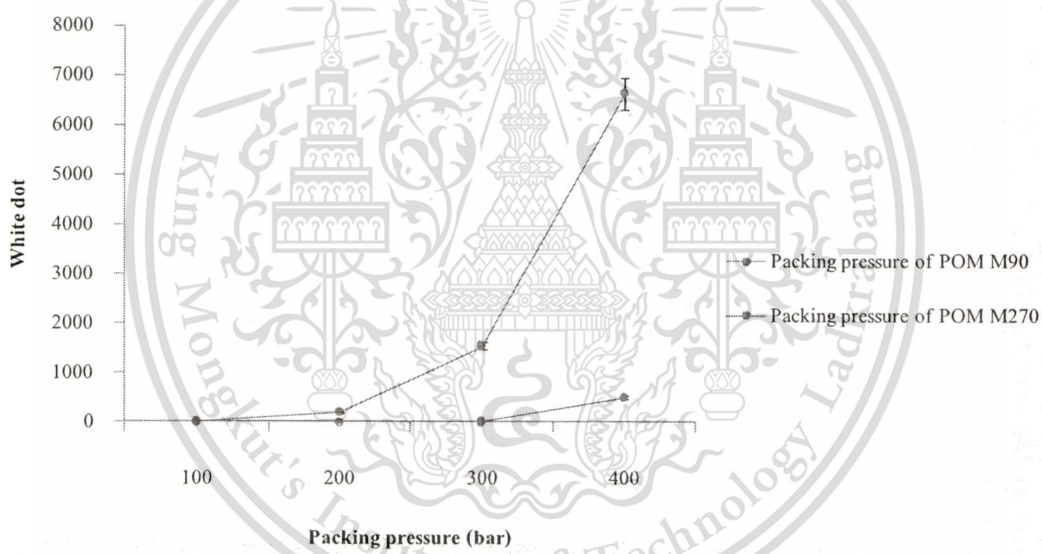

Figure 4.40 The relationship between white dot and packing pressure of POM

4.4 Capillary rheometer result

4.4.1 Effect of viscosities and melt flow index

The relationship between viscosities and shear rates is represented in ABS (see in**4.4.1.1)**. In this experiment, there are three ABSs that are ABS KU901, ABS SP200, and ABS GA300. The various temperatures are three values that are 220 $^{\circ}$C (in **Figure 4.41**), 230 $^{\circ}$C (in **Figure 4.42**), and 240 $^{\circ}$C(in **Figure 4.43**). In this case, the shear viscosities decreased by high melt flow index of ABS. However, ABS GA300 is the highest melt flow index. Then the shear viscosities are the lowest in this test.

The relationship between viscosities and shear rates is represented in POM (see in**4.4.1.2)**. In this experiment, there are two POMs that are POM M90, and POM M270. The various temperatures are three values that are 220 $^{\circ}$C (see in **Figure 4.44**), 230 $^{\circ}$C (see in **Figure 4.45**), and 240 $^{\circ}$C (see in **Figure 4.46**). In this case, the shear viscosities decreased by high melt flow index of POM. However, POM M270 is higher melt flow index than POM M90. But the shear viscosities of POM M270 are lower than the shear viscosities of POM M90.

4.4.1.1 ABS

From the **Figure 4.41**, **Figure 4.42**, and **Figure 4.43**, are shown the viscosities, that against shear rate at the various viscosities in 220°C, 230°C, and 240°C respectively. The trend of these graphs is correlated with melt flow index. The melt flow index of ABS is shown in **Table 3.1**. The viscosities are decreased, when the melt flow index of material was high value. For this case, the melt flow index of ABS GA300 is the highest, although the viscosity is the lowest.

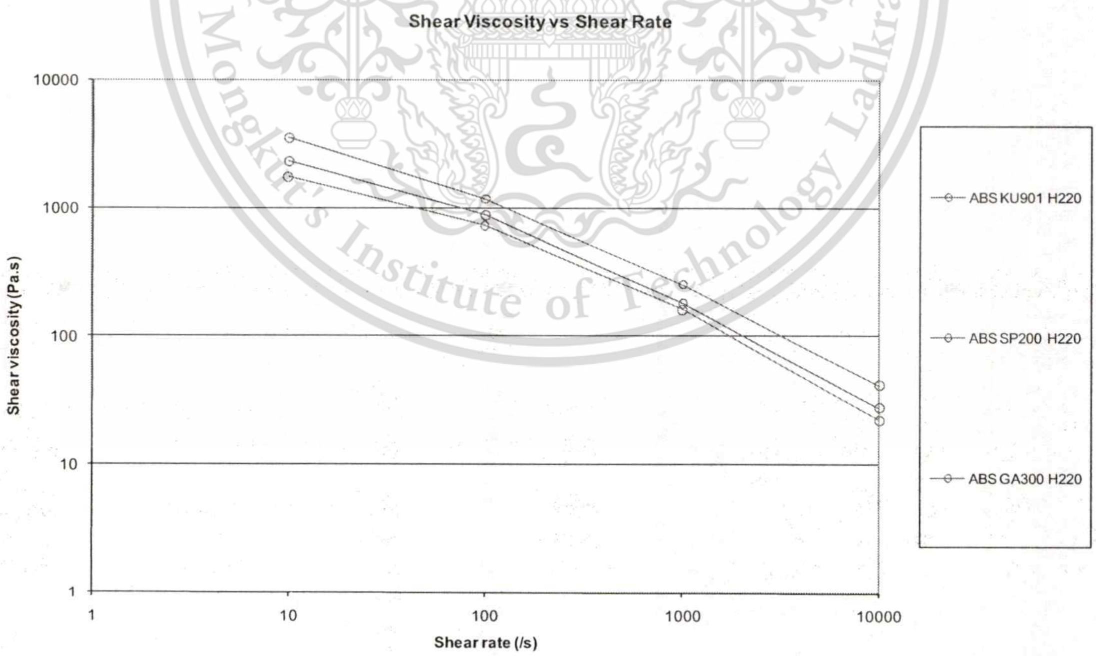

Figure 4.41 Plots of viscosities againt shaer rates at the various viscosities of ABS materials at 220 $^{\circ}$C

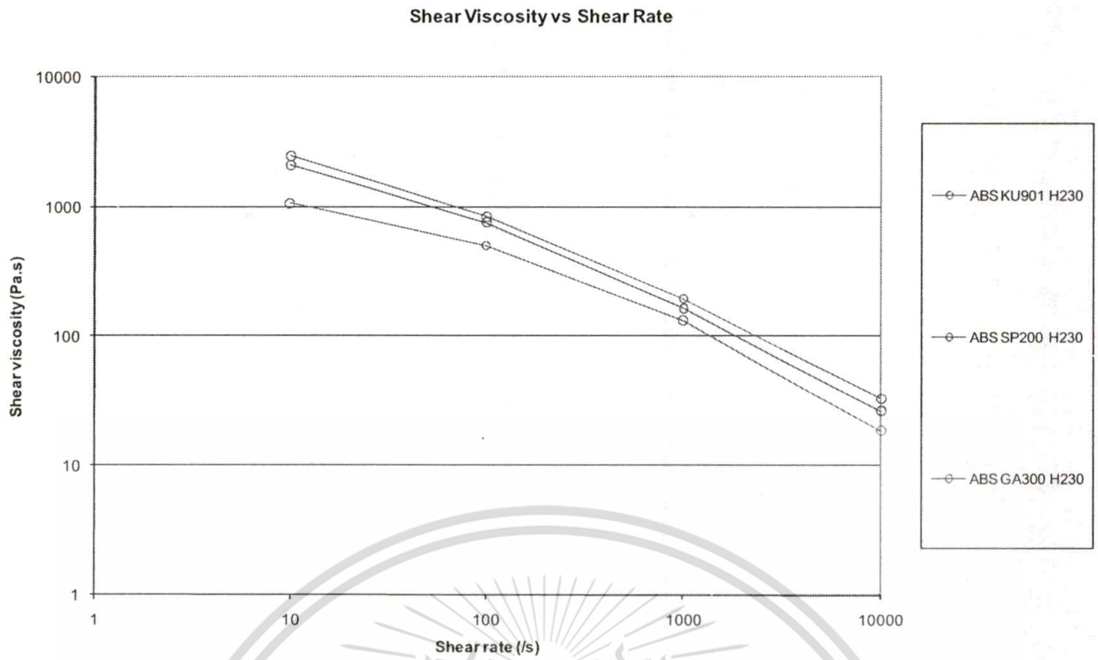

Figure 4.42 Plots of viscosities againt shaer rates at the various viscosities of ABS materials at 230 $^{\circ}$C

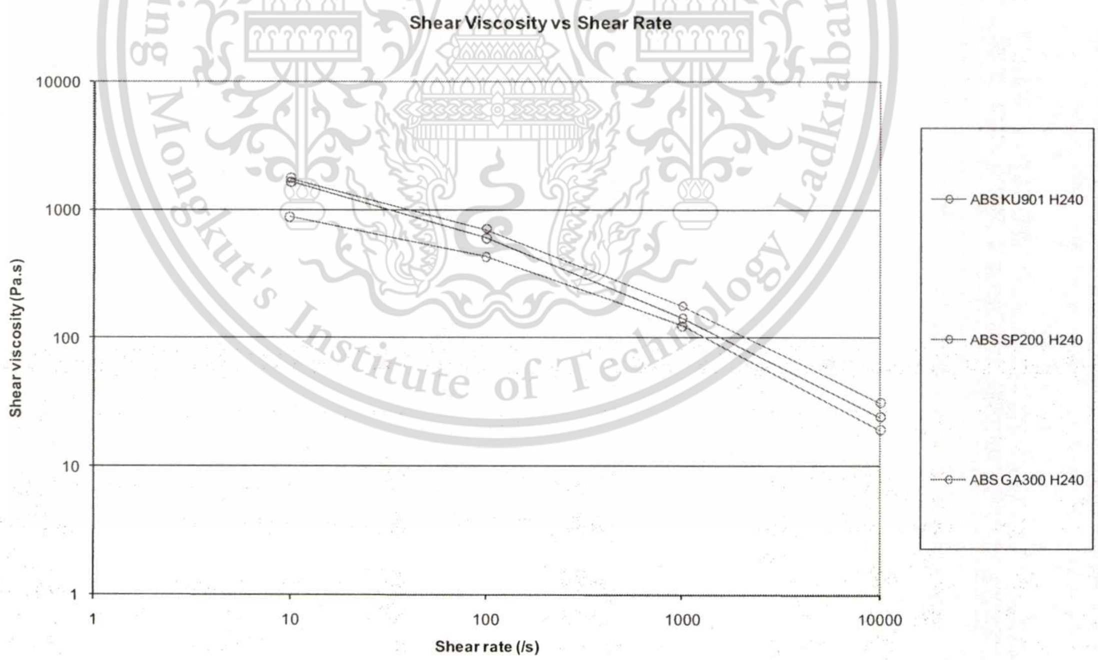

Figure 4.43 Plots of viscosities againt shaer rates at the various viscosities of ABS materials at 240 $^{\circ}$C

4.1.1.2 POM

From the **Figure 4.44 Figure 4.45**, and **Figure 4.46**, are shown the viscosities, that against shear rate at the various viscosities in 220°C, 230°C, and 240°C respectively. The trend of these graphs is correlated with melt flow index. The melt flow index of POM is shown in **Table 3.2**. The viscosities are decreased, when the melt flow index of material was high value. For this case, the melt flow index of POM M270 is higher than POM M90, although the viscosity of POM M270 is lower than the viscosity of POM M90.

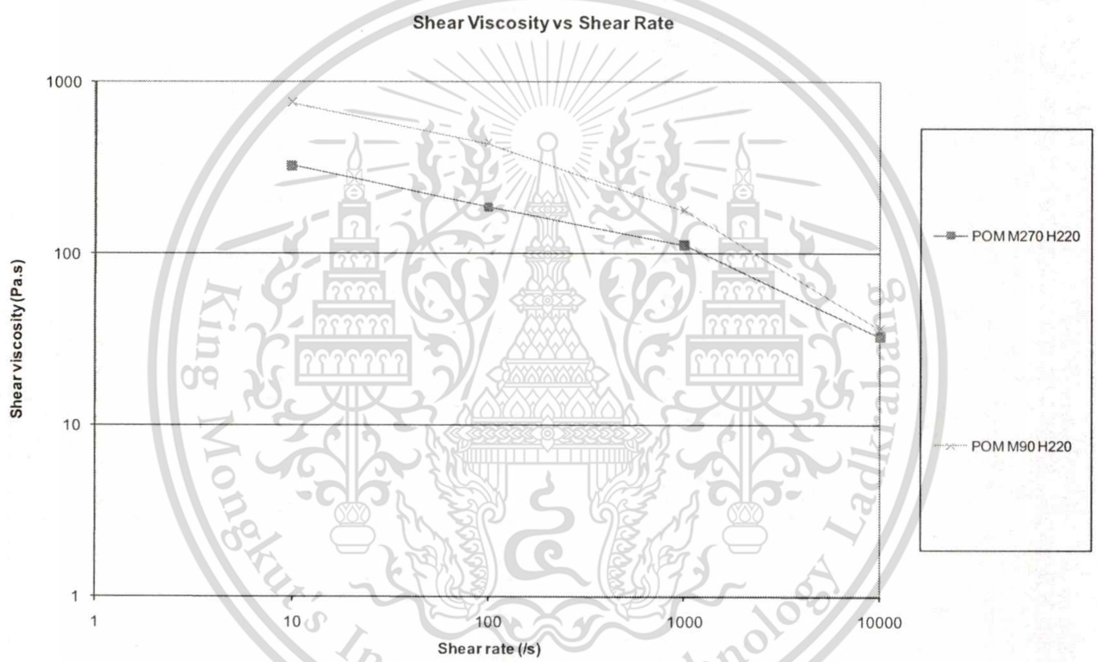

Figure 4.44 Plots of viscosities againt shaer rates at the various viscosities of POM materials at 220°C

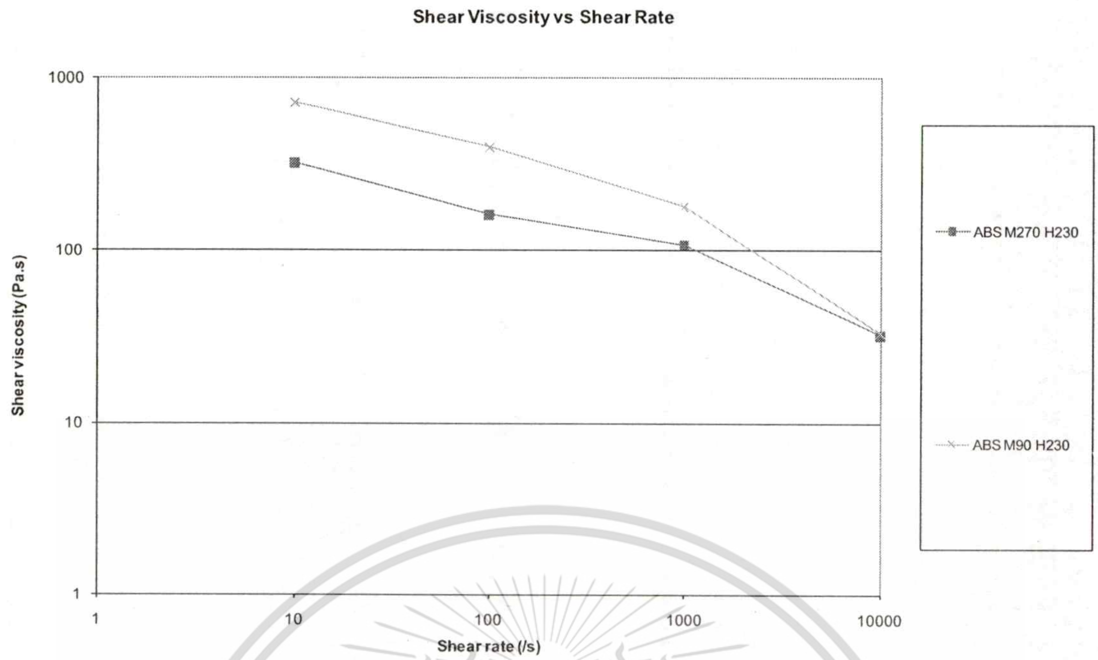

Figure 4.45 Plots of viscosities againt shaer rates at the various viscosities of POM materials at 230°C

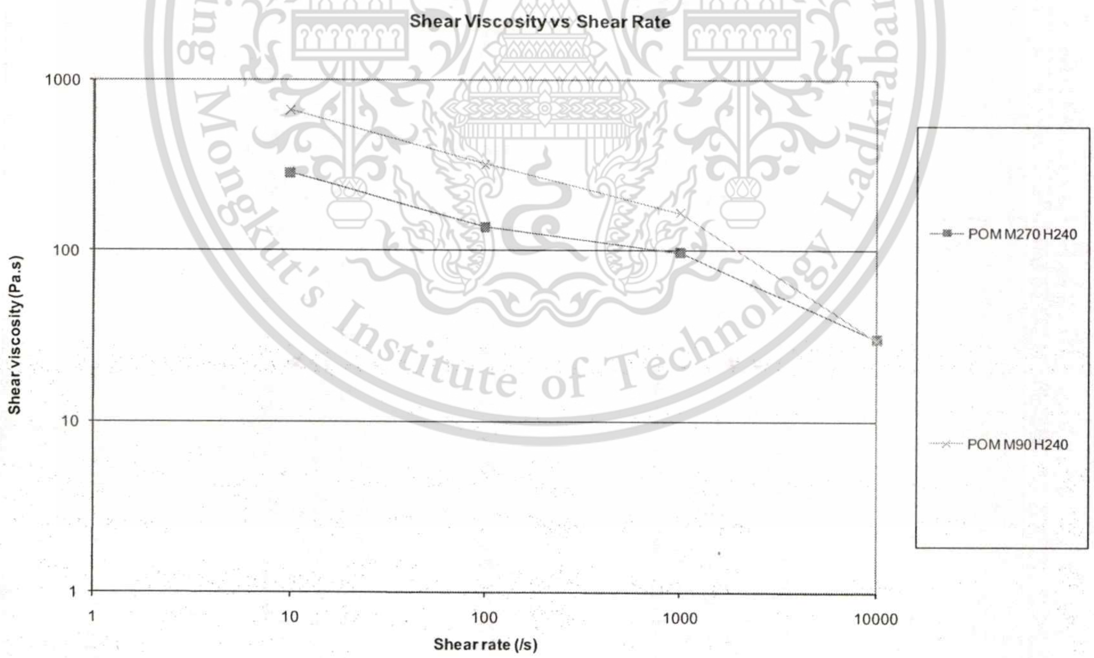

Figure 4.46 Plots of viscosities againt shaer rates at the various viscosities of POM materials at 240°C

4.5 Energy consumption

In the energy consumption, it has been estimated (34) that 65% of the total electricity consumed by an injection molding plant is consumed by the injection machine to run the hydraulic drive and provide heat. The energy is used for shot preparation and forming. Efficiency based on a minimum theoretical energy input per shot is defined by

$$E_{min} = M\int_{T1}^{T0} C_p \, dT + \int_0^{ti} p\,v dt \tag{4.3}$$

Where M is mass of shot, T_1, T_2 is screw inlet and outlet temperatures, respectively, p = injection pressure (function of time), v = volumetric injection rate, and t_i = injection time.

In this case, the energy consumption is defined by the estimated Equation (4.4) that is consist of the energy of mold, the energy of machine, and the energy of plastic. The energy of mold is represented in Equation (4.5). The energy of machine is represented in Equation (4.6). And the energy of plastic is represented in Equation (4.7). From the Equation (4.4) is rewritten the new able equation in Equation (4.6).

$$E_{\min} = E_{mould} + E_{machine} + E_{plastic} \tag{4.4}$$

Where $E_{\min}$ is the minimum theoretical energy input per shot. E_{mould} is the energy of mold. $E_{machine}$ is the energy of machine. $E_{plastic}$ is the energy of plastic.

$$E_{mould} = m_{mould}\int_{T_1}^{T_2} C_{pmould}\,dT \tag{4.5}$$

Where E_{mould} is the energy of mold (kJ). m_{mould} is the mass of BeCu (kg). C_{pmould} is the heat capacity of BeCu (kJ/Kg.K). T_1 is initial temperature (K). T_2 is final temperature (K).

$$E_{machine} = \int_0^{t_i} p\dot{v}dt \tag{4.6}$$

Where $E_{machine}$ is the energy of machine(kJ). t_i is injection time (s). p is injection pressure ($kg.m^{-1}.s^{-2}$). $\dot{v}$ is volumetric rate (m^3).

$$E_{plastic} = m_{plastic}\int_{T_1}^{T_2} C_{pplastic}\,dT \tag{4.7}$$

Where $E_{plastic}$ is the energy of plastic(kJ). $m_{plastic}$ is the mass of plastic (kg). $C_{pplastic}$ is the heat capacity of plastic (kJ/Kg.K). T_1 is initial temperature (K). T_2 is final temperature (K).

$$E_{\min} = m_{mould} \int_{T_1}^{T_2} C_{pmould} dT + \int_{0}^{t_i} p\dot{v} dt + m_{plastic} \int_{T_1}^{T_2} C_{pplastic} dT \qquad (4.8)$$

In this case, The solution in the energy consumption is represent in Appendix D.

4.5.1 The relationship between mold temperature and energy consumption

4.5.1.1 ABS

In **Figure 4.35** is shown the relation between energy consumption and mold temperature of ABS. The materials are ABS KU901, ABS SP200, and ABS GA300. The energy consumption was calculated by Equation (4.8). From the **Figure 4.47**, the energy consumptions are increased, when the mold temperature are going up.

The trend of this relation can be explained by molecular weight of materials. The ABS GA300 is the lowest molecular weight because it is the highest melt flow index in the case. Although, the energy consumption of ABS GA300 is the optimum value.

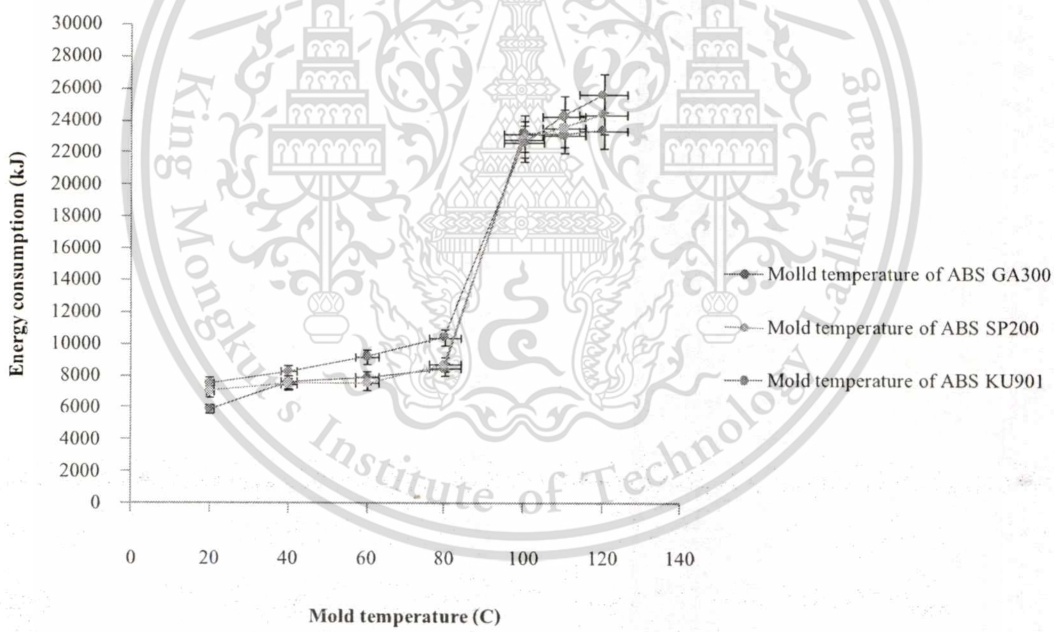

Figure 4.47 The mold temperature and energy consumption in ABS

4.5.1.2 POM

In **Figure 4.48** is shown the relation between energy consumption and mold temperature of POM. The materials are POM M90, and POM M270. The energy consumption was calculated by Equation (4.8). From the **Figure 4.49**, the energy consumptions are increased, when the mold temperature are going up.

The trend of this relation can be explained by molecular weight of materials. The POM M270 is lower molecular weight than POM M90 because it is the higher melt flow index than the other. Although, the energy consumption of POM M270 is lower than POM M90.

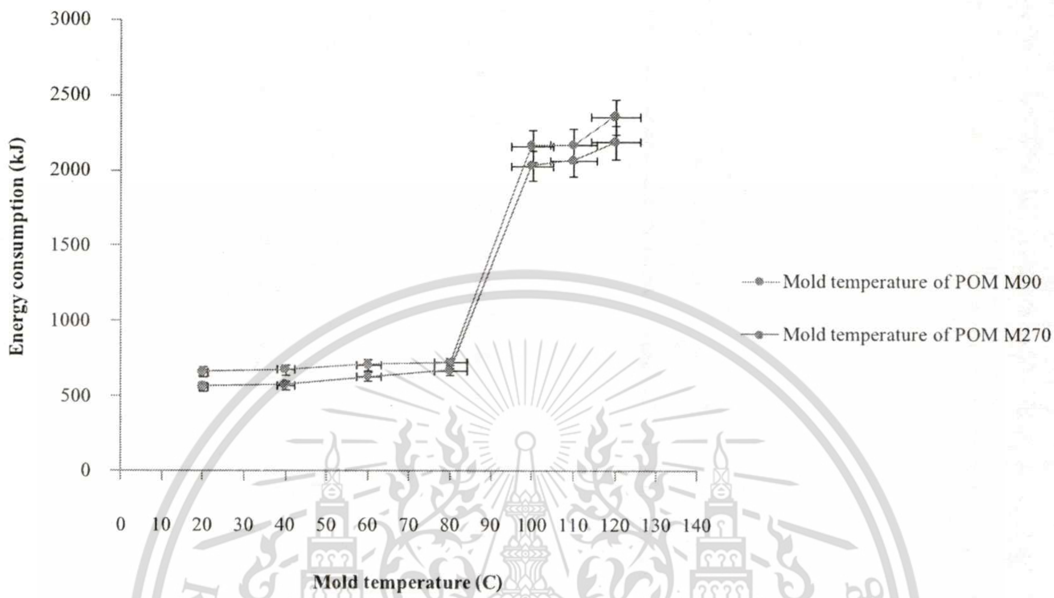

Figure 4.48 The mold temperature and energy consumption in POM

4.5.2 The relationship between energy consumption and roughness

4.5.2.1 ABS

In **Figure 4.49** is shown the relation between energy consumption and roughness of ABS. The condition is mold temperature, that are the beginning temperature at 20°C in conventional injection molding and finishing temperature at 120°C in injection molding via heating and cooling control system.

From this case, the surface's roughness is decreased but energy consumption is increasing. It is the indirect relation because the method for finishing surface use high temperature, that generated by very high power.

The trend of this relation can be explained by molecular weight of materials. The ABS GA300 is the lowest molecular weight because it is the highest melt flow index in the case. Although, the energy consumption of ABS GA300 is the optimum value.

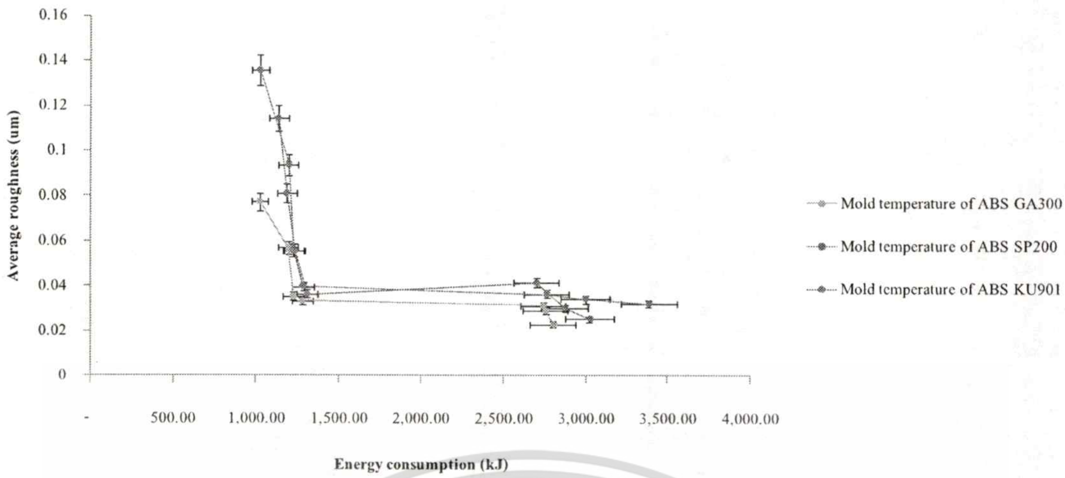

Figure 4.49 The energy consumption and roughness of ABS

The optimum point is considered in energy consumption between about 1,450 kJ and 2,870 kJ is also same average roughness but in 1,450 kJ, the part can not eject from injection machine and the specimen is not compleately. Althouh, the 2,870 kJ is used injection molding via heating and cooling cycle is prefer for the production and quality of surface's roughness is good.

4.5.2.2 POM

In **Figure 4.50** is shown the relation between energy consumption and roughness of POM. The condition is mold temperature, that are the beginning temperature at 20°C in conventional injection molding and finishing temperature at 120°C in injection molding via heating and cooling control system.

From this case, the surface's roughness is decreased but energy consumption is increasing. It is the indirect relation because the method for finishing surface use high temperature, that generated by very high power.

The trend of this relation can be explained by molecular weight of materials. The POM M270 is lower molecular weight than POM M90 because it is the higher melt flow index than the other. Although, the energy consumption of POM M270 is lower than POM M90.

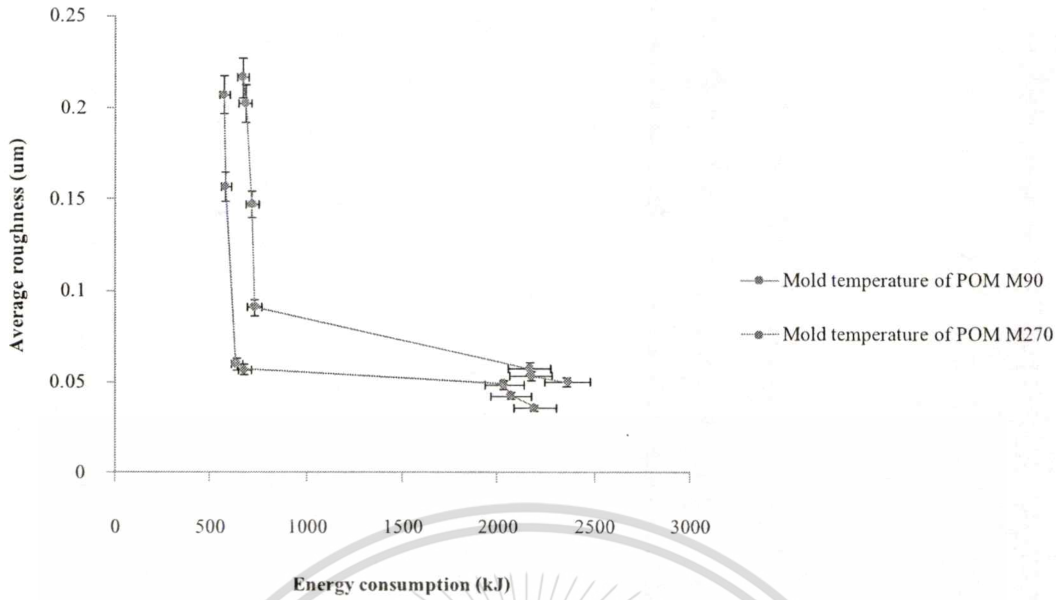

Figure 4.50 The energy consumption and roughness of POM

The optimum point is considered in energy consumption between about 770 kJ and 2,170 kJ is also same average roughness but in 770 kJ, the part can not eject from injection machine and the specimen is not compleately. Althouh, the 2,170 kJ is used injection molding via heating and cooling cycle is prefer for the production and quality of surface's roughness is good.

4.5.3 The statistical process control in heating and cooling cycle

SPC simply means the use of statistical methods to monitor, analyze, and control a process, in particular process variation. SPC can be applied to many different processes. For instance, to manufacturing processes, such as the production of electronic chips, batteries, tires, plastic bottles, and so on. However, it can also be applied to tasks performed in the service industries, such as filling out claim forms, diagnosis of patients by a medical doctor, processing of tax refunds by the IRS, processing of mail by the post office, and so on. A term closely related to SPC is statistical quality control (SQC). Statistical quality control is the application of statistical methods to measure and improve the quality of the process and the articles produced.

Statistics deals with the collection, organization, analysis, and interpretation of numerical data. An integral part of statistics is mathematics; this can make statistics rather imposing and unappetizing. However, the basic mathematical tools necessary to do SPC are straightforward and do not need to be intimidating at all.

The goals of SPC are to improve and ensure quality, and thus reduce process cost to waste as a result of rejects. Quality is determined by how much the characteristic of a product, for instance the outside diameter of a pipe, differs from the target value. The closer the product characteristic is to the target value, the higher the quality.

The SPC is calculated by the equation (4.7) for upper control limit and the equation (4.8) is a lower control limit. From the **4.5.3.1** and **4.5.3.2** are represented the SPC of ABS and SPC of POM, respectively.

$$UCL = \bar{x} + ER \tag{4.7}$$

$$LCL = \bar{x} - ER \tag{4.8}$$

Where UCL is upper control limit, LCL is lower control limit, E is safety factor of surface finish, $\bar{x}$ is average of data and R is range of data.

4.5.3.1 ABS

In the case is studied ABS conditions injection molding are fifty-four conditions. There are five conditions are mold temperature, barrel temperature, packing pressure, packing time and injection speed with 3 grades of ABSs are ABS KU901, ABS SP200, and ABS GA300.

In **Figure 4.51**(a) is the relationship between injection molding conditions and surface roughness. The relation is controlled by statistical process control (SPC) to measure and improve the quality product. The first is calculated the upper control limit (UCL) and lower control limit (LCL) by equation (4.7) and equation (4.8), respectively. From the equation (4.7), the UCL is 0.041 μm when $\bar{x}$ = 0.039 μm, E =0.53, and R = 0.007 μm. And from the equation (4.8), the LCL is 0.020 μm.

In **Figure 4.51**(b) is the relationship between injection molding conditions and energy consumption. The relation is controlled by SPC to calculate the energy consumption and improve the quality product. The UCL is 3,482.67 kJ when $\bar{x}$ = 3,127.08 kJ, E =0.53, and R = 670.3 kJ. And the LCL is 2,771.44 kJ.

In **Figure 4.51** (a) and (b) are also controlled by SPC. SPC to improve the quality product is surface roughness. The range of controllable is between 0.041 μm and 0.02 μm, that is the UCL and the LCL in SPC. In fifty-four injection conditions, there are only two conditions are mold temperature via heating and cooling cycle and packing time via heating and cooling cycle are in the control's range of SPC. The control's range is between the UCL and the LCL, is predicting the quality assurance of the production. But there are using energy consumption higher than the conventional injection molding. In this heating and cooling cycle case, the energy consumption is between 2,771.49 kJ and 3,482.67 kJ, is in range of SPC.

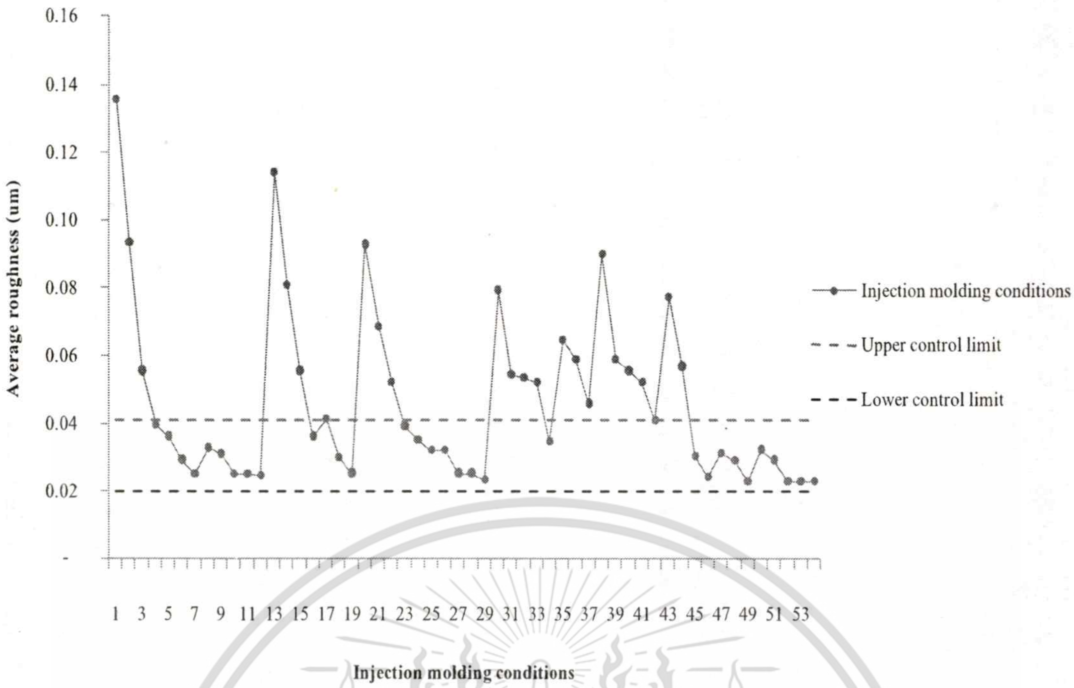

(a)

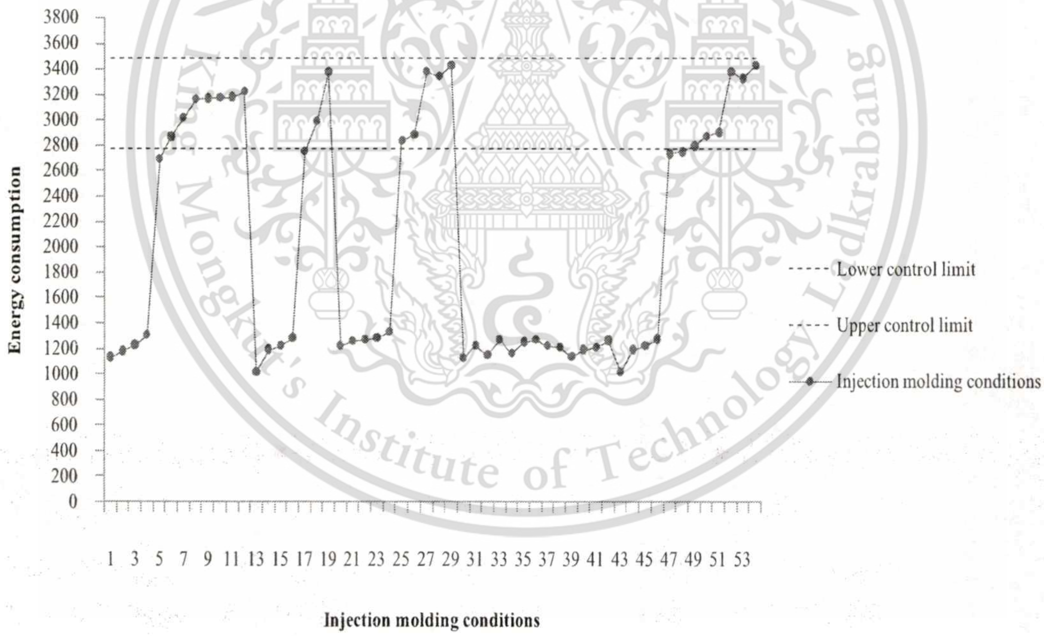

(b)

Figure 4.51 (a) The surface roughness of ABS with SPC, (b) The energy consumption of ABS with SPC

*Remark : fifty-four injection conditions of ABS see in Appendix E.

4.5.3.2 POM

In the case is studied POM conditions injection molding are fifty-seven conditions. There are five conditions are mold temperature, barrel temperature, packing pressure, packing time and injection speed with three grades of POMs are POM M90 and POM M270.

In **Figure 4.52**(a) is the relationship between injection molding conditions and surface roughness. The relation is controlled by statistical process control (SPC) to measure and improve the quality product. The first is calculated the upper control limit (UCL) and lower control limit (LCL) by equation (4.7) and equation (4.8), respectively. From the equation (4.7), the UCL is 0.057 μm when $\overline{x}$ = 0.053 μm, E =0.530, and R = 0.008 μm. And from the equation (4.8), the LCL is 0.020 μm.

In **Figure 4.52**(b) is the relationship between injection molding conditions and energy consumption. The relation is controlled by SPC to calculate the energy consumption and improve the quality product. The UCL is 2,912.16 kJ when $\overline{x}$ = 2,484.870 kJ, E =0.530, and R = 806.590 kJ. And the LCL is 2,057.180 kJ.

In **Figure 4.52**(a) and (b) are also controlled by SPC. SPC to improve the quality product is surface roughness. The range of controllable is between 0.053 μm and 0.020 μm, that is the UCL and the LCL in SPC. In fifty-eight injection conditions, there are only two conditions are mold temperature via heating and cooling cycle and packing time via heating and cooling cycle are in the control's range of SPC. The control's range is between the UCL and the LCL, is predicting the quality assurance of the production. But there are using energy consumption higher than the conventional injection molding. In this heating and cooling cycle case, the energy consumption is between 2,912.16 kJ and 2,057.18 kJ, is in range of SPC.

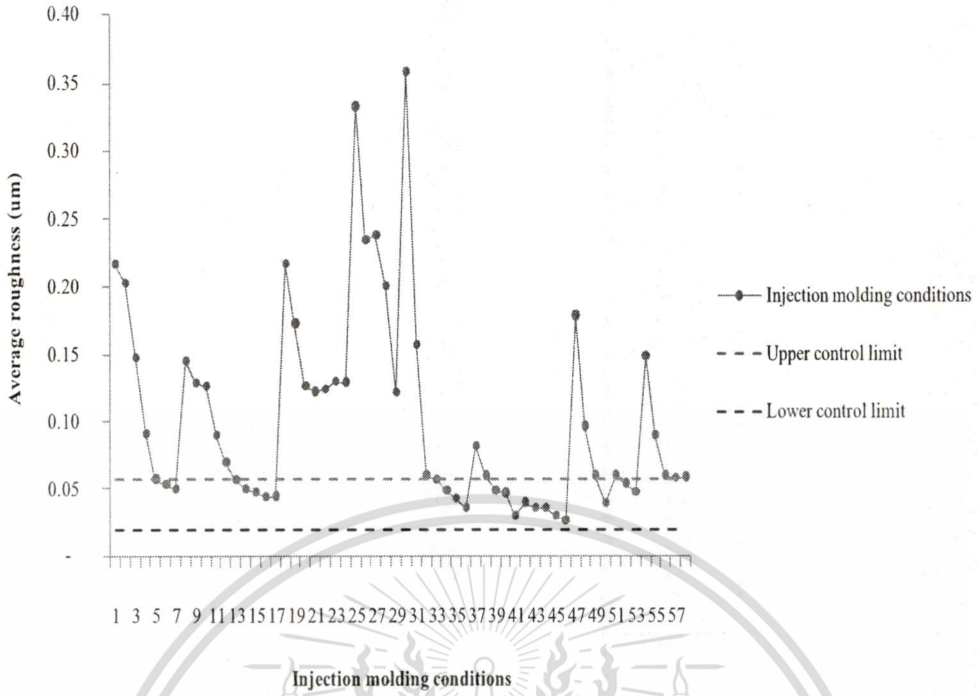

(a)

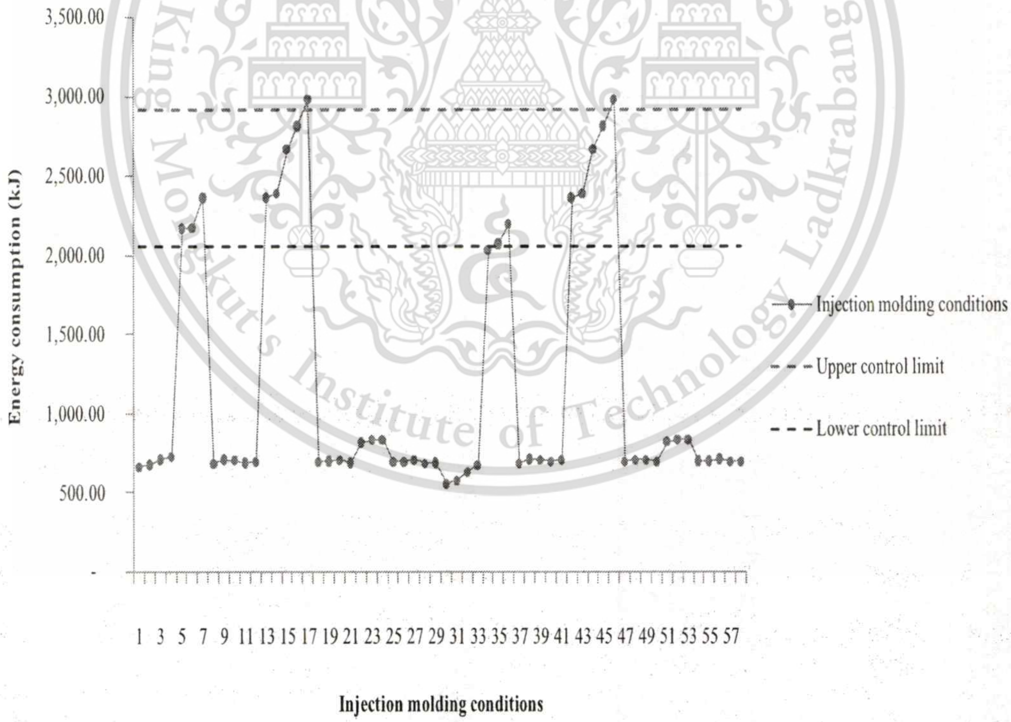

(b)

Figure 4.52 (a) The surface roughness of POM with SPC, (b) The energy consumption of POM with SPC

*Remark : fifty-eight injection condition of POM see in Appendix E.

CHAPTER 5

CONCLUSION AND SUGGESTIONS

5.1 Conclusion

The injection molding parameters, that are mold temperature, barrel temperature, pack pressure, pack pressure time, and injection speed are supported to investigate major and minor parameters involving in surface finish. The result represents the surface finish, that is gloss measurement and roughness measurement. The surface finish shows high gloss and low roughness, when the mold temperature is increasing.

In conventional injection molding, the major of parameter is improving surface finish is mold temperature. In this case, the problem is occurring at high temperature. Using high temperature, the specimen is incompletely part. Although, the solution is using rapid heating and cooling injection molding. In rapid heating and cooling control system, there is a programming that monitor and correcting data from thermocouples and pressure sensor.

The appearance of product is belonging in temperature and pressure conditions. The temperature and pressure are approving the surface's glossiness measurement, surface's roughness measurement, and the scanning electron microscope (SEM). The SEMs are shown the surface structure in ABS and POM. There are related with the parameters in injection molding. The micro structure's picture is very clearly surface finish, when the mold temperature is rising. Although, there are related with the viscosity of melt plastic by direct variant in mold temperature condition.

For the last section, there is investigating in energy consumption. The energy consumption is calculated by the energy consumption's equation. The energy consumption is related with mold temperature in direct variance. From the result in mold temperature condition at100°C, it is the comparison study between conventional injection molding and rapid heating and cooling injection molding. The optimum point is at 100°C condition in heating and cooling injection molding because the surface roughness is better than conventional condition and part is more complete than it.

The modern relation between energy consumption and surface's finish is surface's roughness is shown for instruction of injection molding. It can be predict the quality of product and the injection molding's user can know the trending of energy consumption. In the final experimental in the energy consumption and surface finish is controlled by the statistical process control (SPC) means the use of statistical methods to monitor, analyze, and control a process, in particular process variation. SPC is calculated by SPC's equation is represented the upper control limit and the lower control limit. The experimental of surface finish and energy consumption in temperature condition is calculated the upper control limit and the lower control limit. There is a specific SPC's model is the range between the upper control limit and the lower control limit.

In injection molding conditions, there are only two conditions are mold temperature via heating and cooling cycle and packing time via heating and cooling cycle, are in SPC's range. These conditions can control the quality product is surface roughness by SPC but the energy consumption in these are higher than the energy consumption of conventional injection molding conditions. And they are limited the energy consumption by SPC. The both of relations in surface roughness and in the energy consumption are controlled by SPC. There are useful for preparing in future injection molding, that can predict quality of part and energy consumption.

5.2 Suggestions

However this work was finish, it was only the beginning part of injection moulding via rapid heating and cooling control system. There are some suggestions to the work for further study as follow.

5.2.1 Further examine and analyze the effects of induction heating and cooling system.

5.2.2 The suggestion should be study and in composite polymer, PLA polymer, and green polymer.

5.2.3 The another suggestion should be study in control system in injection molding and heating and cooling machine.

REFERENCES

1. Wang G., Zhao G., Li H., and Guan Y. "Analysis of thermal cycling efficiency and optimal design of heating/cooling systems for rapid cycle injection molding process." **Materials and design.,** vol. 31, 2010. pp 3426-3441.
2. Chris R. S. **SPC Statistical Process Control in Injection Molding and Extrusion.** Munich: Hanser Publishers. 2000.
3. **Modern Plastics Encyclopedia**.New York: McGraw-Hill, Inc. 1982.
4. Turner R. C. "Paper presented at SAE automotive plastics durability conference". **Society of Automotive Engineers.** Vol 1, 1981. pp 79.
5. Rioux J., Yao D. and Kim B. "Characterization of the Weldline Strength in Terms of Crack Growth Resistance in Injection Molded Thermoplastic Elastomers" **Polymer-Plastics Technology and Engineering.** Vol. 37, No. 3, 1998. pp 369-383.
6. Mann J. and Williamson G. R. **The physics Durability Conference.** New York: McGraw-Hill, Inc. 1973.
7. Casale, A., Moroni, A. and Spreafico, C. "ABS reins: The Relationship between. Composition and Rheological Behavior." **Advances in Chemistry Series.** Vol. 142, 1975. pp172.
8. Aoki Y. "Dynamic Viscoelastic Properties of ABS Polymers in the Molten State. II. Relaxation Spectra." **Journal of Rheology.** Vol. 25 (3), 1979. pp 351.
9. Munstedt H. "Rheology of rubber-modified polymer melts". **Polymer Engineering & Science.** 21(5), 1981. pp 259-270.
10. Zosel A. "Rheological properties of disperse systems at low shear stresses". **Rheologic Acta.** 21(1), 1972. pp 72-80.
11. Blyler Jr L. L. The influence of additives on the flow behavior of ABS. **Polymer Engineering & Science**. 14 (11), 1974. pp 806-809.

12. Berardinelli F. M., Dolce T. J. and Walling C. Degradation and stabilization of polyacetal copolymers. **Journal of Applied Polymer Science**. 9 (4), 1965. pp1419-1429.

13. Kekule A. “Zur Kenntniss des Formaldehyds.” **Berichte der deutschen chemischen Gesellschaft**.Vol 25(2),1892. pp 2435-2436.

14. Walker J.F. **Formaldyhyde.** 3 rd ED. New York: Reinhold Publishing Co. 1964. pp 192-194.

15. Spence R. and Wild W. “The Vapour-Pressure Curve of Formaldehyde, and Some Related Data.” **Journal of the Chemical Society**. Vol 138,1935. pp 506-509.

16. Ohe S. **Computer Aided Data Book of Vapor Pressure.** Tokyo: Data book publishing Co. 1976.

17. Gmehling J., Onken U. and Arlt W. “Vapor-Liquid Equilibrium Data Collection.”**Chemistry Data Series**. Vol 1, 1979. pp 414.

18. Stull D.R. and co workers. **The Chemical Thermodynamics of Organic Compounds.** New York : John Wiley & Sons, Inc. 1969.

19. Fire Protection Guide on Hazardous Materials. **National Fire Protection Association.** 6 th ED. 1958.

20. Gallant R.W. **Physical Properties of Hydrocarnons.** Houston: Gulf Publishing Company.

21. Reid R.C. and Sherwood T.K. **The properties of Gases and Liquids.** New York : McGraw-Hill, Inc. 1958.

22. Loew O. Ueber einige katalytische Wirkungen. **Berichte der deutschen chemischen Gesellschaft**. Vol 20(1), 1887. pp 144-145.

23. Auerbach F. and Barschall H. Studien uber Formaldehyde-Die Festen Polymeren des Formaldehyds. **Julius Springer.** Vol 1,1907. pp 38-45.

24. Gerberich H.R. **Krik-Othmer Encyclopedia of Chemical Technology**. 3 rd ED. New York: Wiley-Interscience. 1980.

25. Funck D. L. and Vogl O. **“Thermally Stabilized Polyaldehyde Elastomers”.** U.S. Patent No 3001966 , August, 1961.

26. Price M. B. and Berardinelli F. M. **"relates to a process for purifying acetals where the acetal is purified by contacting with liquid sodium, allowing a precipitate to form and removing the precipitate from the solution".** U.S. Patent No 3580928, May 25, 1971.

27. Schork F. J., Deshpande P.B. and Leffew K. W. "Control of Polymerization Reactors." **AIChE Journal.** Vol 41(5), 1993. pp 1354-1355.

28. Brandon D. and Kaplan W.D. **Microstructural characterization of materials**. 2nd ED. England: John Wiley. 2008.

29. Petrova L. I., Noskava M. P., Balandina V. A. and Guricheva Z. G. "Toxicity of vinyltoluene and its determination in air." **Gig Sanit**. vol 34(7-9),1969. pp. 334-339.

30. Lord H.A. "Mold Filling Studies for the Injection Molding of thermoplastics." **Journal of Engineering Science.** vol 15, 1975. pp. 553

31. Kydonieus N., Spence S.P., Blanks R. F., and James D. E**. "The continuous mass polymerization of HIPS and ABS polyblends."** U.S. Patent **No** 3511895, May 12, 1970.

32. Gesner B. D. "Environmental surface effects on ABS resins." **Journal of Applied Polymer Science.** Vol. 9, 1965. pp 3701–3706.

33. Scott G. "Developments in Polymer Stabilisation." **Applied Science Publishers.** Vol. 4, 1981. pp 181.

34. Injection Molding with Cycolac, Cycoloy, and Cycovin Brand ABS Resins and Alloys, **Technical Publication P-403.** Borg-Warner Chemicals, Inc., 1975.

35. Dalton W.O. **"Continuous process for the preparation of ABS type polyblends".** U.S. Patent **No** 3931356**,** March 21, 1978.

36. Fritch L.W. **Paper presented at the Annual Technical Conference of the Society of Plastics Engineers.** Boston, Mass. Vol. XXVII, 1975. pp 754.

37. Benning, C. J. **Plastic Foams: The Physics and Chemistry of Product Performance and Process Technology.** New York: John Wiley & Sons Inc.1969.

38. Landrock, A.H. **Polyurethane Foams: Technology Properties and Applications**, Plastic Technical Evaluation Center. 1969.

39. NASA. **Thermal Insulation Systems-A Survey.** Washington, D.C. 1967.

40. Miller,R.N. Bailey,C.D. Beal, R.T. and Freeman,J.M."Advances in Cryogenic Engineering". **Plenum Press**. Vol.8, 1963. pp. 417-424.

41. An Assessment of Thermal Insulation Materials and Systems for Building Applications, **DOE Report BNL-50862 UC-95d. U.S. Dept. of Energy**. Washington, D.D., 1978.

42. Nunn R.E. and Ackerman K. "Energy Efficiency in Injection Molding." **Society of Plastics Engineers.** Vol. 27, 1981. pp. 786.

43. Olmsted Bernie B.A. and Davis M.E. "Practical Injection Molding." **Plastics Engineering.** Vol. 36 , 1980. pp 51.

44. Schott N.R. and Derby H. **ACS Symposium Series.** Washington: American Chemical Society.1979.

45. Wang G, Zhao G, Wang X. "Effects of cavity surface temperature on reinforced plastic part surface appearance in rapid heat cycle moulding." **Materials and Design.**, vol. 44, 2012.pp509-520

46. Tsai K, Hsieh C, Lo W. "A study of the effects of process parameters for injection molding on surface quality of optical lenses." **Journal of materials processing technology.**, vol.209,2009.pp 3469-3477

APPENDIX A

HEATING AND COOLING CYCLE

A.1 Heating Up Stage

Mold surface temperature in heating up stage of Heating and Cooling cycle is increasing temperature. The mold surface temperature is higher or equal than Heat Distortion Temperature (HDT) of finishing surface polymer. Heating up stage is shown in **Figure A-1**.

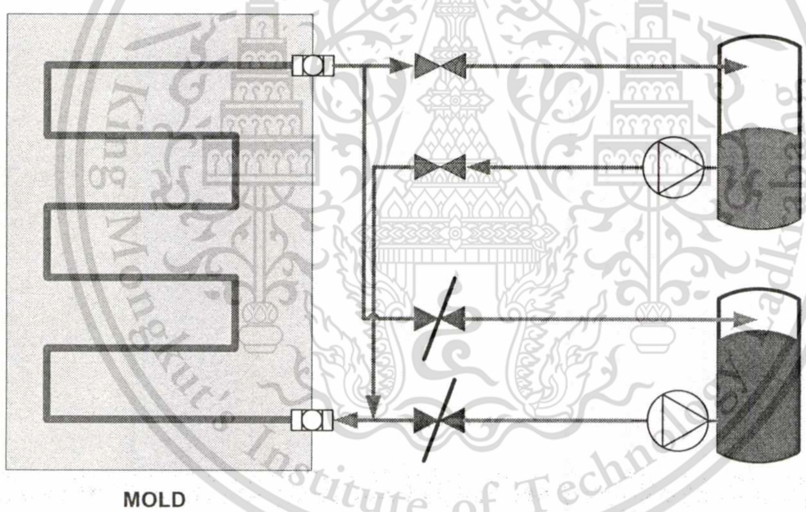

Figure A-1 Heating Up Stage

A.2 Cooling Down Stage

Mold surface temperature in cooling down stage of HC System (Heating and Cooling) is decreasing temperature. The mold surface temperature is lower or equal than ejection Temperature (HDT-30°C) of finishing surface polymer. Cooling down stage is shown in Figure A-2.

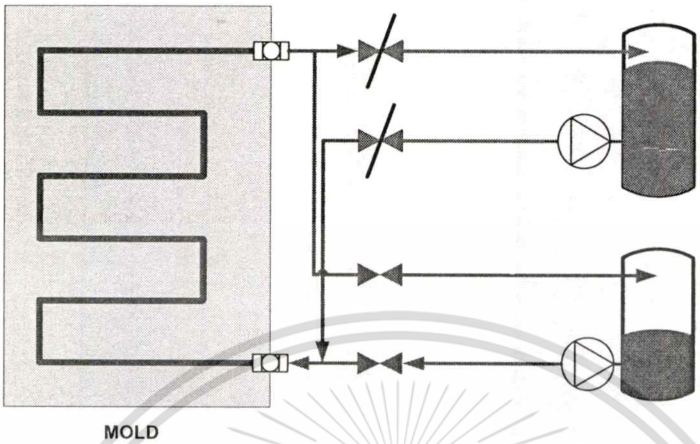

Figure A-2 Cooling Down Stage

In this study, Heating and cooling cycle is designed, assembly and installed heating and cooling control system by Plastic Technology Laboratory in MTEC. The specification of HC System is shown in **Table A-1** and the real HC System is shown in **Figure A-3**.

Table A-1 Specification of HC System

Temperature range	$5^{\circ}C$ - $120^{\circ}C$
Pressure	10 bar
Flow rate	2 - 4 liter/minute

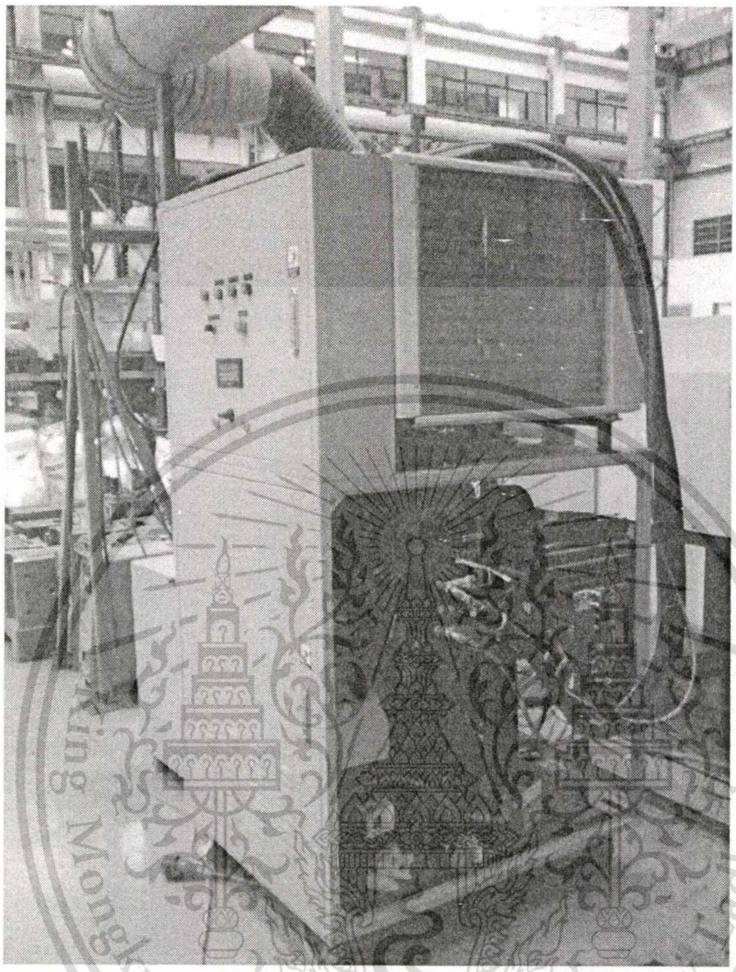

Figure A-3 Real HC System

APPENDIX B

Data Measurement

B.1 Thermocouple

The structure of thermocouple is represented in Figure B-1.

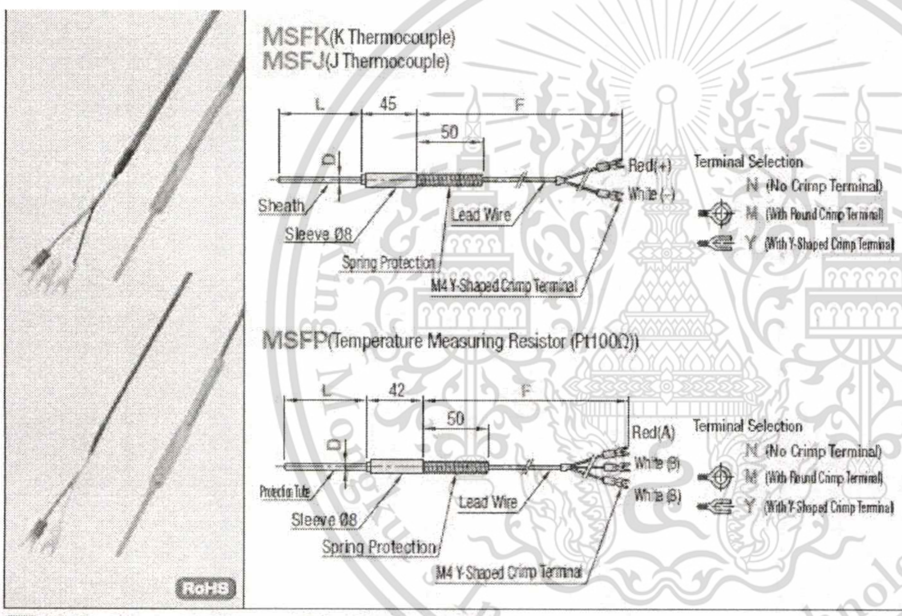

MSFK / MSFJ		MSFK	MSFJ
Type of Thermocouple		K Thermocouple	J Thermocouple
Precision		JIS Class 2	
Temperature Measurement Contact Point		Isolated Neutral Type	
Temperature Measurement Range	Ø1.0, 1.6	0~650°C	0 ~ 450°C
	Ø3.2	0~750°C	0~650°C
	Ø4.8	0~800°C	0~750°C
M Material	Sheath	316 Stainless Steel	
	Sleeve	304 Stainless Steel	
Heat Resistance Temperature of Sleeve		80°C	
Lead Wire (Operating Temperature Range)		Glass Wool Coating (0~150°C)	

MSFP

Type of Device		Pt100Ω
Precision		JIS Class B
Lead Type		3-lead Type
Measurement Temperature Range		0 ~ 300°C
M Material	Protection Tubes	316 Stainless Steel
	Sleeve	304 Stainless Steel
Heat Resistance Temperature of Sleeve		80°C
Lead Wire (Operating Temperature Range)		Vinyl Coating (-20~70°C)

■K Thermocouple - J Thermocouple

Part Number		L 10mm Increment	Lead Wire Length F 0.1m Increment	Terminal Selection
Type	D			
(K Thermocouple) MSFK	1.0	50~200	0.3~5.0	N M Y
	1.6	50~500		
(J Thermocouple) MSFJ	3.2	50~1000		
	4.8	50~1500		

FigureB-1 Thermocouple specification

B.2 Pressure sensor

The structure of pressure sensor is represented in **Figure B-2**.

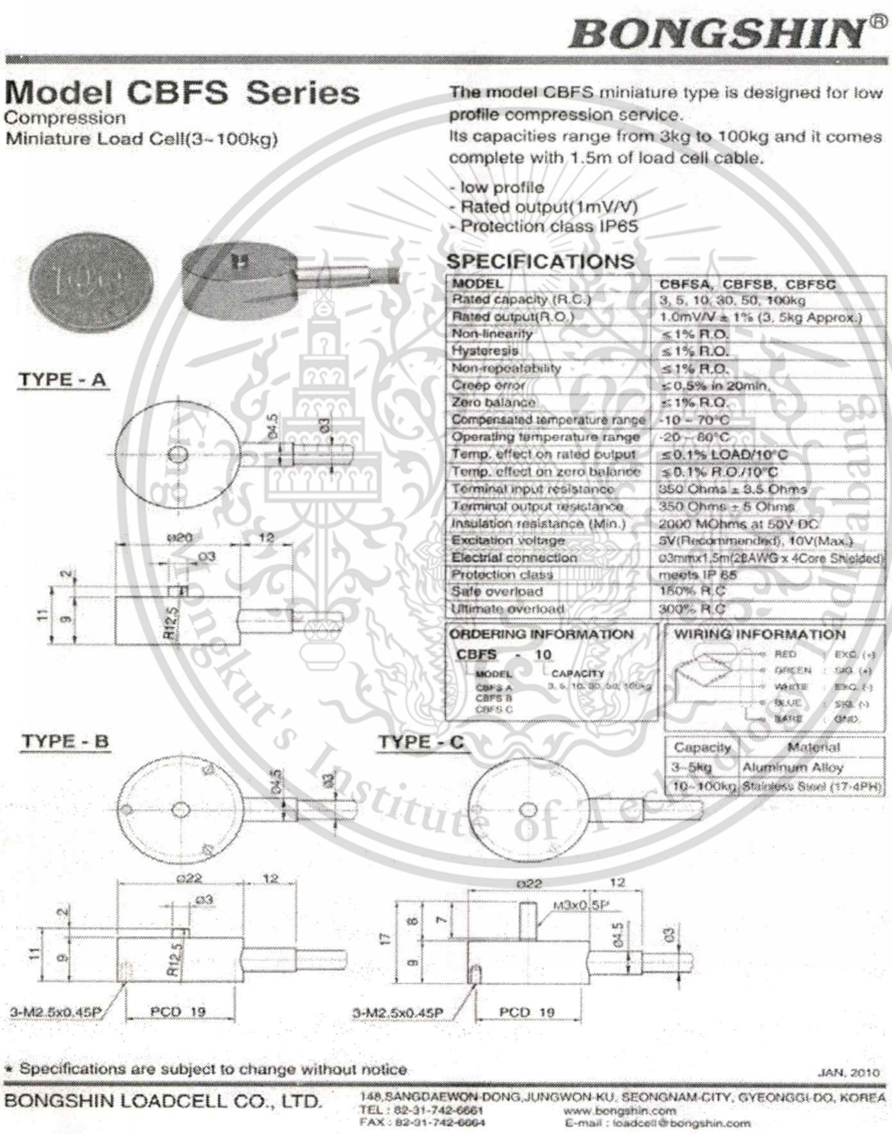
BONGSHIN®

Model CBFS Series

Compression
Miniature Load Cell(3~100kg)

The model CBFS miniature type is designed for low profile compression service.
Its capacities range from 3kg to 100kg and it comes complete with 1.5m of load cell cable.

- low profile
- Rated output(1mV/V)
- Protection class IP65

TYPE - A

SPECIFICATIONS

MODEL	CBFSA, CBFSB, CBFSC
Rated capacity (R.C.)	3, 5, 10, 30, 50, 100kg
Rated output(R.O.)	1.0mV/V ± 1% (3, 5kg Approx.)
Non-linearity	≤1% R.O.
Hysteresis	≤1% R.O.
Non-repeatability	≤1% R.O.
Creep error	≤0.5% in 20min.
Zero balance	≤1% R.O.
Compensated temperature range	-10 ~ 70°C
Operating temperature range	-20 ~ 80°C
Temp. effect on rated output	≤0.1% LOAD/10°C
Temp. effect on zero balance	≤0.1% R.O./10°C
Terminal input resistance	350 Ohms ± 3.5 Ohms
Terminal output resistance	350 Ohms ± 5 Ohms
Insulation resistance (Min.)	2000 MOhms at 50V DC
Excitation voltage	5V(Recommended), 10V(Max.)
Electrial connection	ø3mmx1.5m(28AWG x 4Core Shielded)
Protection class	meets IP 65
Safe overload	150% R.C
Ultimate overload	300% R.C

ORDERING INFORMATION

CBFS - 10
MODEL: CBFS A, CBFS B, CBFS C
CAPACITY: 3, 5, 10, 30, 50, 100kg

WIRING INFORMATION

RED : EXC. (+)
GREEN : SIG. (+)
WHITE : EXC. (-)
BLUE : SIG. (-)
BARE : GND.

Capacity	Material
3~5kg	Aluminum Alloy
10~100kg	Stainless Steel (17-4PH)

TYPE - B

TYPE - C

★ Specifications are subject to change without notice

JAN. 2010

BONGSHIN LOADCELL CO., LTD.
148,SANGDAEWON-DONG,JUNGWON-KU, SEONGNAM-CITY, GYEONGGI-DO, KOREA
TEL : 82-31-742-6661
FAX : 82-31-742-6664
www.bongshin.com
E-mail : loadcell@bongshin.com

Figure B-2 Pressure sensor specification

APPENDIX C

Data logger and Programming

C.1 Assembly data logger

C.1.1 Install NI-9211 at the top of box as called Temperature zone.

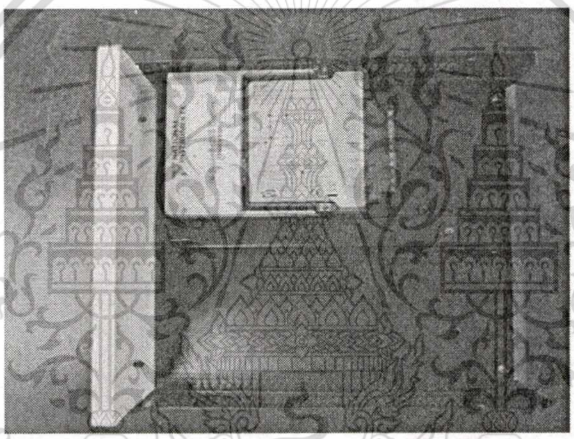

Figure C-1 Wisco WT95 into box

C.1.2 Install NI-9215 and Wisco WT95 at the bottom of box as called pressure zone.

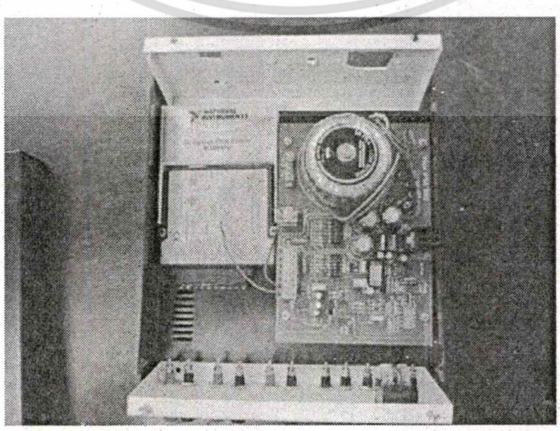

Figure C-2 NI-9211 into box

C.1.3 Drilling at the front of the box.

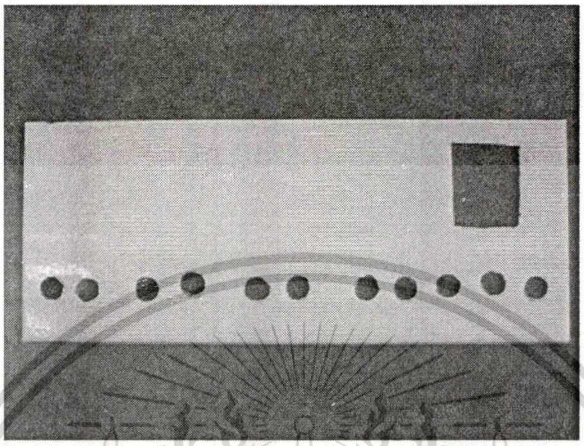

Figure C-3 Drilling at the front of the box

C.1.4 Install switch and plugs at the front of the box.

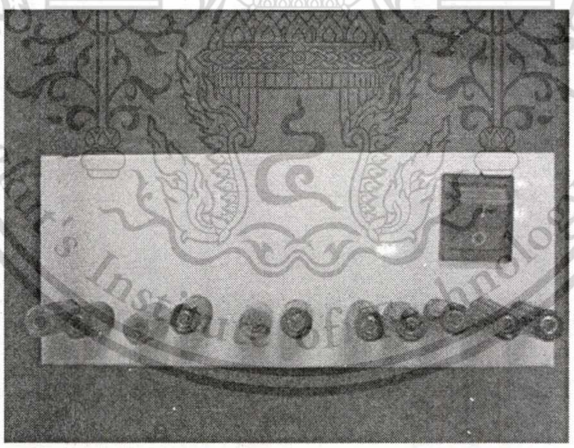

Figure C-4 Switch and plugs at the front of the box

C.1.5 Install power plug, flues and drilling at the front of the box.

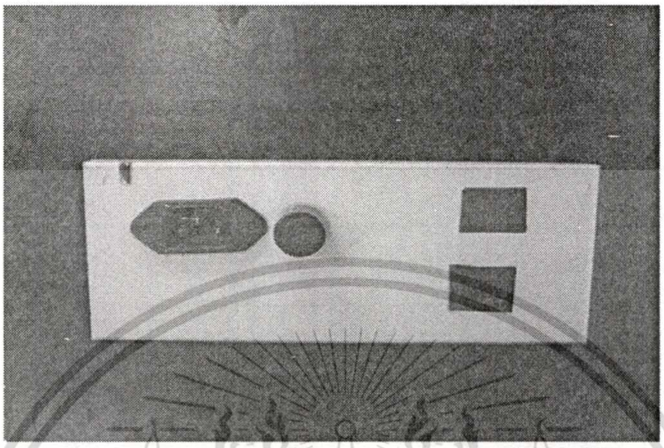

Figure C-5 Power plug , flues and drilling at the front of the box

C.1.6 Assembly a part of box and stick a label.

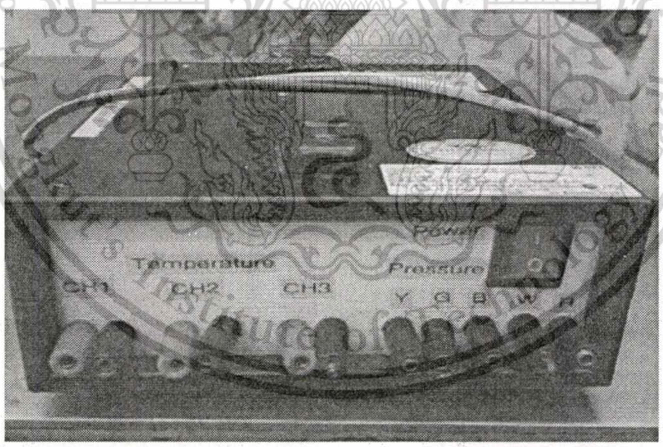

Figure C-6 Completely data logger

C.2 manual Data logger

C.2.1 Connect power plug into data logger in **Figure C-7**.

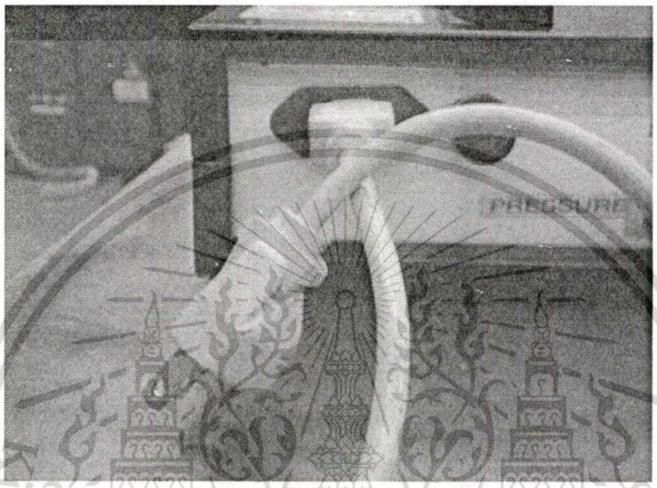

Figure C-7 Completely data logger

C.2.2 Connect thermocouple data wires into data logger in **Figure C-8**

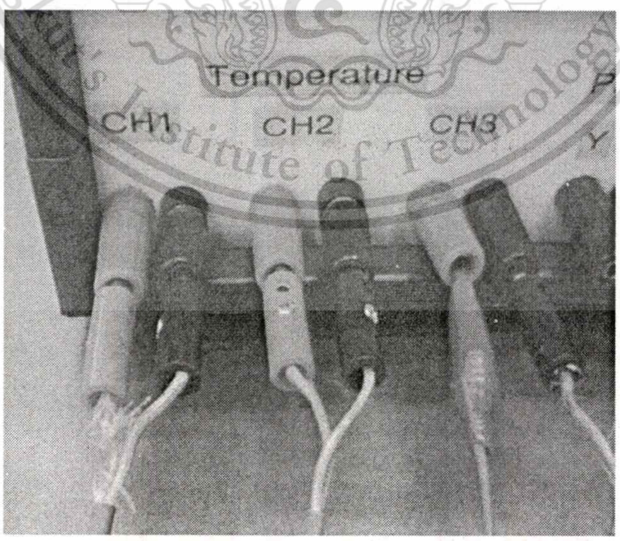

Figure C-8 Thermocouple data wires connect data logger

C.2.3 Connect pressure data wires into data logger in **Figure C-9**

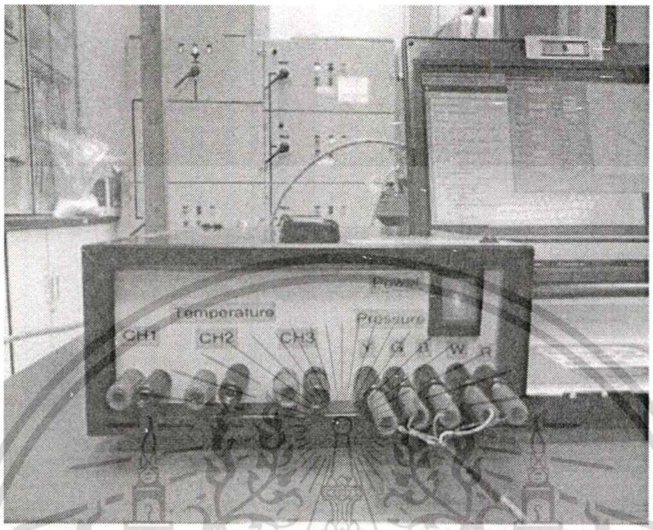

Figure C-9 Pressure data wires connect data logger

C.2.4 Turn on power switch in **Figure C-10**.

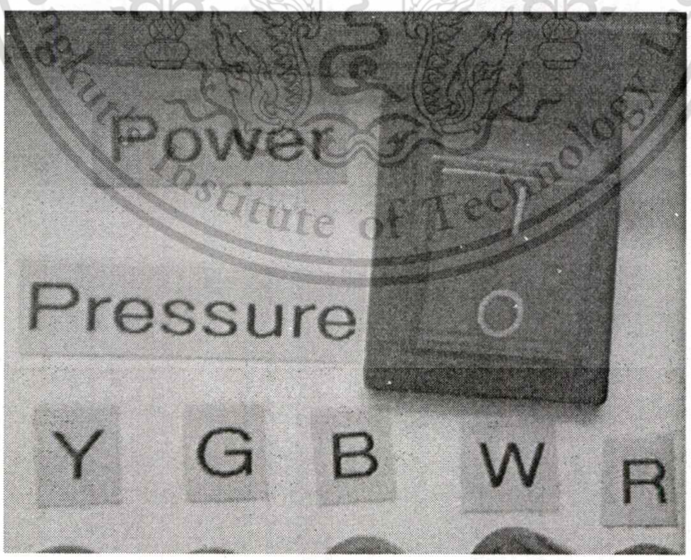

Figure C-10 On power switch

C.2.5 **Connect data logger into computer in Figure C-11.**

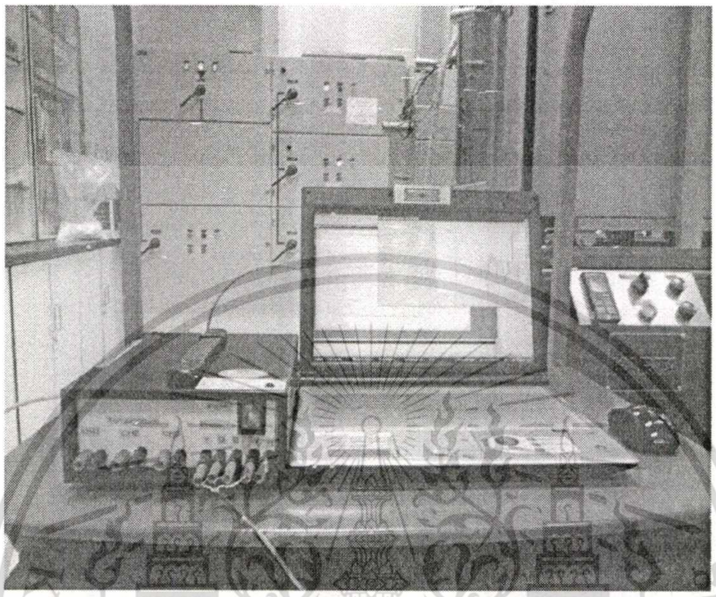

Figure C-11 Data logger connect computer

C.3 Programming

C.3.1 Flowchart of temperature programming

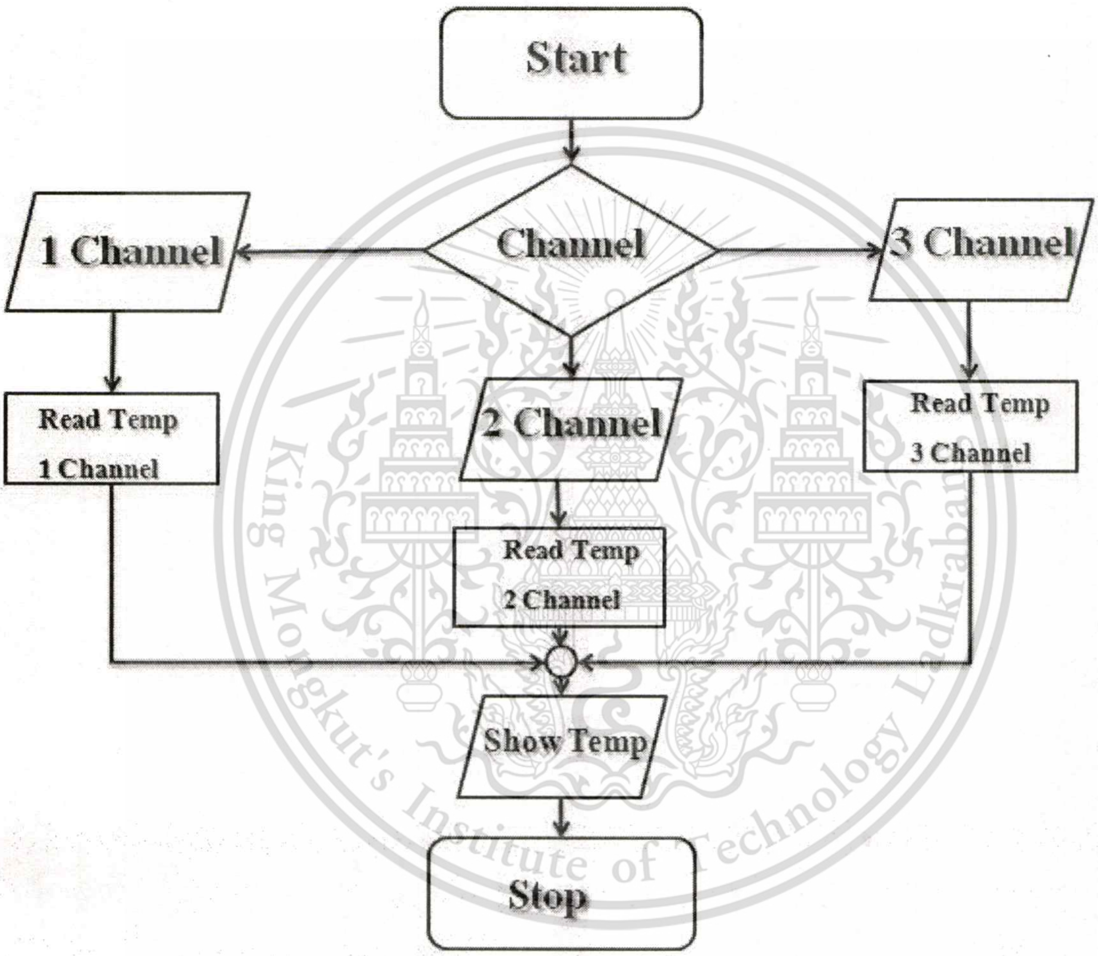

Figure C-12 Flowchart of temperature programming

C.3.2 Temperature programming

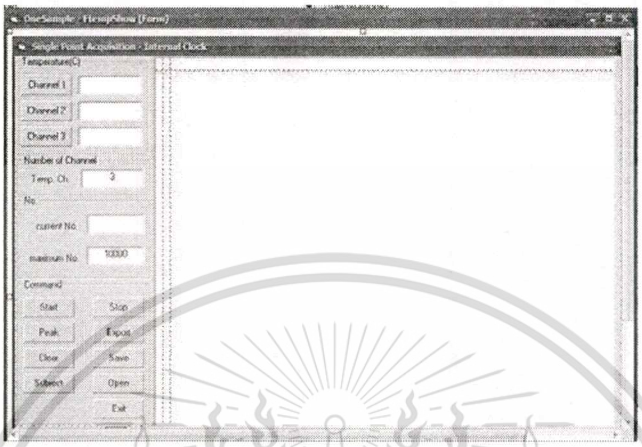

Figure C-13 Temperature software

C.3.3 Code programming of temperature

C.3.3.1 Main of temperature programming

```
Option Explicit
Private Declare Sub Sleep Lib
"kernel32" (ByVal
dwMilliseconds As Long)
Private Sub End_Click()
End
End Sub
Private Sub
btnDisconnect_Click()
 If MSComm1.PortOpen =
True Then
   MSComm1.PortOpen =
False
   Label5.Caption = "Port
Closed"
  Label5.ForeColor = vbBlack
 End If
End Sub
Private Sub
BTNoffCh1_Click()
MSComm1.Output = "@1 F1"
& vbCr
End Sub
Private Sub
BTNoffCh2_Click()
  MSComm1.Output = "@1
F2" & vbCr
End Sub
Private Sub
BTNoffCh3_Click()
MSComm1.Output = "@1 F3"
& vbCr
End Sub
Private Sub
BTNonCh1_Click()
 MSComm1.Output = "@1
N1" & vbCr
End Sub
Private Sub
BTNonCh2_Click()
```

```
MSComm1.Output = "@1 N2"
& vbCr
End Sub
Private Sub
BTNonCh3_Click()
MSComm1.Output = "@1 N3"
& vbCr
End Sub
Private Sub btnStatus1_Click()
Call ClearInpBuffer 'clear
existing input buffer data
 MSComm1.Output = "@1
S1" & vbCr
 Sleep (50)
 MsgBox (MSComm1.Input)
End Sub
Private Sub btnStatus3_Click()
ClearInpBuffer 'clear existing
input buffer data
MSComm1.Output = "@1 S3"
& vbCr
 Sleep (50)
 MsgBox (MSComm1.Input)
End Sub
Private Sub
Cmd_clear_plot_Click()
plot_t.Cls
End Sub
Private Sub
Cmd_export_temp_Click()
mExport
End Sub
Private Sub
Cmd_Open_T1_Click()
mOpen
End Sub
Private Sub cmd_peak_Click()
FpeakTemp.Show
End Sub
Private Sub
Cmd_save_T_Click()
mSave
End Sub
Private Sub
Cmd_Temp_Back_Click()
'FtempShow.Hide
'FselectChannel.Show
End Sub
Private Sub
Cmd_Temp_Exit_Click()
End
End Sub

Private Sub
Cmd_Temp_Stop_Click()
    Timer1.Enabled = False
    StartTemp.Enabled = True
    Cmd_Temp_Stop.Enabled =
False
    End Sub
Private Sub
Command1_Click()
    mExport
End Sub
Private Sub
cmdMoldParameters_Click()
Fmp.Show
End Sub
Private Sub Command_Click()
 Call Autoclick
 End Sub
Private Sub
plot_t_MouseDown(Button As
Integer, Shift As Integer, X As
Single, Y As Single)
    Dim Yv As Single
    Dim Yi As Single
    Dim Yt As Single
    Dim Xv As Single
    Dim Xi As Single
    Dim Xt As Single
    Dim xxX1 As Single
    Dim xxY1 As Single
    Dim xxX2 As Single
```

```
Dim xxY2 As Single
Dim xxX3 As Single
Dim xxY3 As Single
Dim xxPlot As Single
Dim xyPlot As Single
Dim xxPlot1 As Single
Dim xyPlot1 As Single
'Pointer
If ShowPointerStatus = True
Then
    Line1.Y1 = Y
    Line1.Y2 = Y
    Line2.X1 = X
    Line2.X2 = X
        If X >= 3 * lpx_T
And X <= 13 * lpx_T Then
        Xi = (X - (3 *
lpx_T)) / lpx_T

        Xv = XPointMin_T
+ ((XPointMax_T -
XPointMin_T) * 0.1 * Xi)
    End If
    If Y >= 2 * lpy_T And Y
<= 12 * lpy_T Then
        Yi = 10 - ((Y - (2 *
lpy_T)) / lpy_T)
                Yv = YPointMin_T
+ ((YPointMax_T -
YPointMin_T) * 0.1 * Yi)
        End If
                If
Abs(XPointMax_T -
XPointMin_T) <> 0 And
Abs(YPointMax_T -
YPointMin_T) <> 0 Then
                xxPlot = (3 *
lpx_T) + (10 * lpx_T * ((X -
XPointMin_T) /
Abs(XPointMax_T -
XPointMin_T)))
                xyPlot = (12
* lpy_T) - (10 * lpy_T * ((Y -
YPointMin_T) /
Abs(YPointMax_T -
YPointMin_T)))
FtempShow.plot_t.Circle
(xxPlot, xyPlot), 5000,
QBColor(2)
'
fMain.plot.Line (xxPlot,
xyPlot - 40)-(xxPlot, xyPlot +
40), QBColor(2)
'                MsgBox
xxPlot & "," & xyPlot
                End If
        fPeakU.PointerText.Text
= "" & Format(Xv, "####.#0")
& " , " & Format(Yv,
"####.#0") & ""
    End If
    'baseline
    If ShowBaselineStatus =
True Then
        If Y >= 2 * lpy_T And
Y <= 12 * lpy_T Then
            Yi = 10 - ((Y - (2 *
lpy_T)) / lpy_T)
            Yv = YPointMin_T
+ ((YPointMax_T -
YPointMin_T) * 0.1 * Yi)

            YBaseline = Yv
fPeakU.BaselineText.Text =
Format(YBaseline, "####.#0")
            If
Abs(XPointMax_T -
XPointMin_T) <> 0 And
Abs(YPointMax_T -
YPointMin_T) <> 0 Then
                xxPlot = 3 *
lpx_T
                xxPlot1 = 13
* lpx_T
```

```
                xyPlot1 =
(12 * lpy_T) - (10 * lpy_T *
((YBaseline - YPointMin_T) /
Abs(YPointMax_T -
YPointMin_T)))
FtempShow.plot_t.Line
(xxPlot, xyPlot1)-(xxPlot1,
xyPlot1), QBColor(2)
            End If
        Else
     fPeakU.BaselineText.Text
=
Format(YBaseline,"####.#0")

        End If
   End If
   'X1
   If ShowX1Status = True
Then
      If X >= 3 * lpx_T And X
<= 13 * lpx_T Then
        Line1.Y1 = Y
        Line1.Y2 = Y
        Line2.X1 = X
        Line2.X2 = X
          Xi = (X - (3 *
lpx_T)) / lpx_T
                Xv = XPointMin_T
+ ((XPointMax_T -
XPointMin_T) * 0.1 * Xi)
                RangeX1 = Xv
fPeakU.RangeX1Text.Text =
Format(RangeX1, "####.#0")
                  If
Abs(XPointMax_T -
XPointMin_T) <> 0 And
Abs(YPointMax_T -
YPointMin_T) <> 0 Then
xxPlot = (3 * lpx_T) + (10 *
lpx_T * ((RangeX1 -
XPointMin_T) /
Abs(XPointMax_T -
XPointMin_T)))
xyPlot = 2 * lpy_T
xyPlot1 = 12 * lpy_T
FtempShow.plot_t.Line
(xxPlot, xyPlot)-(xxPlot,
xyPlot1), QBColor(2)
                  End If
        Else
fPeakU.RangeX1Text.Text =
Format(RangeX1, "####.#0"
        End If
     End If
     'X2
  If ShowX2Status = True
Then
     If X >= 3 * lpx_T And X
<= 13 * lpx_T Then
        Line1.Y1 = Y
        Line1.Y2 = Y
        Line2.X1 = X
        Line2.X2 = X
          Xi = (X - (3 *
lpx_T)) / lpx_T
          Xv = XPointMin_T
+ ((XPointMax_T -
XPointMin_T) * 0.1 * Xi)
          RangeX2 = Xv
fPeakU.RangeX2Text.Text =
Format(RangeX2, "####.#0")
               If
Abs(XPointMax_T -
XPointMin_T) <> 0 And
Abs(YPointMax_T -
YPointMin_T) <> 0 Then
xxPlot = (3 * lpx_T) + (10 *
lpx_T * ((RangeX2 -
XPointMin_T) /
Abs(XPointMax_T -
XPointMin_T)))
 xyPlot = 2 * lpy_T
xyPlot1 = 12 * lpy_T
```

```
FtempShow.plot_t.Line
(xxPlot, xyPlot)-(xxPlot,
xyPlot1), QBColor(3)
            End I
      Else
fPeakU.RangeX2Text.Text =
Format(RangeX2, "####.#0")
      End If

   End If
   'Zoom1
   If Zoom1Status = True
Then
      Line1.Y1 = Y
      Line1.Y2 = Y
      Line2.X1 = X
      Line2.X2 = X
      If X >= 3 * lpx_T And X
<= 13 * lpx_T Then
            Xi = (X - (3 *
lpx_T)) / lpx_T
            Xv = XPointMin_T
+ ((XPointMax_T -
XPointMin_T) * 0.1 * Xi)
      End If
      If Y >= 2 * lpy_T And Y
<= 12 * lpy_T Then
            Yi = 10 - ((Y - (2 *
lpy_T)) / lpy_T)
            Yv = YPointMin_T
+ ((YPointMax_T -
YPointMin_T) * 0.1 * Yi)
      End If
FtempShow.ZoomX1Text.Tex
t = Format(Xv, "####.#0")

FtempShow.ZoomY1Text.Tex
t = Format(Yv, "####.#0")
      Zoom1Status = False
      Line1.Visible = False
      Line2.Visible = False
   End If
   'Zoom2
   If Zoom2Status = True
Then
      Line1.Y1 = Y
      Line1.Y2 = Y
      Line2.X1 = X
      Line2.X2 = X
      If X >= 3 * lpx_T And X
<= 13 * lpx_T Then
 Xi = (X - (3 * lpx_T)) / lpx_T
Xv = XPointMin_T +
((XPointMax_T -
XPointMin_T) * 0.1 * Xi)

End If
If Y >= 2 * lpy_T And Y <=
12 * lpy_T Then Yi = 10 - ((Y
- (2 * lpy_T)) / lpy_T)
Yv = YPointMin_T
((YPointMax_T -
YPointMin_T) * 0.1 * Yi)
End If
FtempShow.ZoomX2Text.Tex
t = Format(Xv, "####.#0")
FtempShow.ZoomY2Text.Tex
t = Format(Yv, "####.#0")
Zoom2Status = False
Line1.Visible = False
Line2.Visible = False
End If
End Sub
Private Sub
plot_t_MouseMove(Button As
Integer, Shift As Integer, X As
Single, Y As Single)
 Dim Yv As Single
   Dim Yi As Single
   Dim Yt As Single
   Dim Xv As Single
   Dim Xi As Single
   Dim Xt As Single
   'Pointer
If ShowPointerStatus = True
Then
```

```
        Line1.Y1 = Y

        Line1.Y2 = Y
        Line2.X1 = X
        Line2.X2 = X
    If X >= 3 * lpx_T And X
<= 13 * lpx_T Then
            Xi = (X - (3 *
lpx_T)) / lpx_T
            Xv = lpy_T +
((XPointMax_T -
XPointMin_T) * 0.1 * Xi)
    End If
    If Y >= 2 * lpy_T And Y
<= 12 * lpy_T Then
            Yi = 10 - ((Y - (2 *
lpy_T)) / lpy_T)
            Yv = YPointMin_T
+ ((YPointMax_T -
YPointMin_T) * 0.1 * Yi)
    End If
    fPeakU.LabelP.Caption =
"Position :(" & Format(Xv,
"####.#0") & "," &
Format(Yv, "####.#0") & ")"
  End If
  'Baseline
  If ShowBaselineStatus =
True Then
    If Y >= 2 * lpy_T And Y
<= 12 * lpy_T Then
        Line1.Y1 = Y
        Line1.Y2 = Y
        Line2.X1 = X
        Line2.X2 = X
            Yi = 10 - ((Y - (2 *
lpy_T)) / lpy_T)
            Yv = YPointMin_T
+ ((YPointMax_T -
YPointMin_T) * 0.1 * Yi)
            Yt = Yv
fPeakU.LabelB.Caption =
"Baseline : " & Format(Yt,
"####.#0")
    End If
  End If
  'X1
  If ShowX1Status = True
Then
If X >= 3 * lpx_T And X <=
13 * lpx_T Then
 Line1.Y1 = Y

        Line1.Y2 = Y
        Line2.X1 = X
        Line2.X2 = X
 Xi = (X - (3 * lpx_T)) / lpx_T
            Xv = XPointMin_T
+ ((XPointMax_T -
XPointMin_T) * 0.1 * Xi)
            Xt = Xv
fPeakU.LabelX1.Caption =
"From X1 : " & Format(Xt,
"####.#0")
End If
End If
'X2
If ShowX2Status = True Then
    If X >= 3 * lpx_T And X
<= 13 * lpx_T Then
        Line1.Y1 = Y
        Line1.Y2 = Y
        Line2.X1 = X
        Line2.X2 = X
Xi = (X - (3 * lpx_T)) / lpx_T
            Xv = XPointMin_T
+ ((XPointMax_T -
XPointMin_T) * 0.1 * Xi)
            Xt = Xv
fPeakU.LabelX2.Caption =
"To X2 : " & Format(Xt,
"####.#0")
    End If
  End If
  'Zoom1
```

```
If Zoom1Status = True
Then
        Line1.Y1 = Y
        Line1.Y2 = Y
        Line2.X1 = X
        Line2.X2 = X
    If X >= 3 * lpx_T And X
<= 13 * lpx_T Then
            Xi = (X - (3 *
lpx_T)) / lpx_T
            Xv = XPointMin_T
+ ((XPointMax_T -
XPointMin_T) * 0.1 * Xi)
    End If
    If Y >= 2 * lpy_T And Y
<= 12 * lpy_T Then
            Yi = 10 - ((Y - (2 *
lpy_T)) / lpy_T)
            Yv = YPointMin_T
+ ((YPointMax_T -
YPointMin_T) * 0.1 * Yi)
    End If
FtempShow.LabelZoom.Capti
on = "(X,Y ):dddddd(" &
Format(Xv, "####.#0") & ","
& Format(Yv, "####.#0") &
")"
    End If
    'Zoom2
    If Zoom2Status = True
Then
        Line1.Y1 = Y
        Line1.Y2 = Y
        Line2.X1 = X
        Line2.X2 = X
    If X >= 3 * lpx_T And X
<= 13 * lpx_T Then
            Xi = (X - (3 *
lpx_T)) / lpx_T
Xv = XPointMin_T +
((XPointMax_T -
XPointMin_T) * 0.1 * Xi)
    End If
    If Y >= 2 * lpy_T And Y
<= 12 * lpy_T Then
            Yi = 10 - ((Y - (2 *
lpy_T)) / lpy_T)
            Yv = YPointMin_T
+ ((YPointMax_T -
YPointMin_T) * 0.1 * Yi)
    End
IfFtempShow.LabelZoom.Cap
tion = "(X,Y ):(" &
Format(Xv, "####.#0") & ","&
Format(Yv, "####.#0") & ")"
End If
End Sub
Private Sub startTemp_Click()
StartTemp.Enabled = False
Cmd_Temp_Stop.Enabled =
True
Timer1.Enabled = True
Initial_Data_T
Start_Time_T = Timer
Counter_T = 0
'MsgBox Start_Time_T
End Sub
Private Sub Form_Load()
taskIsRunning = 0
nPoint_T = 0
End Sub
Private Sub
Form_Unload(Cancel As
Integer)
'  Quit the program.
If taskIsRunning = True Then
StopTask
End If
End
End Sub
Private Sub Timer1_Timer()
DoEvents
'Temperature sensor @
```

```
channel 1
Counter_T = Counter_T + 1
nPoint_T = Counter_T
currentdata.Text = nPoint_T
'findPeakTemperatureMax
'MsgBox Counter_T
XPoint_T(Counter_T) = Timer
- Start_Time_T

'    MsgBox
XPoint_T(Counter_T)
A_ReadTempAll
'findPeakTemperatureMax
XYMaxMin_T
PlotCurve_Temp
Call AutoclickTempmax
Call AutoclickTempmin
End Sub
Private Sub Timer2_Timer()
Dim xxxxx1 As String
Open App.Path & "\s.txt" For
Input As #1
 Input #1, xxxxx
Input #1, xxxxx1
Close #1
Open App.Path & "\s.txt" For
Input As #2
Input #2, xxxxx
Input #2, xxxxx1
Close #2
If xxxxx = 1 Then
Timer2.Enabled = False
startTemp_Click
 ElseTimer2.Enabled = True
Cmd_Temp_Stop_Click

   End If
End Sub
Private Sub Form_Load1()
ConnectPort
End Sub
Private Sub
btnConnect_Click()
Call ConnectPort
End Sub
Private Sub ConnectPort()
If MSComm1.PortOpen =
False Then 'check if port
already open
MSComm1.CommPort =
CInt(Text1.Text)
MSComm1.PortOpen = True
Label5.Caption = "Port
Opened"
Label5.ForeColor = vbBlue
End If
End Sub
Private Sub ClearInpBuffer()
Dim strInpBuffer As String
strInpBuffer =
MSComm1.Input
End Sub

Private Sub btnStatus2_Click()
ClearInpBuffer 'clear existing
input buffer data
MSComm1.Output = "@1 S2"
& vbCr  Sleep (50)
MsgBox (MSComm1.Input)
End Sub
Private Sub
Form_Unload1(Cancel As
Integer)
On Error Resume Next
MSComm1.PortOpen = False
'close the port
End Sub
Private Sub Timer3_Timer()
'Dim yyyyy1 As String
 'Open App.Path & "\t.txt" For
Input As #1
'    Input #1, yyyyy
'   Input #1, yyyyy1
'Close #1
'Open App.Path & "\t.txt" For
Input As #2
'    Input #2, yyyyy
```

```
'    Input #2, yyyyy1
'Close #2
If Temp1.Text >= "23" Then
Timer3.Enabled = False
BTNonCh1_Click
Else
Timer3.Enabled = True
Cmd_Temp_Stop_Click
End I
End Sub
```

C.3.4 Flowchart of pressure programming

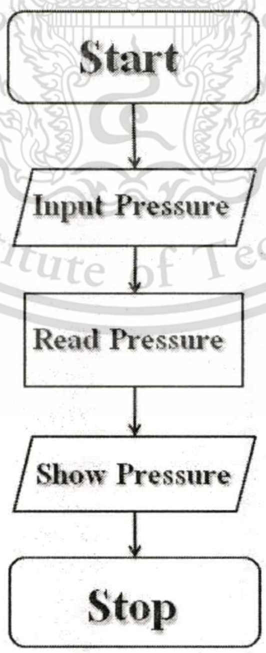

FigureC-13 Flow chart of pressure programming

C.3.5 Pressure programming

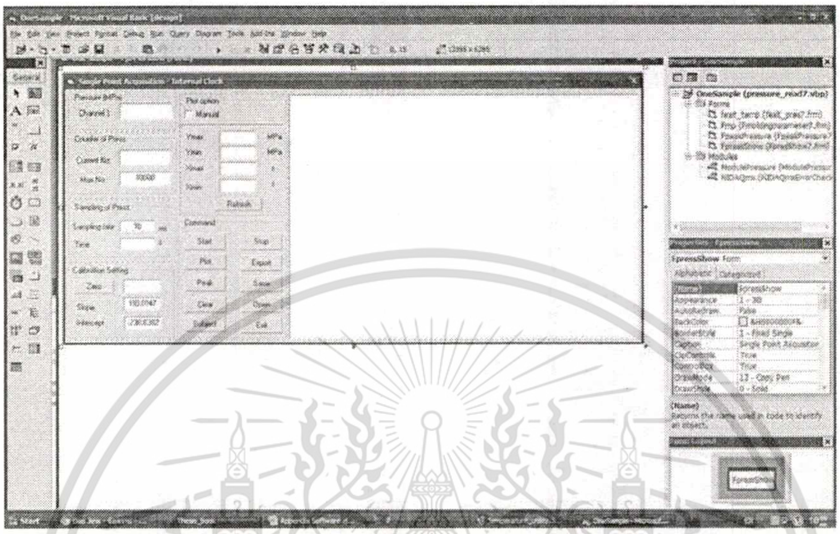

Figure C-14 Pressure program

C.3.6 Code programming of pressure

```
Option Explicit
Private Sub
End_Click()
End
End Sub
Private Sub
Cmd_clear_plot_Clic
k()
plot_press.Cls
End Sub
Private Sub
Cmd_export_press_Cl
ick()
mExportPressure
'Export Pressure data
End Sub
Private Sub
Cmd_Open_T1_Click
()
mOpenPressure
'Open Pressure data
End Sub

Private Sub
cmd_peak_Click()
FpeakPressure.Show
'FpeakTemperature
open
End Sub
Private Sub
cmd_plot_Click()
 Dim TC1 As Single
  Dim TC2 As Single
  TC1 = Timer
  If nPoint_P = 0
Then
 MsgBox "Error
plotting data! Because
of number of data is
```

```
zero."
Exit Sub
End If
'gen_random_data
plot_press.DrawMode
= 13
 plot_press.DrawStyle
= 0
XYMaxMin_P
plot_press.Cls
DrawScale_Press
DrawGrid_Press
DrawAxis_Press
LabelScale_Press
LabelScale1_Press
PlotDATA_Press
TC2 = Timer - TC1
'Text2.Text =Str(TC2)
End Sub
Private Sub
Cmd_save_T_Click()
mSavePressure
'Save Pressure data
End Sub
Private Sub
Cmd_Temp_Exit_Cli
ck()
FpressShow.Hide
fexit_temp.Show
End Sub
Private Sub
Cmd_Press_Stop_Clic
k()
 'Timer1.Enabled =
False
'Timer1 stop as
Temperature
measurement stop
Timer2.Enabled =
False
'Timer2 stop as
Pressure measurement
stop
startPress.Enabled =
True
'Start button able click
Cmd_Press_Stop.Ena
bled = False
'Stop button unable
click
'XPoint_P(Counter_P)
= 0
 'Timer = 0
End Sub
Private Sub
cmd_refresh_Click()
    PlotOptions
PlotOpionMaxMin
FpressShow.plot_pres
s.Cls
DrawScale_Press
DrawGrid_Press
DrawAxis_Press
LabelScale_Press
LabelScale1_Press
PlotDATA_Press
End Sub
Private Sub
Command2_Click()
PlotOptions
PlotOpionMaxMin

FpressShow.plot_pres
s.Cls
DrawScale_Press
DrawGrid_Press
DrawAxis_Press
LabelScale_Press
LabelScale1_Press
PlotDATA_Press
End Sub
Private Sub
Timer1_Timer()
```

```
Dim xxxxx1 As String
Open App.Path &
"\s.txt" For Input As
#1
Input #1, xxxxx
Input #1, xxxxx1
Close #1
If xxxxx = 1 Then
Timer1.Enabled =
False
startPress_Click
Else
Timer1.Enabled =
True
Cmd_Press_Stop_Click
End If
End Sub
Private Sub YZero_Click()
Y0 =
Val(Out_Pressure(1).Text)
Text5.Text = Y0
Y0 = Slope * Y0 + Intercept
End Sub
Private Sub
cmdMoldParameters_Click()
Fmp.Show
End Sub
Private Sub startPress_Click()
'When click this buttom,
temperature and pressure is
running
startPress.Enabled = False
'start button unable click
Cmd_Press_Stop.Enabled =
True                'stop button able
click
'Pressure measurement
'Initial_Data_P
'Initial_Data_P run
Start_Time_P = Timer
 Slope =
Val(FpressShow.Tslope.Text)
'Put value in slope box
Intercept =
Val(FpressShow.Tintercept.Te
xt)  'Put value in intercept box
Timer2.Interval =
Val(TSamplingRate.Text)
'Timer2 for pressure
measurement
PlotOptions
'PlotOptionMaxMin run
PlotOpionMaxMin
'PlotOptionMaxMin run
'MsgBox Autoplot
Timer2.Enabled = True
'Timer2 run
 'Start_Time_P = Timer2
'Start_Time_p = Timer
Counter_P = 0
'Counter_P = 0
'MsgBox Str(Timer1.Interval)
& ":" & Str(Timer2.Interval)
End Sub

Private Sub
 Form_Load()
taskIsRunning = 0
nPoint_P = 0
End Sub
Private Sub
Form_Unload(Cancel As
Integer)
' Quit the program.
If taskIsRunning = True Then
StopTask
 End If
End
End Sub
'Private Sub Timer1_Timer()
'   DoEvents
'   'Temperature sensor @
channel 1
'   Counter_T = Counter_T + 1
```

```
'Counter_T = Counter_T+1
'   nPoint_T = Counter_T
'get Counter_T into nPoint_T
'   currentdata.Text =
nPoint_T
'get currentdata into nPoint_T
'MsgBox Counter_T'

XPoint_T(Counter_T) =
Timer - Start_Time_T
'XPoint_T(Counter_T) =
Timer-Start_Time_T
'MsgBox
XPoint_T(Counter_T)

''****************

'  read and plot temperature  '
data
'**********************'
A_ReadTempAll
'A_ReadTempAll run
'   findPeakTemperatureMax
'find Peak Temperature
'   XYMaxMin_T
'XYMaxMin_T run
'   PlotCurve_Temp
'PlotCurve_Temp run
'End Sub
Private Sub Timer2_timer()
DoEvents
'pressure sensor @ channel 1
Counter_P = Counter_P + 1
'Counter_P = Counter_P+1

 nPoint_P = Counter_P
'get Counter_P into nPoint_P
CurrentdataPress.Text =
nPoint_P           'get Current
data pressure into nPoint_P
'MsgBox
Counter_T
XPoint_P(Counter_P) = Timer
- Start_Time_P
'XPoint_P(Counter_P) =
Timer-Start_Time_T
'MsgBox Timer
' MsgBox
XPoint_P(Counter_P)
 XpointPress.Text =
XPoint_P(Counter_P)
'XpointPress.Text =
XPoint_P(Counter_P)
'MsgBox
XPoint_P(Counter_T)
'****************
 ' read pressure data
*'****************
A_ReadPressureAll
'A_ReadPressureAll run

        findPeakPressureMax
        '***************'
        plot pressure data
        * '***********
         If Autoplot = 1 Then
        'check condition auto
        plot XYMaxMin_P
        'XYMaxMin_P run
         PlotCurve_Pressure
        'PlotCurve_Pressure
        run
        ElseIf Autoplot = 0
        Then
        'check condition
        manual plot

'MsgBox YPointMax_P
PlotDATA_Press_man
'PlotData_Press_man run
End If
End Sub
```

APPENDIX D

Calculation of Energy consumption

From the equation, $E_h = M_p \int_{T_1}^{T_2} C_m dT + \int_0^{t_i} p\dot{v}dt + M_p \int_{T_3}^{T_4} C_p dT$ is defined by

$$E_{\min} = m_{mould} \int_{T_1}^{T_2} C_{pmould} dT + \int_0^{t_i} p\dot{v}dt + m_{plastic} \int_{T_1}^{T_2} C_{pplastic} dT \cdot \tag{D.1}$$

The energy consumption, there are three parts as;

D.1 Mold Energy

The mold temperature is defined as;

$$E_{mold} = m_{mold} \int_{T_1}^{T_2} C_{pmold} dT \tag{D.2}$$

Where E_{mald} is mold energy, m_{mold} is mass of mold that is 2.037 kg, and C_{pmold} is 0.42 kJ/kg.K. There are integrate in graph is shown in **Figure D-1**.

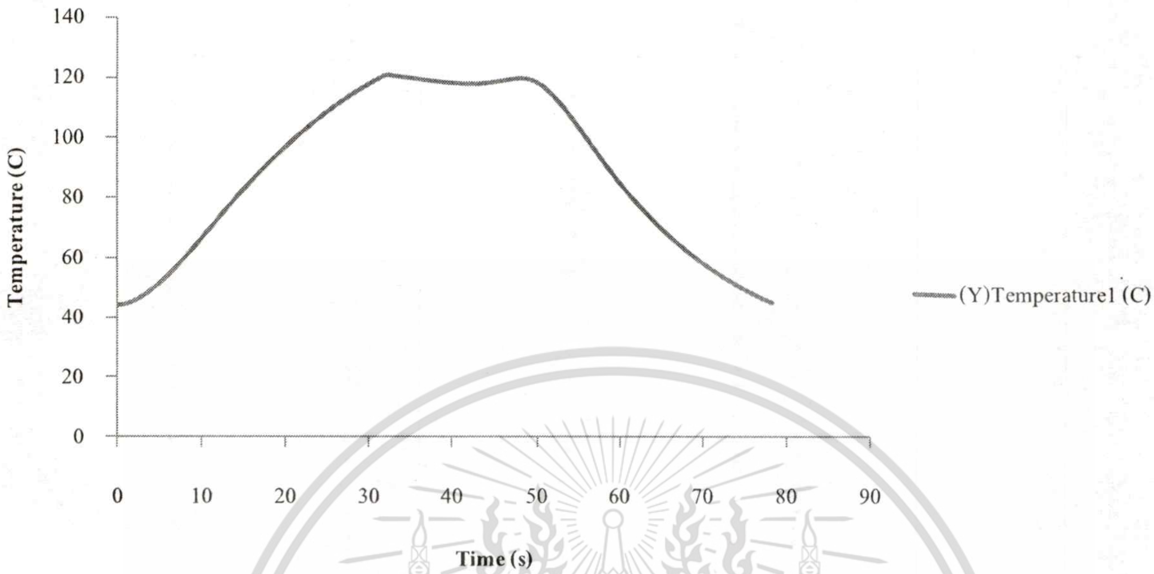

Figure D-1 Temperature and time

The area of this graph (Figure D-1) is $\int_{T_1}^{T_2} dT$. For this is 2,831.90 K.s. The mold energy is 2,422.836 kJ.

D.2 Machine Energy

The machine energy is defined as;

$$E_{machine} = \int_{0}^{t_i} p\dot{v}dt \tag{D.3}$$

Where $E_{machine}$ is the energy of machine(kJ). t_i is injection time (s). p is injection pressure ($kg.m^{-1}.s^{-2}$). $\dot{v}$ is volumetric rate (m^3). There are integrate in **Figure D-2**.

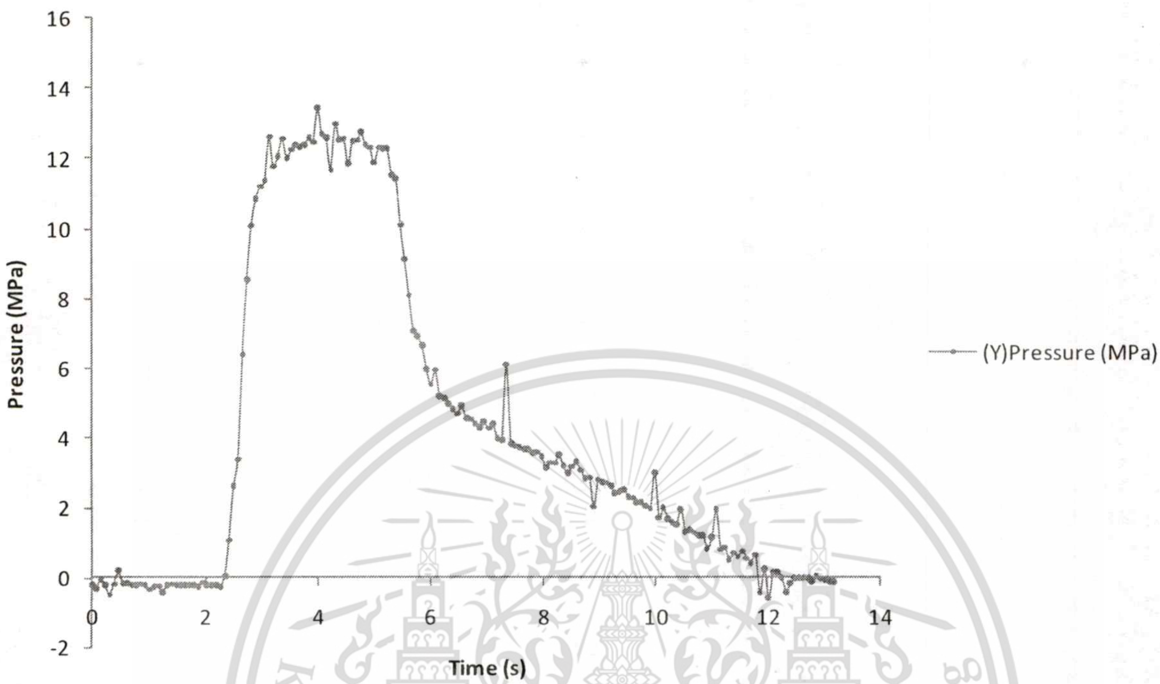

Figure D-2 Pressure and time

The area of this graph (Figure D-2) is $\int_0^{t_1} pdt$. For this case is 4,506,286.93 $kg.m^{-1}.s^{-2}$. $\dot{v}$ is 0.00016 m^3.

The machine energy is 0.721 kJ.

D.3 Plastic Energy

The plastic energy is defined as;

$$E_{plastic} = m_{plastic} \int_{T_1}^{T_2} C_{pplastic} dT \tag{D.4}$$

Where $E_{plastic}$ is the energy of plastic(kJ). $m_{plastic}$ is the mass of plastic (kg), in this is 0.02 kg. $C_{pplastic}$ is the heat capacity of plastic (kJ/kg.K) in this is 1.3 kJ/kg.K . T_1 is initial temperature (K). T_2 is final temperature (K).

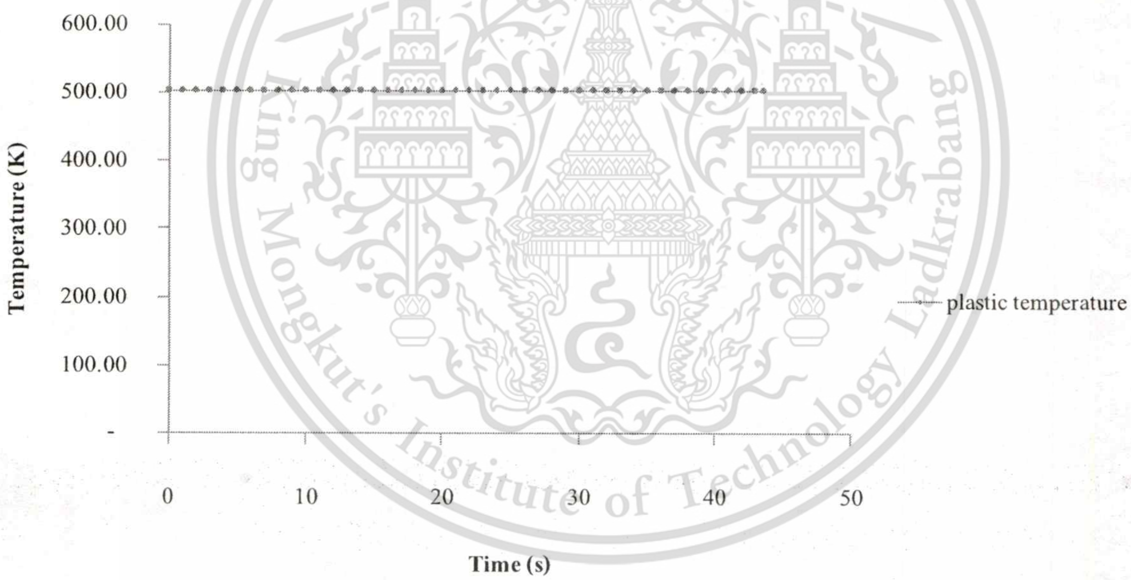

Figure D-3 Plastic temperature and time

The area of this graph (Figure D-3) is $\int_{T_1}^{T_2} dT$. For this case is 2,195.83 K.s. The plastic energy is 456.27 kJ.

Then energy consumption is Mold Energy + Machine Energy + Plastic Energy. Although in this case, the energy consumption is 2,422.836 kJ + 0.721 kJ + 456.27 kJ = 2,879.827 kJ.

Remark* In this case is SP200 injection molding via heating and cooling cycle in packing time is 3 sec.

APPENDIX E

Injection molding conditions

E.1 ABS

Table E.1 Injection molding conditions of ABS

Number	Mterials	Condition	Number	Mterials	Condition
1	KU901	mt20-h230-hp450-hpt5-v30	11	KU901	mt120-h230-hp450-hpt7-v30
2	KU901	mt40-h230-hp450-hpt5-v30	12	KU901	mt120-h230-hp450-hpt9-v30
3	KU901	mt60-h230-hp450-hpt5-v30	13	SP200	mt20-h230-hp450-hpt5-v30
4	KU901	mt80-h230-hp450-hpt5-v30	14	SP200	mt40-h230-hp450-hpt5-v30
5	KU901	mt100-h230-hp450-hpt5-v30	15	SP200	mt60-h230-hp450-hpt5-v30
6	KU901	mt110-h230-hp450-hpt5-v30	16	SP200	mt80-h230-hp450-hpt5-v30
7	KU901	mt120-h230-hp450-hpt5-v30	17	SP200	mt100-h230-hp450-hpt5-v30
8	KU901	mt120-h230-hp450-hpt1-v30	18	SP200	mt110-h230-hp450-hpt5-v30
9	KU901	mt120-h230-hp450-hpt3-v30	19	SP200	mt120-h230-hp450-hpt5-v30
10	KU901	mt120-h230-hp450-hpt5-v30	20	SP200	mt60-h230-hp450-hpt1-v30

Table E.1 Injection molding conditions of ABS (CON.)

Number	Mterials	Condition	Number	Mterials	Condition
21	SP200	mt60-h230-hp450-hpt3-v30	31	SP200	mt60-h230-hp200-hpt3-v30
22	SP200	mt60-h230-hp450-hpt5-v30	32	SP200	mt60-h230-hp300-hpt3-v30
23	SP200	mt60-h230-hp450-hpt7-v30	33	SP200	mt60-h230-hp450-hpt3-v30
24	SP200	mt60-h230-hp450-hpt9-v30	34	SP200	mt60-h230-hp500-hpt3-v30
25	SP200	mt120-h230-hp450-hpt1-v30	35	SP200	mt60-h220-hp450-hpt3-v30
26	SP200	mt120-h230-hp450-hpt3-v30	36	SP200	mt60-h230-hp450-hpt3-v30
27	SP200	mt120-h230-hp450-hpt5-v30	37	SP200	mt60-h240-hp450-hpt3-v30
28	SP200	mt120-h230-hp450-hpt7-v30	38	SP200	mt60-h230-hp450-hpt3-v10
29	SP200	mt120-h230-hp450-hpt9-v30	39	SP200	mt60-h230-hp450-hpt3-v20
30	SP200	mt60-h230-hp100-hpt3-v30	40	SP200	mt60-h230-hp450-hpt3-v30

Table E.1 Injection molding conditions of ABS (CON.)

Number	Mterials	Condition	Number	Mterials	Condition
41	SP200	mt60-h230-hp450-hpt3-v50	48	GA300	mt110-h230-hp450-hpt5-v30
42	SP200	mt60-h230-hp450-hpt3-v70	49	GA300	mt120-h230-hp450-hpt5-v30
43	GA300	mt20-h230-hp450-hpt5-v30	50	GA300	mt120-h230-hp450-hpt1-v30
44	GA300	mt40-h230-hp450-hpt5-v30	51	GA300	mt120-h230-hp450-hpt3-v30
45	GA300	mt60-h230-hp450-hpt5-v30	52	GA300	mt120-h230-hp450-hpt5-v30
46	GA300	mt80-h230-hp450-hpt5-v30	53	GA300	mt120-h230-hp450-hpt7-v30
47	GA300	mt100-h230-hp450-hpt5-v30	54	GA300	mt120-h230-hp450-hpt9-v30

Where;

mt = mold temperature

h = barrel temperature

hp = packing pressure

hpt = packing time

v = injection speed

E.2 POM

Table E.2 Injection molding conditions of POM

Number	Mterials	Condition	Number	Mterials	Condition
1	M90	mt20-h230-hp300-hpt3-v30	11	M90	mt60-h230-hp300-hpt7-v30
2	M90	mt40-h230-hp300-hpt3-v30	12	M90	mt60-h230-hp300-hpt9-v30
3	M90	mt60-h230-hp300-hpt3-v30	13	M90	mt120-h230-hp300-hpt1-v30
4	M90	mt80-h230-hp300-hpt3-v30	14	M90	mt120-h230-hp300-hpt3-v30
5	M90	mt100-h230-hp300-hpt3-v30	15	M90	mt120-h230-hp300-hpt5-v30
6	M90	mt110-h230-hp300-hpt3-v30	16	M90	mt120-h230-hp300-hpt7-v30
7	M90	mt120-h230-hp300-hpt3-v30	17	M90	mt120-h230-hp300-hpt9-v30
8	M90	mt60-h230-hp300-hpt1-v30	18	M90	mt60-h230-hp100-hpt3-v30
9	M90	mt60-h230-hp300-hpt3-v30	19	M90	mt60-h230-hp200-hpt3-v30
10	M90	mt60-h230-hp300-hpt5-v30	20	M90	mt60-h230-hp300-hpt3-v30

Table E.2 Injection molding conditions of POM (CON.)

Number	Mterials	Condition	Number	Mterials	Condition
21	M90	mt60-h230-hp400-hpt3-v30	31	M270	mt40-h230-hp300-hpt3-v30
22	M90	mt60-h220-hp300-hpt3-v30	32	M270	mt60-h230-hp300-hpt3-v30
23	M90	mt60-h230-hp300-hpt3-v30	33	M270	mt80-h230-hp300-hpt3-v30
24	M90	mt60-h240-hp300-hpt3-v30	34	M270	mt100-h230-hp300-hpt3-v30
25	M90	mt60-h230-hp300-hpt3-v10	35	M270	mt110-h230-hp300-hpt3-v30
26	M90	mt60-h230-hp300-hpt3-v20	36	M270	mt120-h230-hp300-hpt3-v30
27	M90	mt60-h230-hp300-hpt3-v30	37	M270	mt60-h230-hp300-hpt1-v30
28	M90	mt60-h230-hp300-hpt3-v50	38	M270	mt60-h230-hp300-hpt3-v30
29	M90	mt60-h230-hp300-hpt3-v70	39	M270	mt60-h230-hp300-hpt5-v30
30	M270	mt20-h230-hp300-hpt3-v30	40	M270	mt60-h230-hp300-hpt7-v30

Table E.2 Injection molding conditions of POM (CON.)

Number	Mterials	Condition	Number	Mterials	Condition
41	M270	mt60-h230-hp300-hpt9-v30	50	M270	mt60-h230-hp400-hpt3-v30
42	M270	mt120-h230-hp300-hpt1-v30	51	M270	mt60-h220-hp300-hpt3-v30
43	M270	mt120-h230-hp300-hpt3-v30	52	M270	mt60-h230-hp300-hpt3-v30
44	M270	mt120-h230-hp300-hpt5-v30	53	M270	mt60-h240-hp300-hpt3-v30
45	M270	mt120-h230-hp300-hpt7-v30	54	M270	mt60-h230-hp300-hpt3-v10
46	M270	mt120-h230-hp300-hpt9-v30	55	M270	mt60-h230-hp300-hpt3-v20
47	M270	mt60-h230-hp100-hpt3-v30	56	M270	mt60-h230-hp300-hpt3-v30
48	M270	mt60-h230-hp200-hpt3-v30	57	M270	mt60-h230-hp300-hpt3-v50
49	M270	mt60-h230-hp300-hpt3-v30	58	M270	mt60-h230-hp300-hpt3-v70

Where;

mt = mold temperature

h = barrel temperature

hp = packing pressure

hpt = packing time

v = injection speed

BIOGRAPHY

Name:	Mr. Wasan Palapinyo
Date of Birth:	June 23, 1986
Place of Birth:	Chonburi, Thailand
Education:	
2005-2008	B. Eng. in Control Engineering, Department of Control Engineering, King Mongkut's Institute of Technology Ladkrabang (KMITL)
2009-2012	M. Eng. in Automotive Engineering (International program), International College, King Mongkut's Institute of Technology Ladkrabang (KMITL)
Honour and Scholarship:	
2009-2012	Full scholarship for study in the master degree from National Science and Technology Development Agency (NSTDA)

Publications:

1. Wasan Palapinyo, Wuttipong Rungseesantivanon, Nattawoot Depaiwa, Takushi Saito, Isao Satoh, Natcha Prakymoramas, Bongkoth Hararak, Dumrong Thanomjirt. "Injection molding process parameter for ABS surface finish." **The 4th KKU International Engineering Conference**, Khon Kaen, Thailand, May 10-12, 2012.